Cosmology

Jacobo Asorey Barreiro

TAE 2024 - International Workshop on High Energy Physics

1 -14 September 2024, Centro de Ciencias de Benasque Pedro Pascual

Contents

I) Rise of ΛCDM

II) Inhomogeneous Universe

III) Cosmological probes and tensions

Galaxy Surveys

Spectroscopic:

good or very good radial resolution (0.1-1Mpc/h), but less deep (small Volume)

WiggleZ, BOSS, e-BOSS, Subaru/Sumire, OzDES, DESI, HETDEX, SKA, VISTA/Spec, Euclid, WFIRST

***Photometric*:**

poor radial (redshift) resolution (~300 Mpc/h) but deeper (more Volume, more evolution)

DES, VISTA, Pan-STARRS, Subaru/HSC, KIDS, Skymapper, LSST, Euclid, WFIRST

Photometric surveys

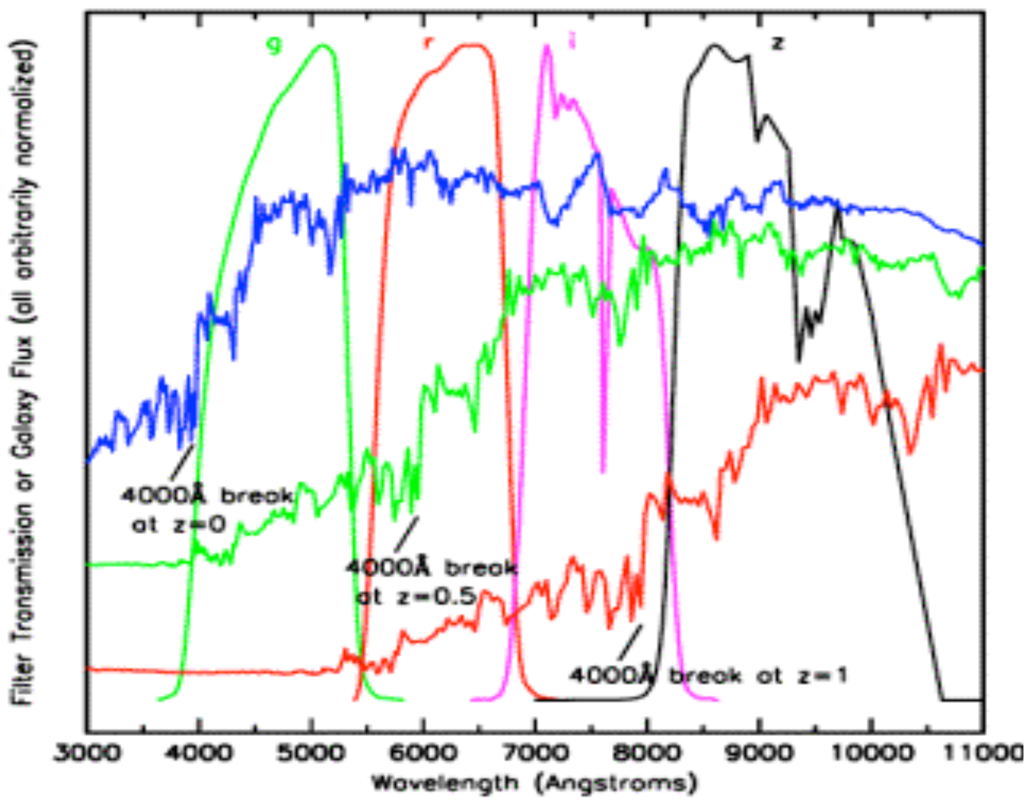

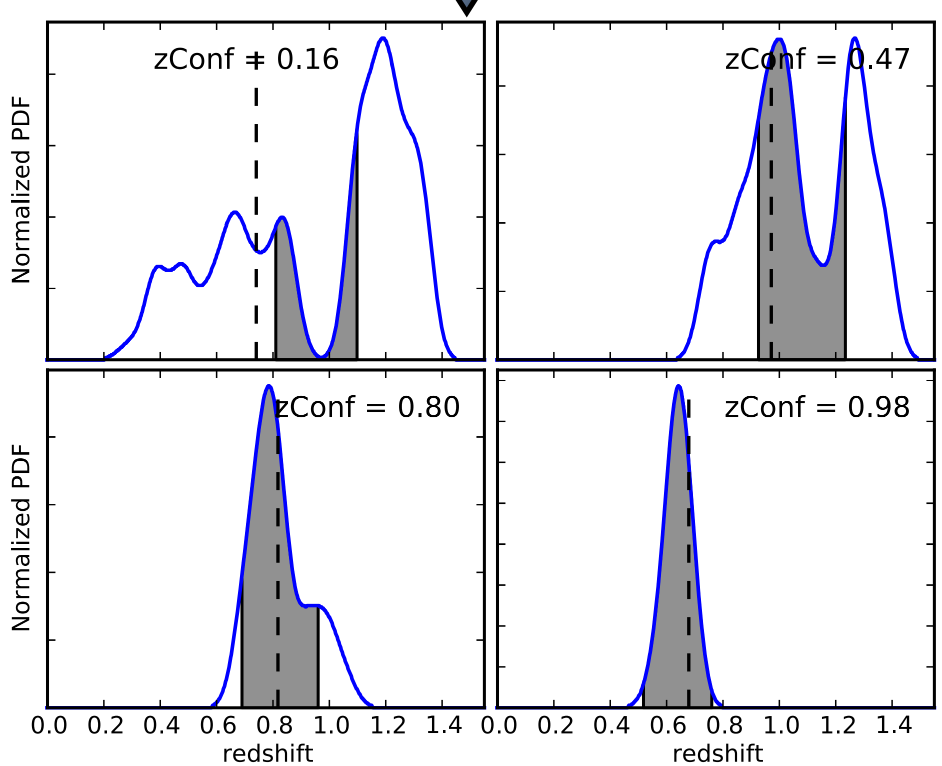

Carrasco Kind & Brunner 2013a (MNRAS, 432, 1483)

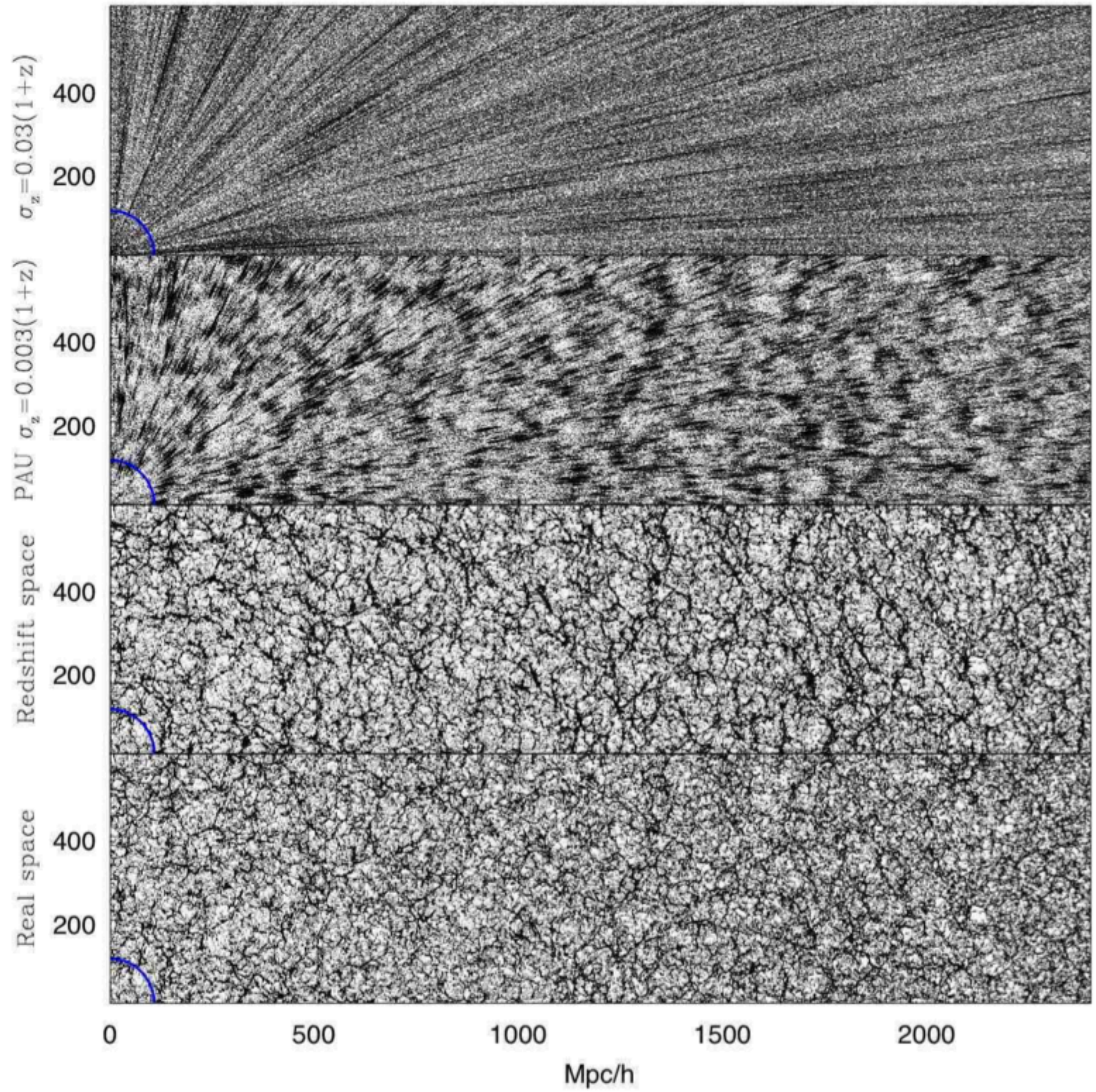

Benitez et al., 2009

Dark Energy survey

- 570 Mpixel DECam situated at 4-m Blanco Telescope, at Cerro Tololo (Chile)
- 2.2 degrees FoV.
- 5 broad-band filters grizY
- Expects to record over 300 million galaxies to depth i_{AB}~ 24
- Two surveys:
  - Wide: 5000 deg^2 during 5 years
  - Deep: 30 deg^2 repeated visits for transients (e.g. SN Type 1a)

DARK ENERGY SURVEY

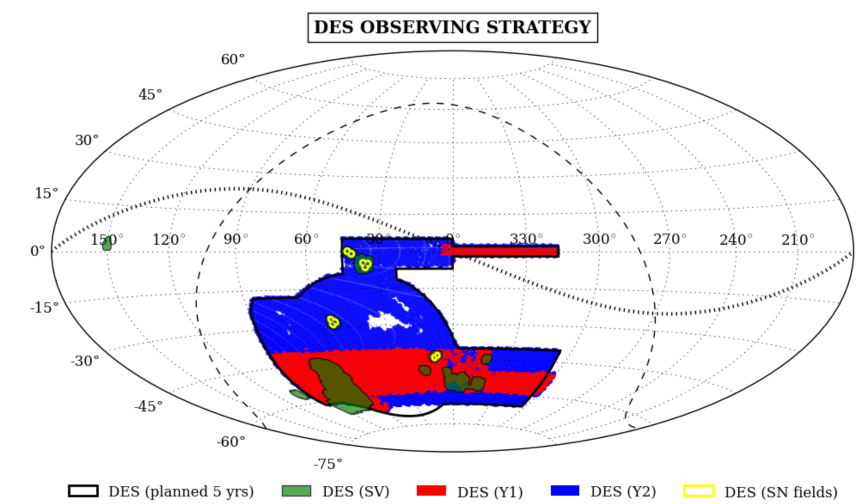

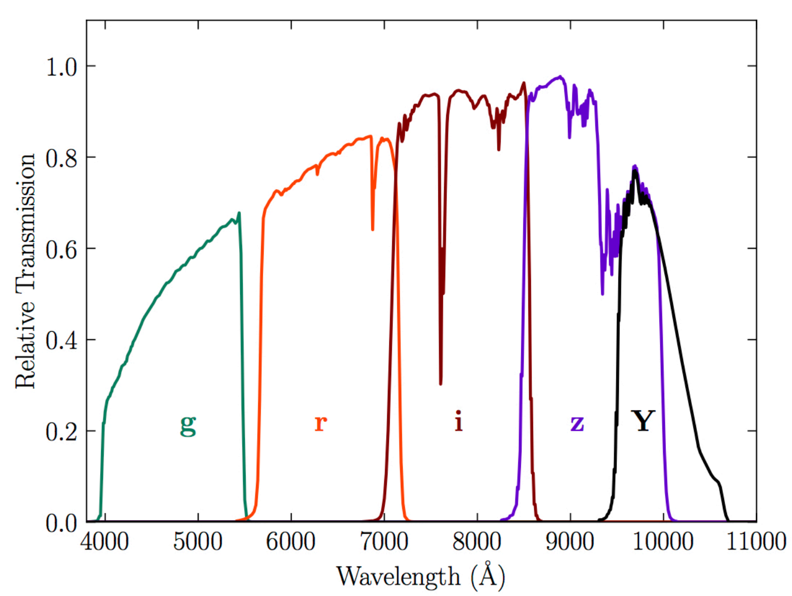

Searching for Dark Energy

The Dark Energy Survey main goal is to test the nature of Dark Energy

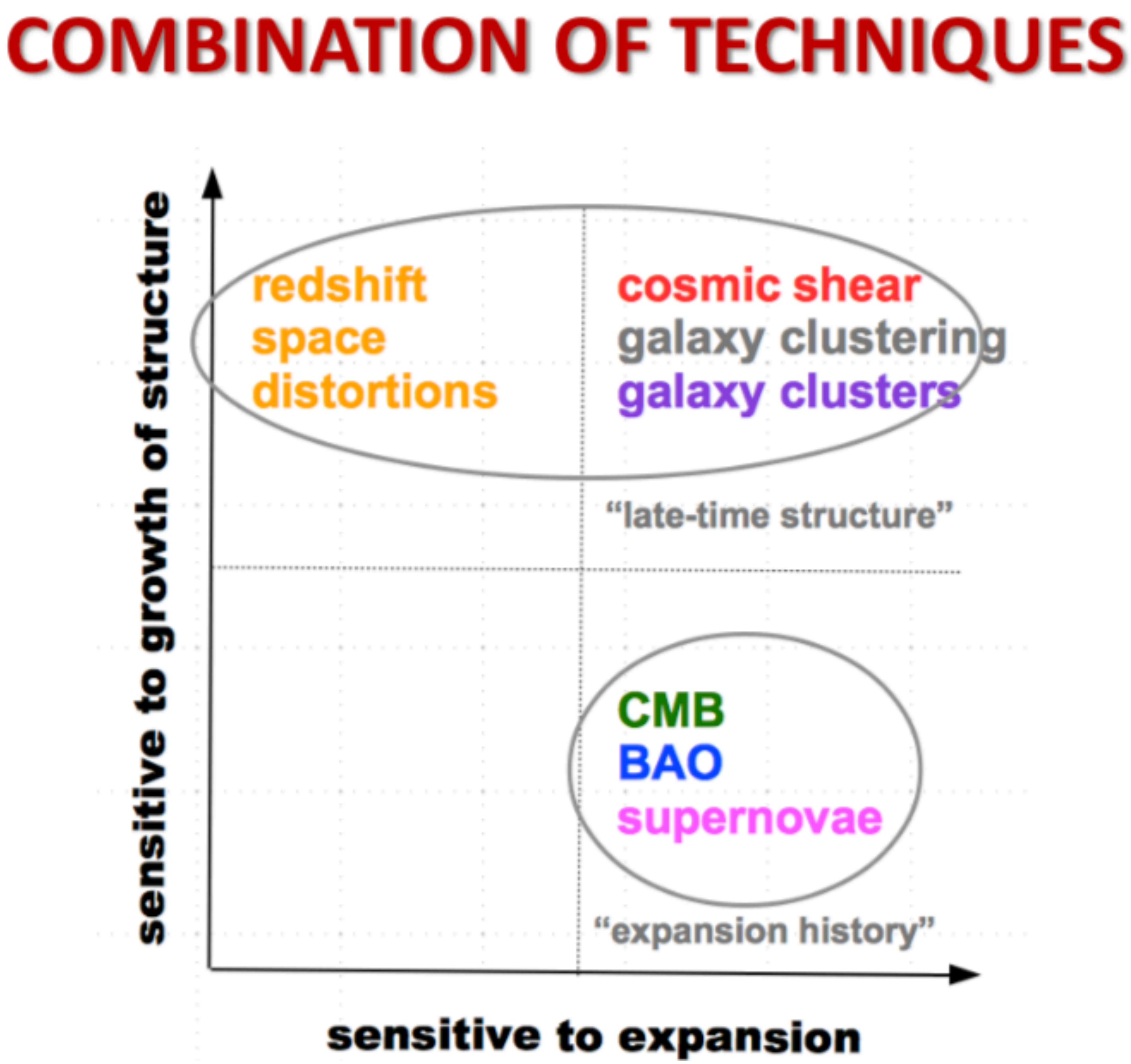

Gravitational lensing

As light its affected by gravity, the bright and shape of lensed objects change. -> Potential cosmological observable.

Depending on the distance to the lens and source and the properties between them, we can define 2 lensing effects

Strong lensing

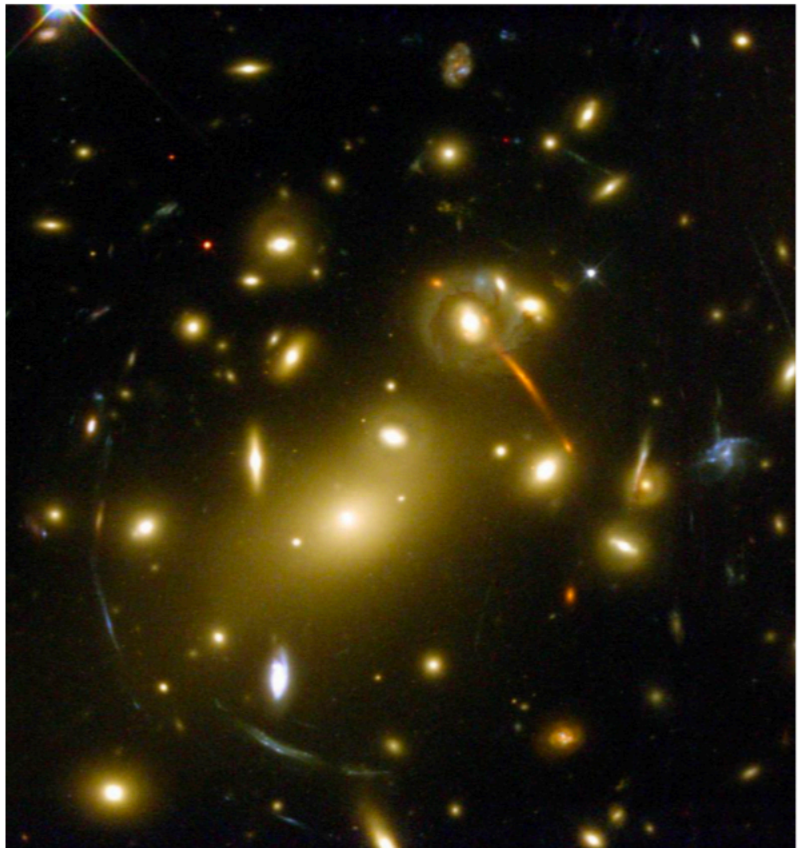

Weak lensing

Gravitational lensing

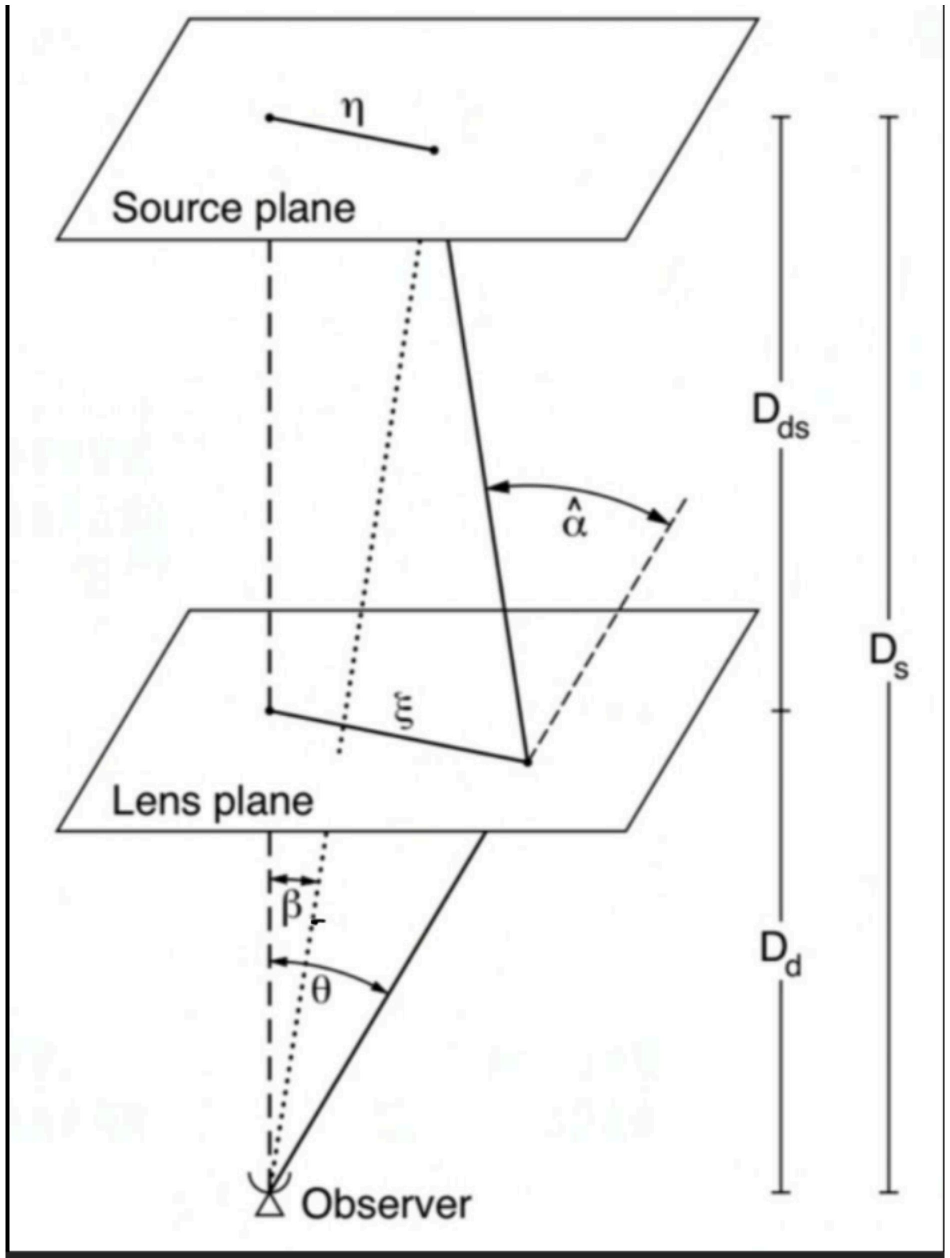

Bartelmann & Schneider 2001

For a point source:

$$\hat{\alpha} = \alpha \frac{Ds}{Dds} = \frac{4GM}{\xi c^2}$$

$$\theta - \alpha = \beta$$

For an extended potential:

$$\hat{\alpha}(\xi) = \frac{4GM(\xi)}{\xi c^2}$$

$$M(\xi) = 2\pi \int_0^{\xi} \Sigma(\xi')\xi' d\xi'$$

Gravitational lensing

An extended object change shape and brightness by the lensing of multiple light trajectories. Described by the Jacobian between the unlensed and lensed coordinates.

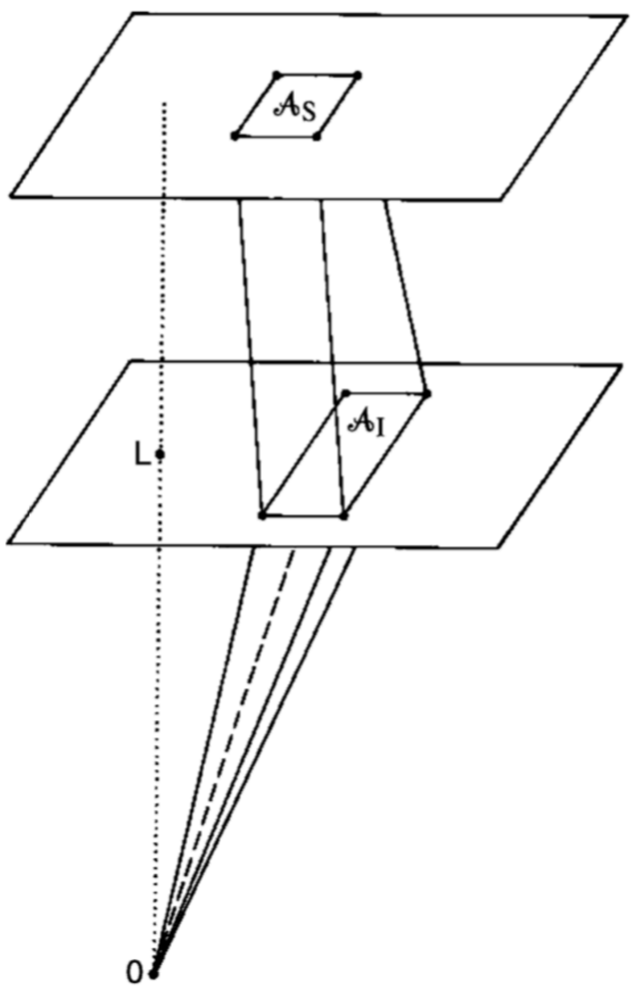

Fig. 2.23. Light beams are deflected differentially, leading to changes of the shape and the cross-sectional area of the beam. As a consequence, the observed solid angle subtended by the source, as seen by the observer, is modified by gravitational light deflection. In the example shown, the observed solid angle $\mathcal{A}_I/D_d^2$ is larger than the one subtended by the undeflected source, $\mathcal{A}_S/D_s^2$ – the image of the source is thus magnified

$$A_{ij} = \frac{\partial \beta_i}{\partial \theta_j} = \delta_{ij} - \frac{\partial \alpha_i}{\partial \theta_j} = \delta_{ij} - \frac{\partial^2 \psi}{\partial \theta_i \partial \theta_j} = \begin{bmatrix} 1-\kappa-\gamma_1 & \gamma_2 \\ \gamma_2 & 1-\kappa+\gamma_1 \end{bmatrix}$$

$$\vec{\theta} - \vec{\beta} = \vec{\alpha}(\vec{\theta}) = \vec{\nabla}\psi(\vec{\theta})$$

$$\kappa(\vec{\theta}) = \frac{1}{2}\nabla^2\psi(\vec{\theta})$$

κ is the convergence (change of brightness) -> magnification

γ define the shape change -> (shear)

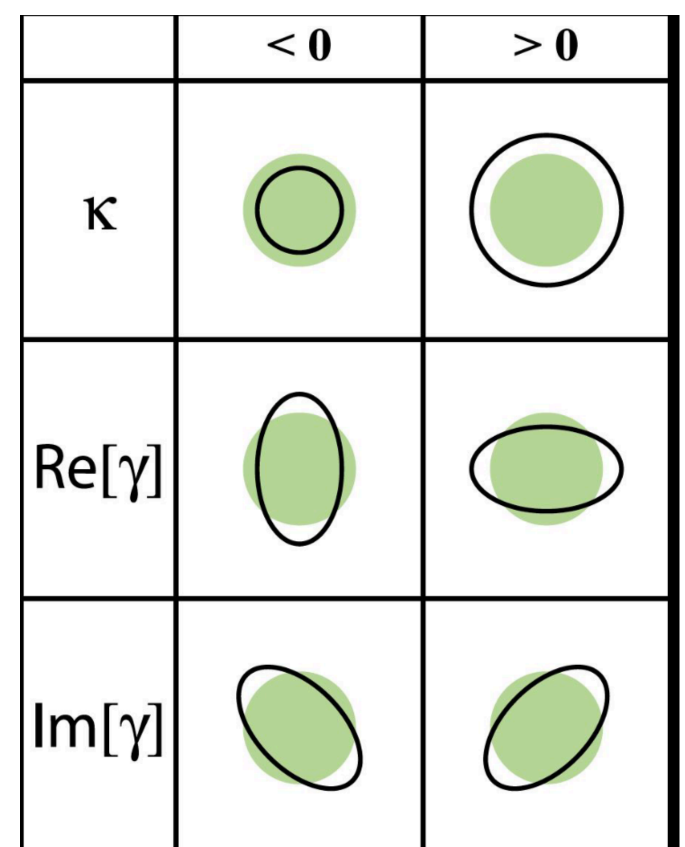

Figure by Jim Bosch

Weak lensing Shear

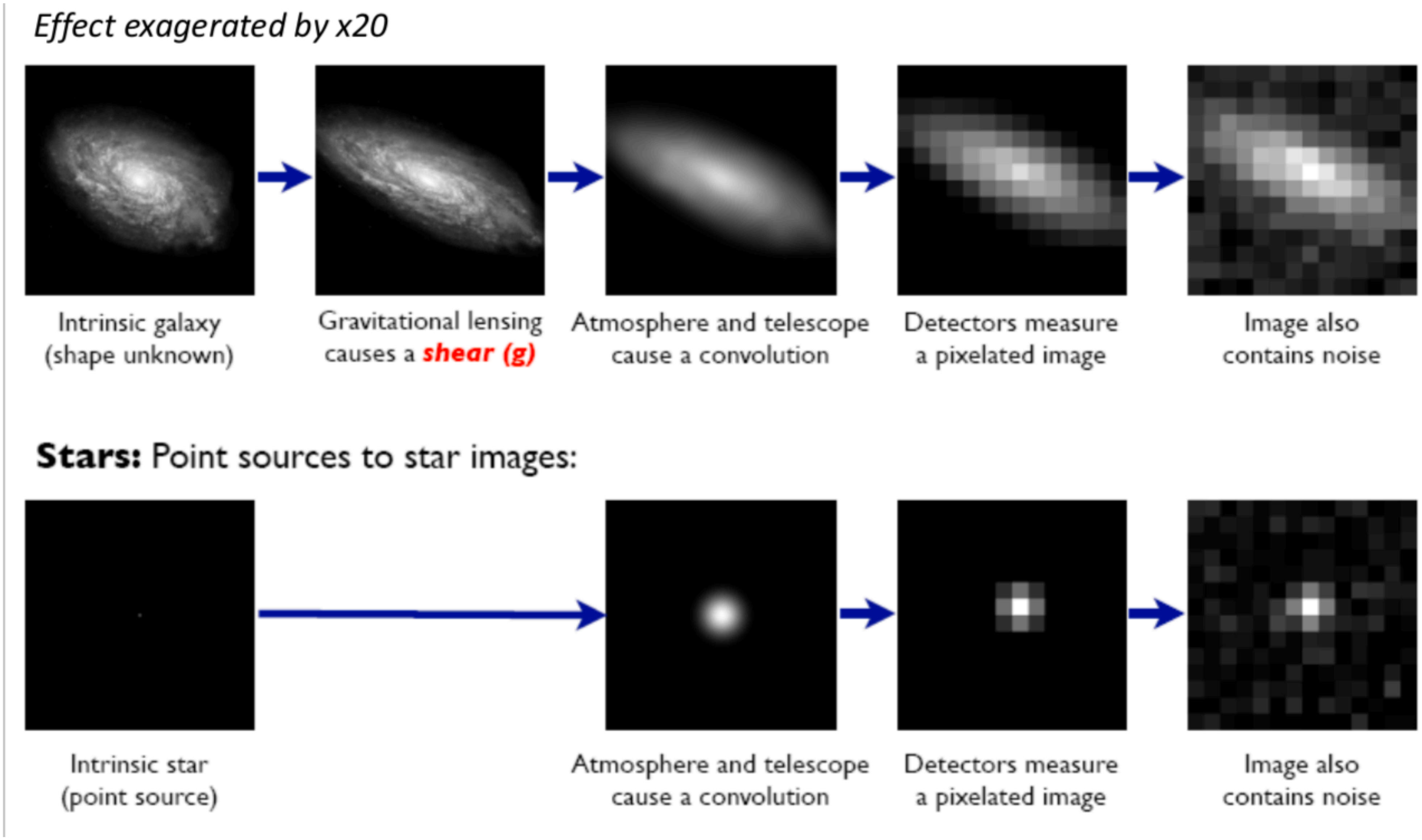

The measurement of shear from images requires the calibration with stars images.

Cosmology 3x2pt (with DES)

Combination of clustering with gravitational shear.

Main observational problems, the photometric uncertainty and the shear measurements.
Main theory problem. Intrinsic alignments

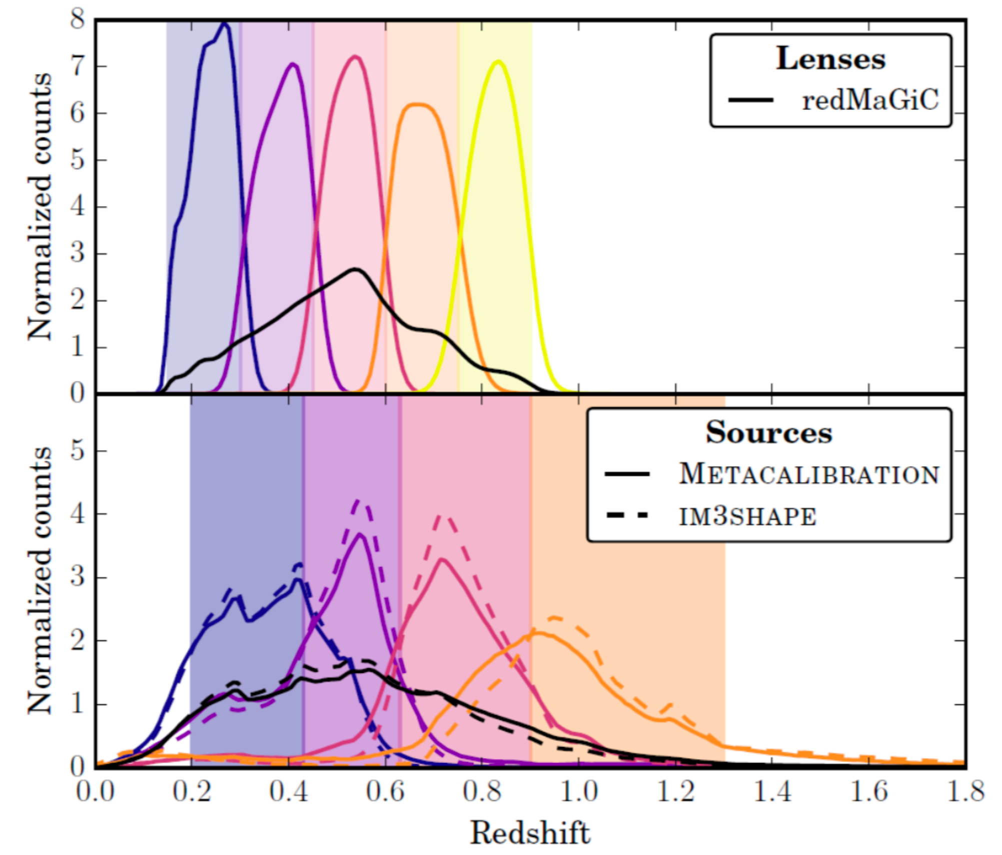

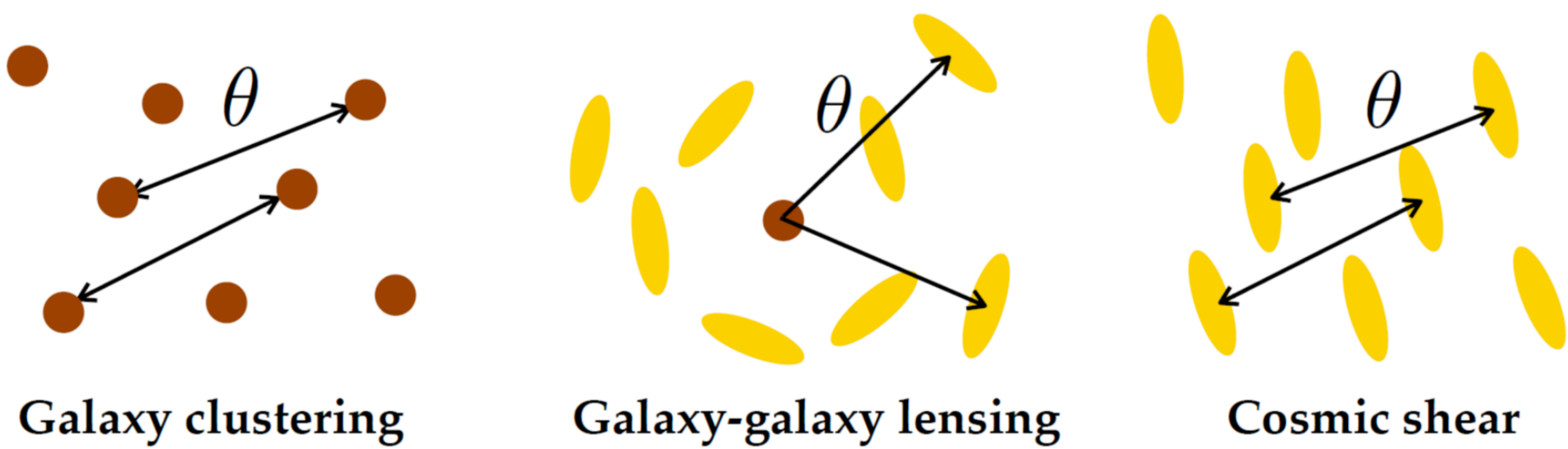

Cosmology 3x2pt (with DES)

Dataset composed by three different types with multiple redshift bin combinations and angular scales

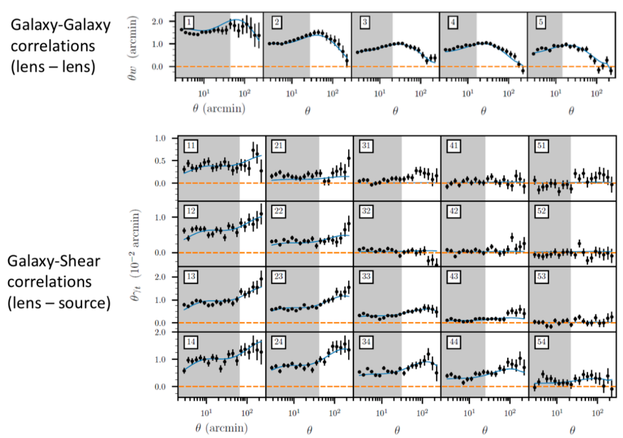

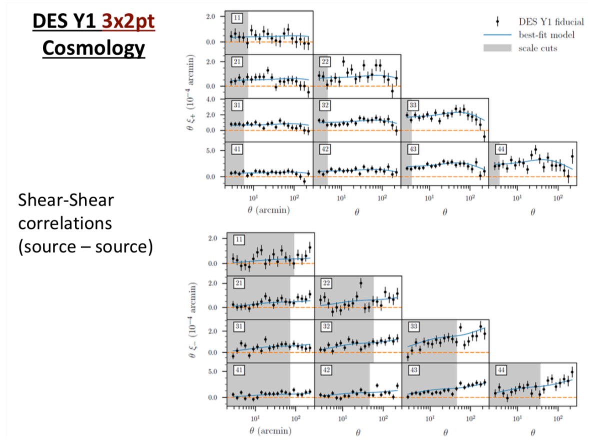

$$w^i(\theta) = (b^i)^2 \int \frac{dl\, l}{2\pi} J_0(l\theta) \int d\chi \times \frac{\left[n_l^i(z(\chi))\right]^2}{\chi^2 H(z)} P_{\rm NL}\left(\frac{l+1/2}{\chi}, z(\chi)\right)$$

Galaxy Clustering Correlation position-position

$$\gamma_t^{ij}(\theta) = b^i(1+m^j) \int \frac{dl\, l}{2\pi} J_2(l\theta) \int d\chi n_l^i(z(\chi)) \times \frac{q_s^j(\chi)}{H(z)\chi^2} P_{\rm NL}\left(\frac{l+1/2}{\chi}, z(\chi)\right)$$

Galaxy-Glaxy Lensing Correlation position-shape

$$q_s^i(\chi) = \frac{3\Omega_m H_0^2}{2} \frac{\chi}{a(\chi)} \int_\chi^{\chi(z=\infty)} d\chi' n_s^i(z(\chi')) \frac{dz}{d\chi'} \frac{\chi'-\chi}{\chi'} \quad \text{(IV.3)}$$

$$\xi_{+/-}^{ij}(\theta) = (1+m^i)(1+m^j) \int \frac{dl\, l}{2\pi} J_{0/4}(l\theta) \int d\chi \times \frac{q_s^i(\chi) q_s^j(\chi)}{\chi^2} P_{\rm NL}\left(\frac{l+1/2}{\chi}, z(\chi)\right)$$

Cosmic Shear Correlation shape-shape

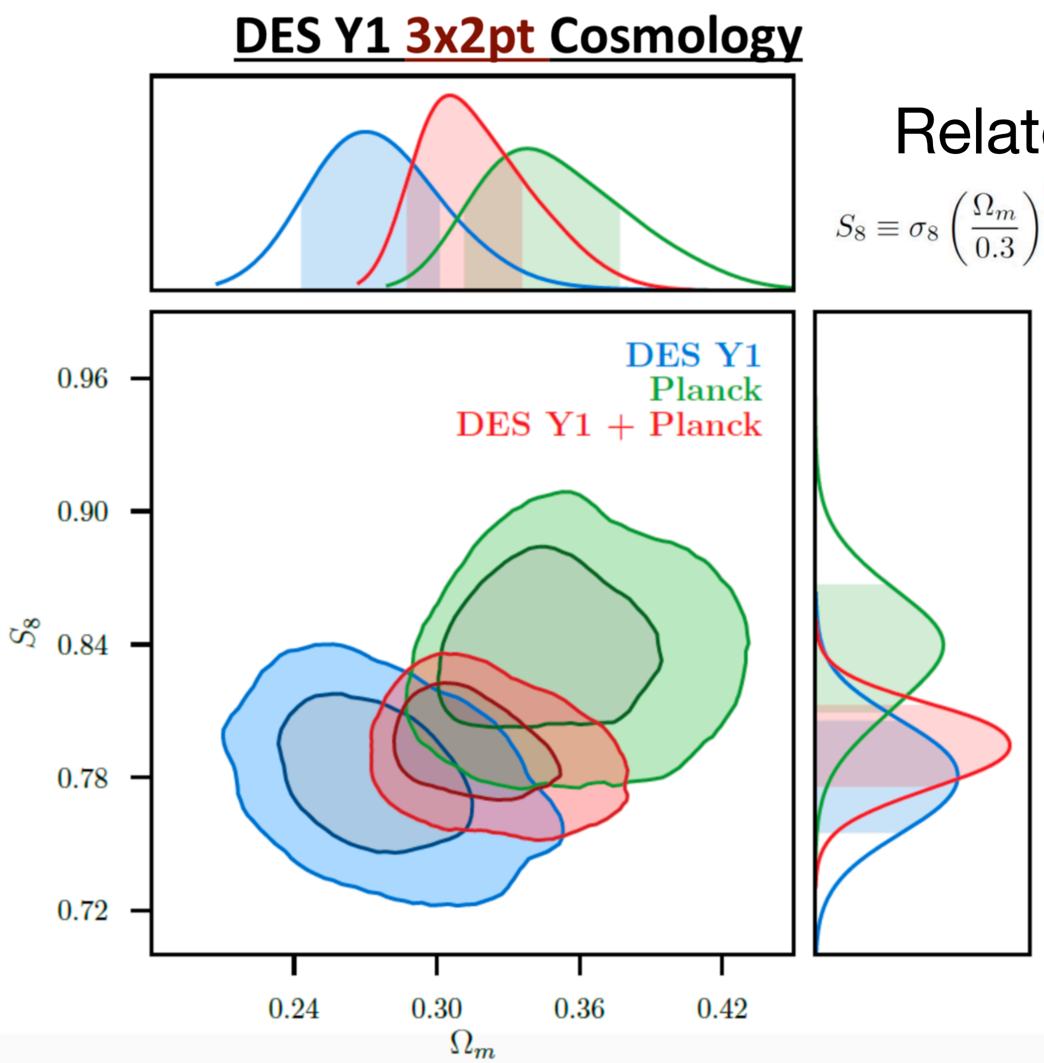

Related with A_S

$$S_8 \equiv \sigma_8 \left(\frac{\Omega_m}{0.3}\right)^{0.5}$$

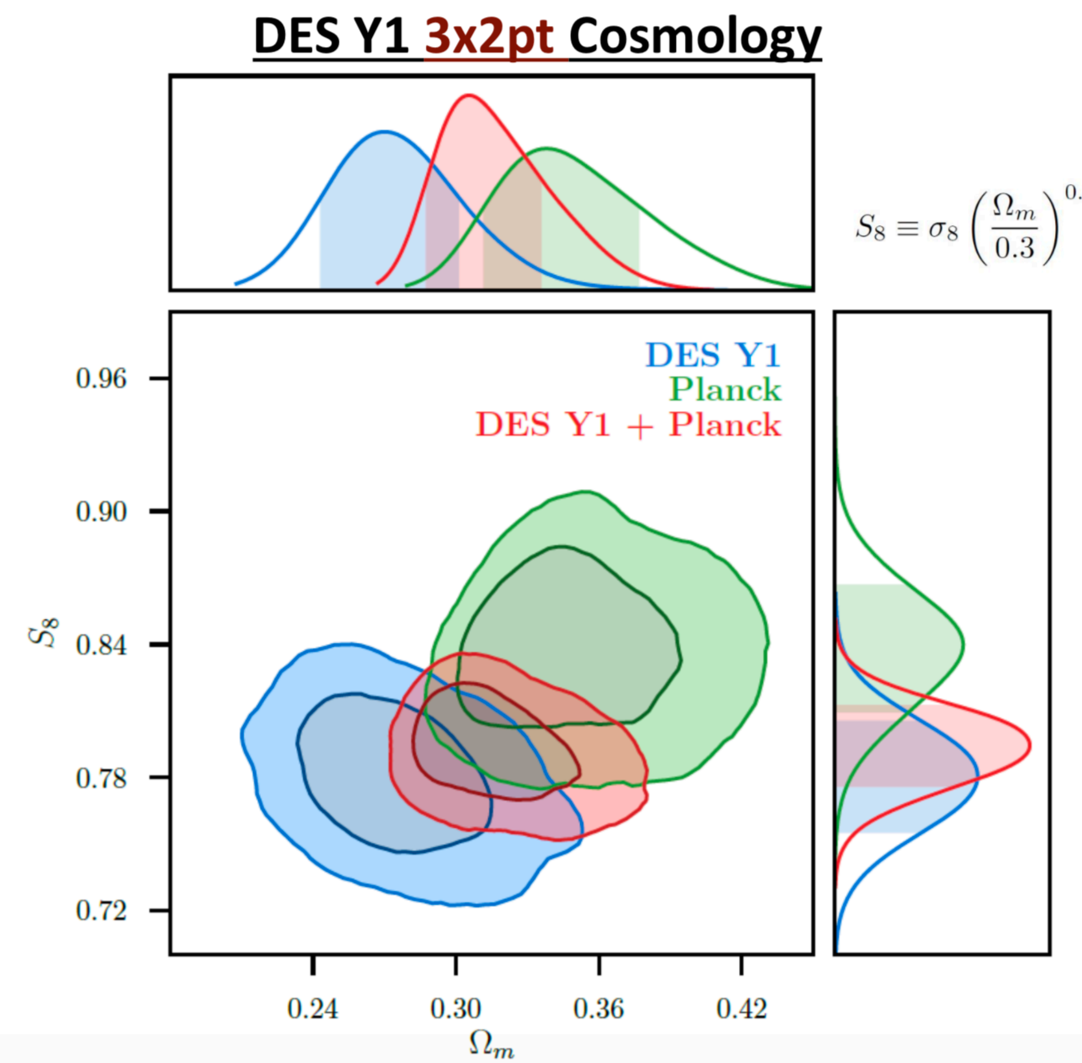

$$S_8 \equiv \sigma_8 \left(\frac{\Omega_m}{0.3}\right)^{0.5}$$

Combining multiple probes

DES was able to combine multiple probes with just one single telescope.

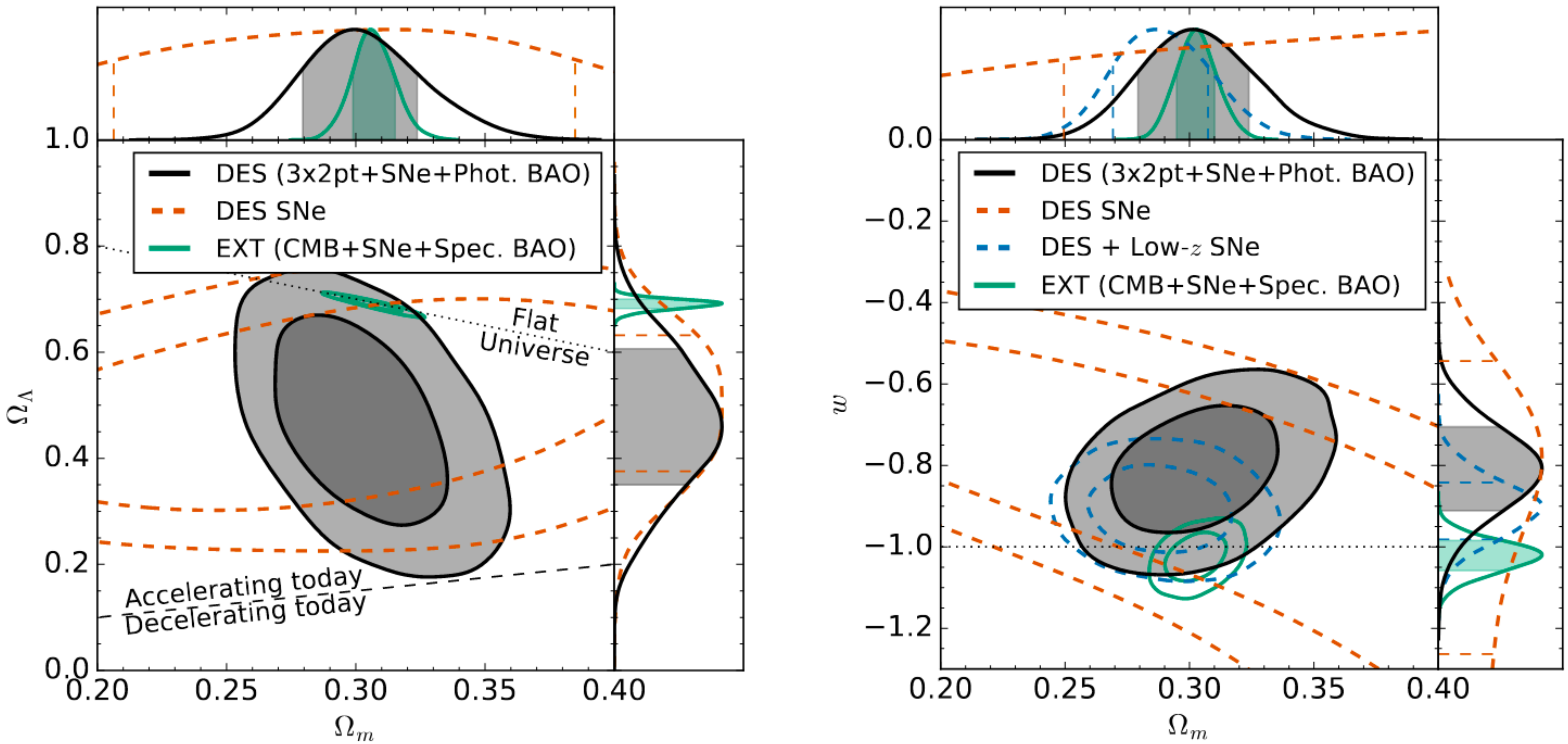

2-σ significance with only one “experiment”.

Extended models

- Dark Energy equation of state (CPL):

$$\frac{H(a)}{H_0} = \left[\Omega_m a^{-3} + (1-\Omega_m) a^{-3(1+w_0+w_a)} e^{-3w_a(1-a)}\right]^{1/2} .$$

- Metric perturbations and GR test:

$$ds^2 = a^2(\tau)\left[(1+2\Psi)d\tau^2 - (1-2\Phi)\delta_{ij}dx_i dx_j\right]$$

$$k^2\Psi = -\,4\pi G a^2 (1+\mu(a))\rho\delta\,,$$
$$k^2(\Psi+\Phi) = -\,8\pi G a^2(1+\Sigma(a))\rho\delta\,,$$

$$\mu(z) = \mu_0 \frac{\Omega_\Lambda(z)}{\Omega_\Lambda}\,,\quad \Sigma(z) = \Sigma_0 \frac{\Omega_\Lambda(z)}{\Omega_\Lambda}$$

Extended models

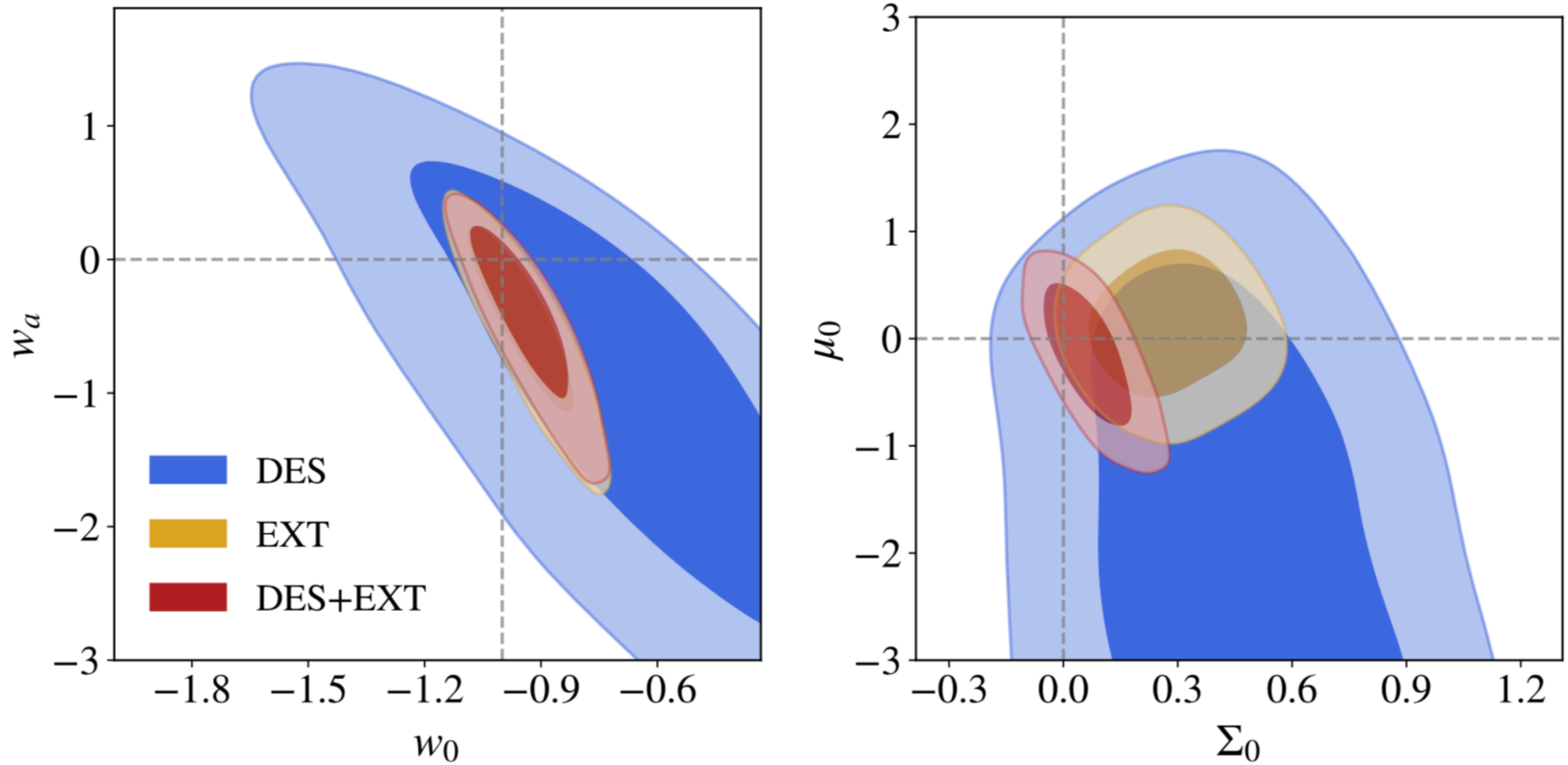

Dark Energy Survey Collaboration,2019a

How to survey Dark Matter

Model	Probe	Parameter	Value
Warm Dark Matter	Halo Mass	Particle Mass	$m \sim 18\,\text{keV}$
Self-Interacting Dark Matter	Halo Profile	Cross Section	$\sigma_{\text{SIDM}}/m_\chi \sim 0.1\text{–}10\,\text{cm}^2/\,\text{g}$
Baryon-Scattering Dark Matter	Halo Mass	Cross Section	$\sigma \sim 10^{-30}\,\text{cm}^2$
Axion-Like Particles	Energy Loss	Coupling Strength	$g_{\phi e} \sim 10^{-13}$
Fuzzy Dark Matter	Halo Mass	Particle Mass	$m \sim 10^{-20}\,\text{eV}$
Primordial Black Holes	Compact Objects	Object Mass	$M > 10^{-4} M_\odot$
WIMPs	Indirect Detection	Cross Section	$\langle\sigma v\rangle \sim 10^{-27}\,\text{cm}^3/\,\text{s}$
Light Relics	Large-Scale Structure	Relativistic Species	$N_{\text{eff}} \sim 0.1$

Table 1: Probes of fundamental dark matter physics in the LSST era, organized by dark matte
model and associated ol

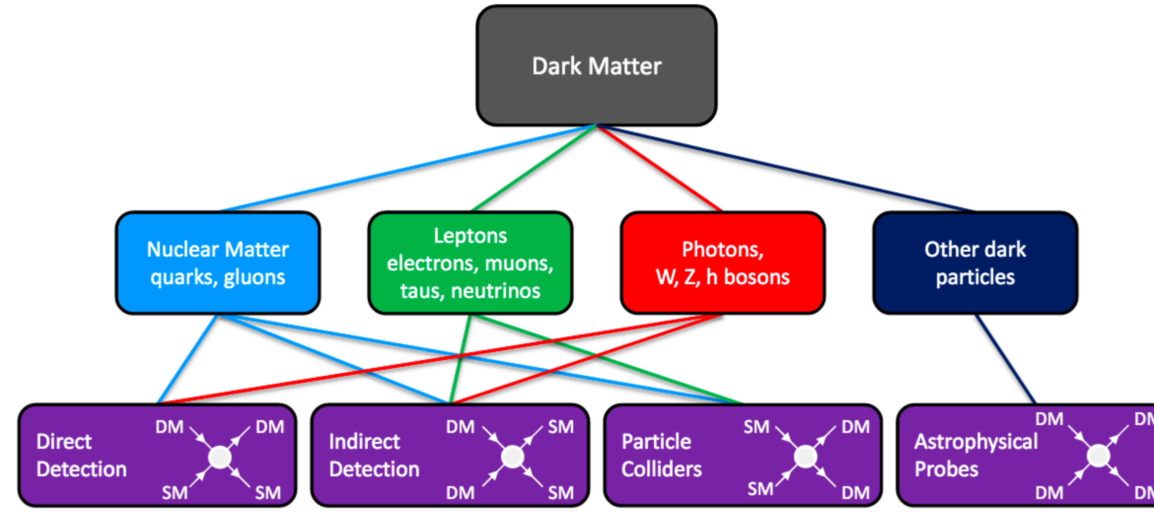

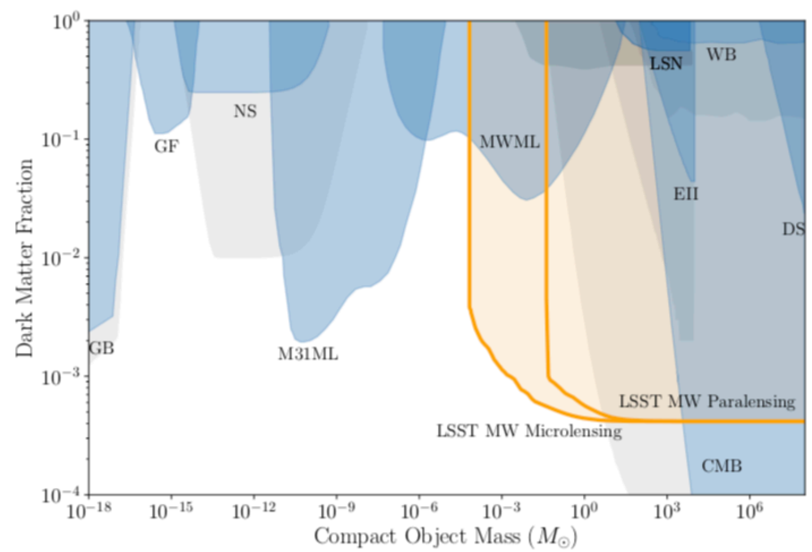

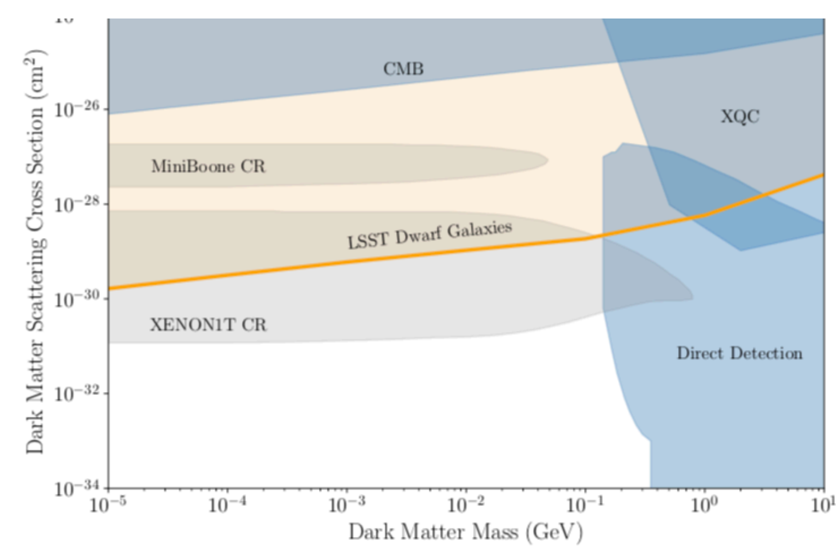

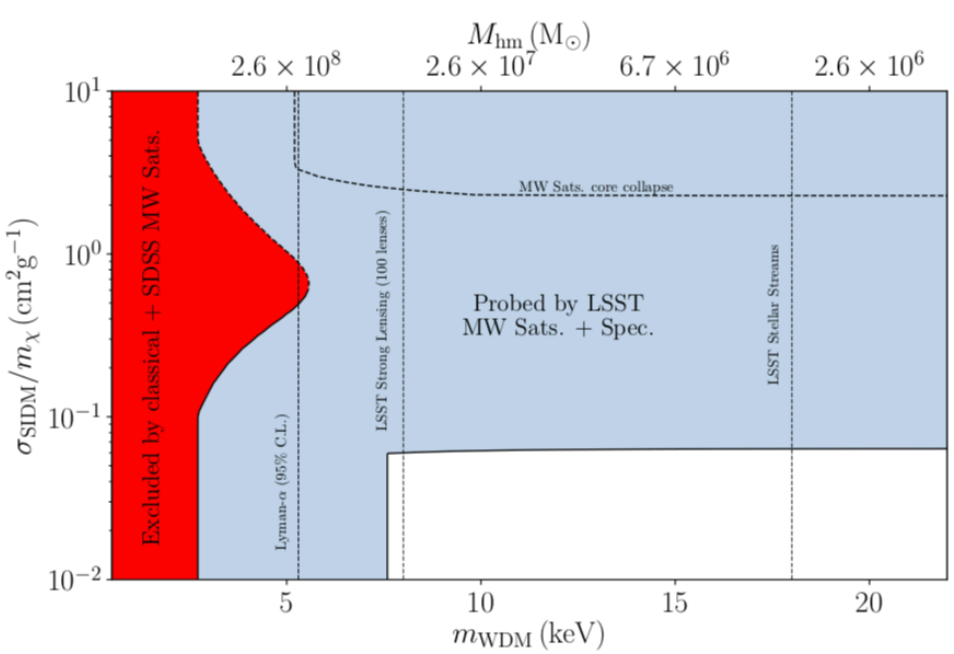

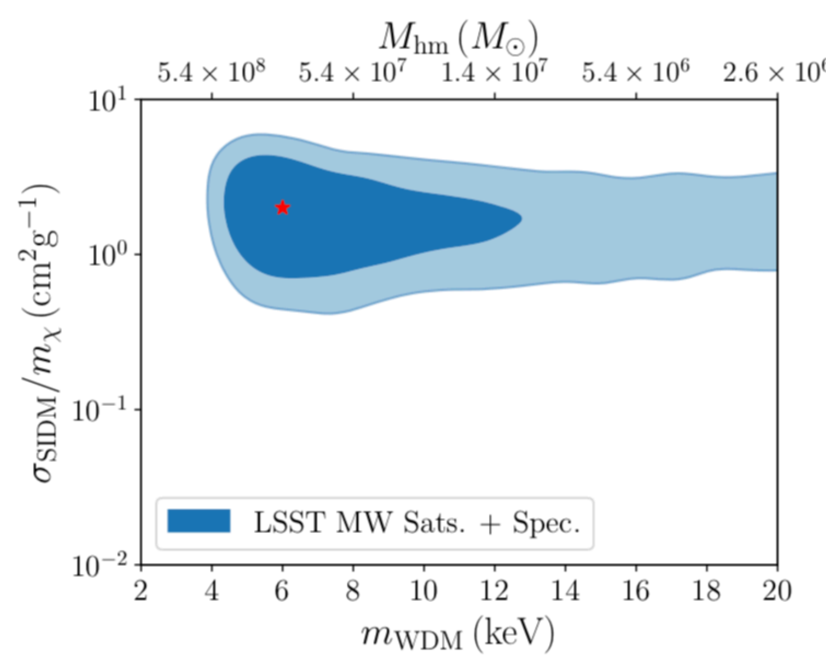

Vera C. Rubin Observatory

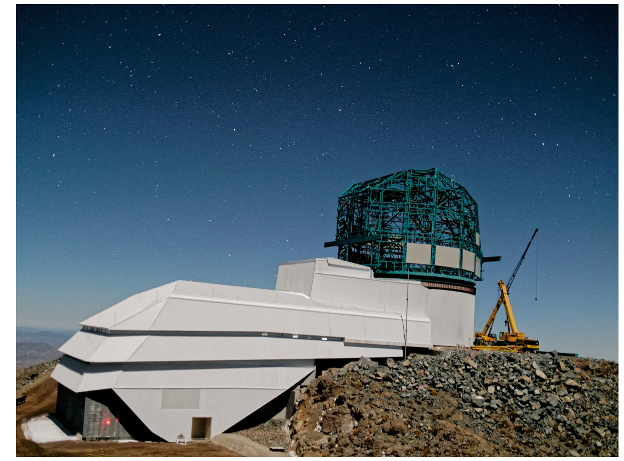

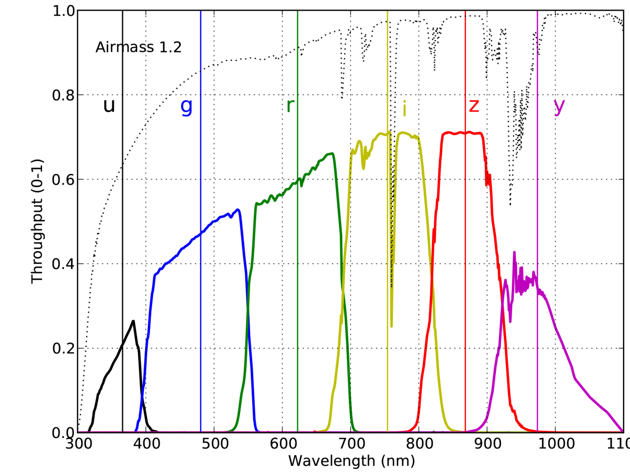

- 3.2 Gpixel camera at 8.4m Simonyi telescope situated Vera C. Rubin Observatory, at Cerro Pachón (Chile)
- 3.5 degrees FoV.
- 6 broad-band filters ugrizY
- Expects to record over 20000 million galaxies to depth i_{AB}~ 26.8
- Legacy Survey of Space and Time (LSST): Wide fast survey of 18000 sq. deg.

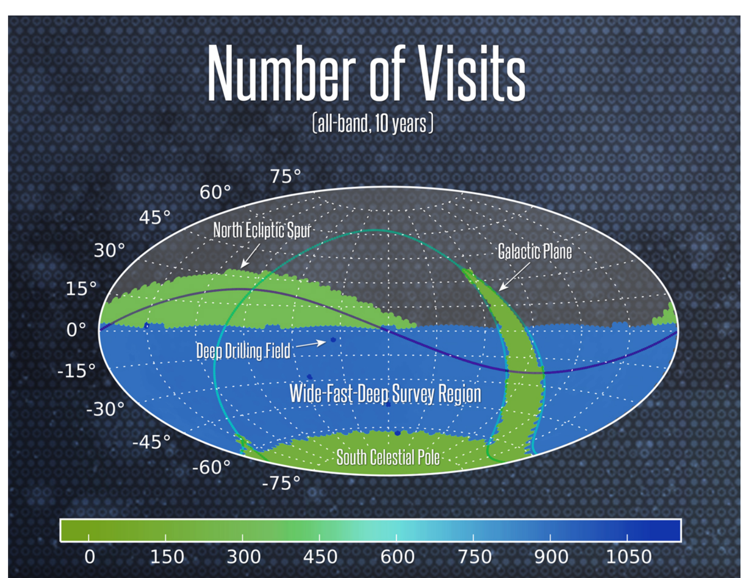

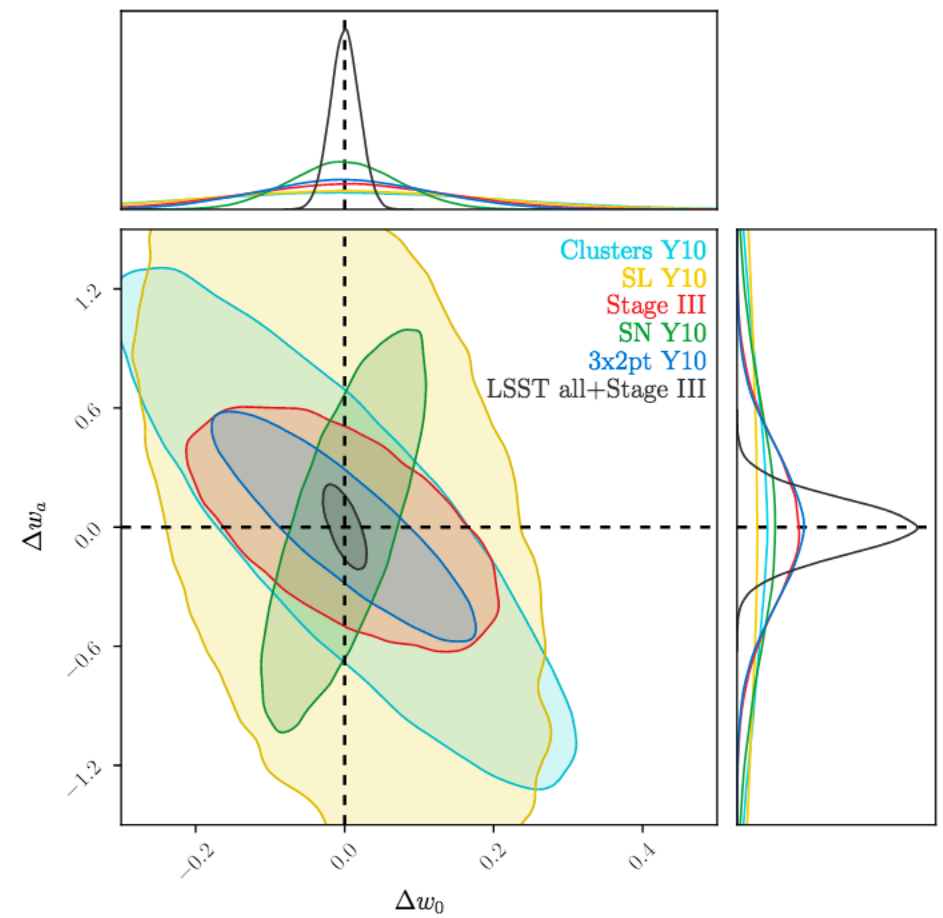

LSST Collab (2018)

LSST DESC Dark Energy Science Collaboration

Euclid Constortium

ESA mission of class M. Launched at 2023
1.2m spatial telescope with 2 instruments:

VISP: Imager
NISP: Near Infrared Spectrometer and Photometer

Wide field survey: 15000 sq. deg. $AB_{VIS} < 24.5$
Deep field survey: 40 sq. deg $AB_{VIS} < 26.5$

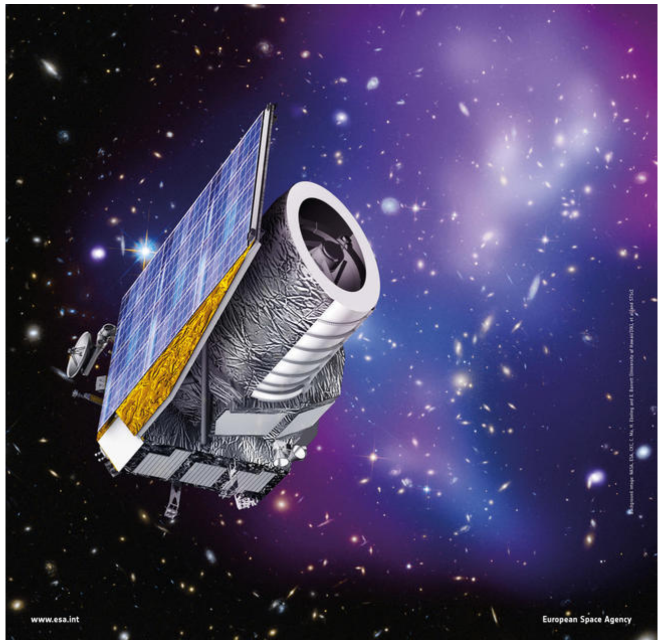

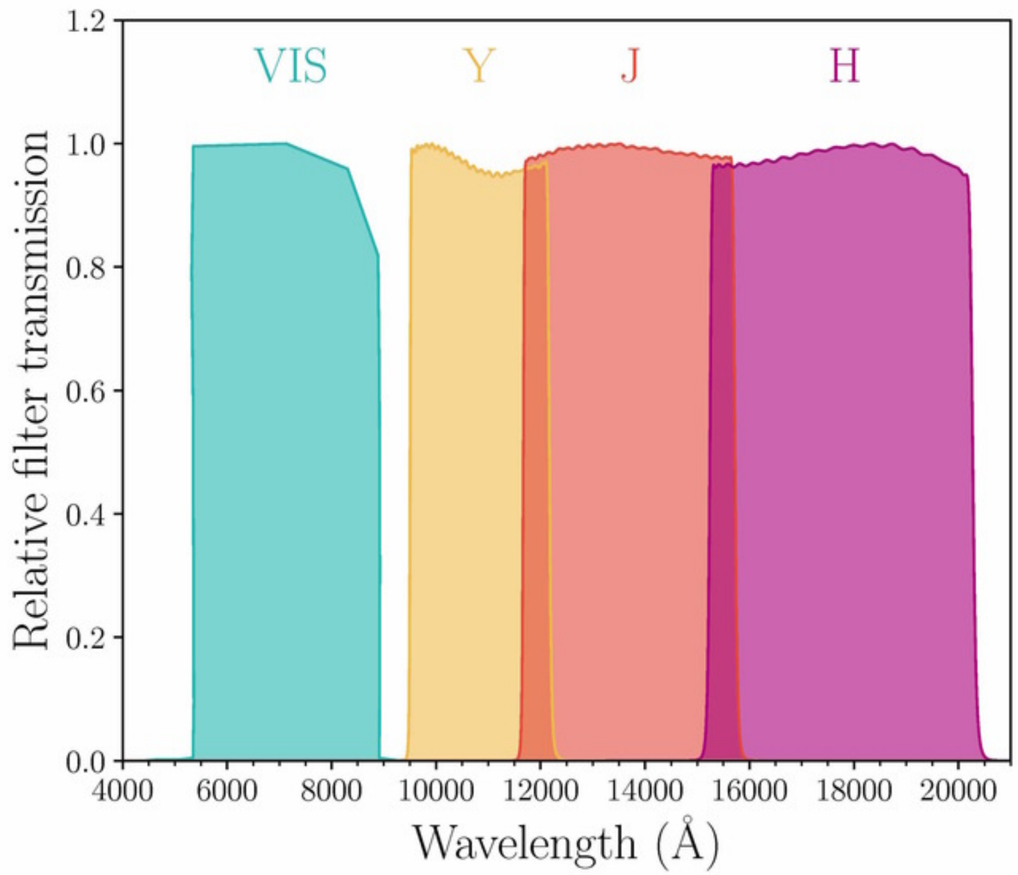

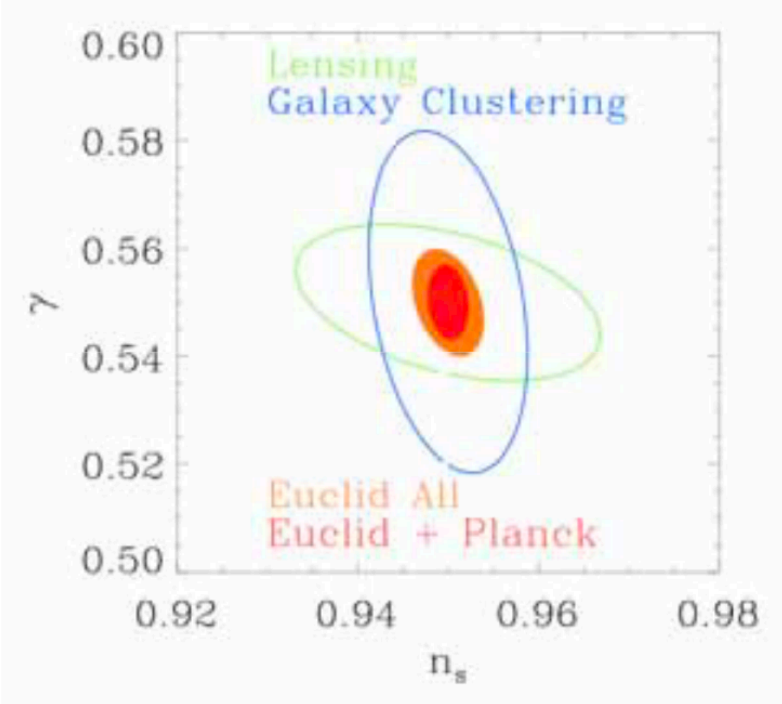

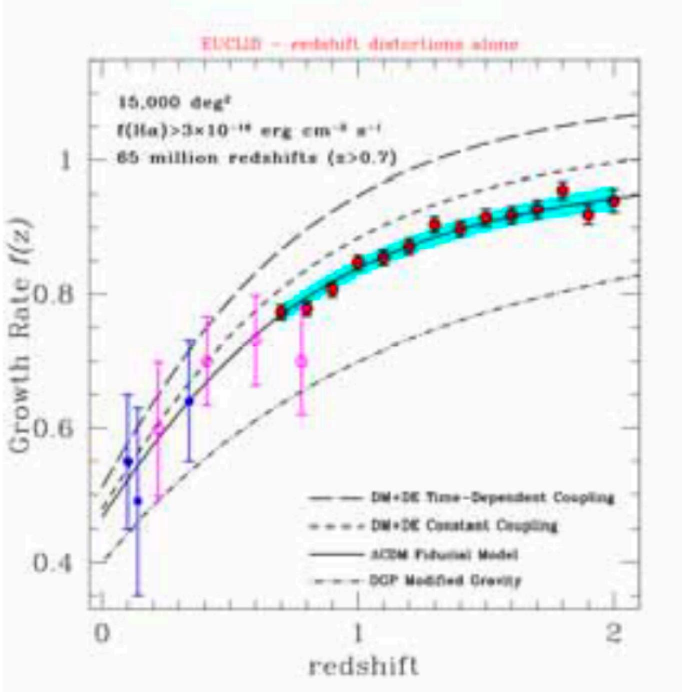

Latest results and anomalies

- Up to here we have shown the most relevant probes establishing the ΛCDM model.

- But there are some problems regarding some of the observations.

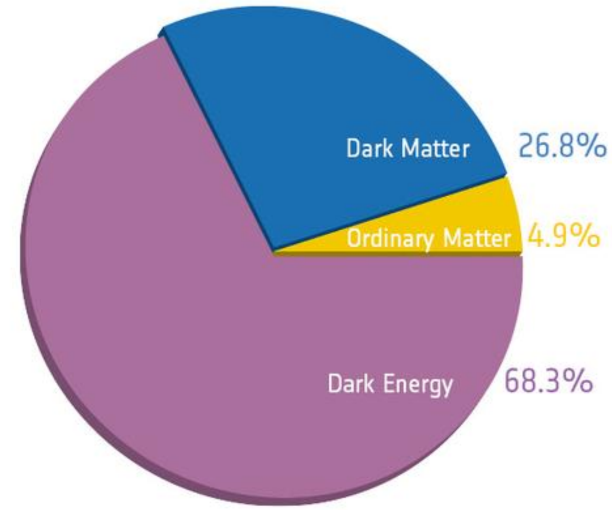

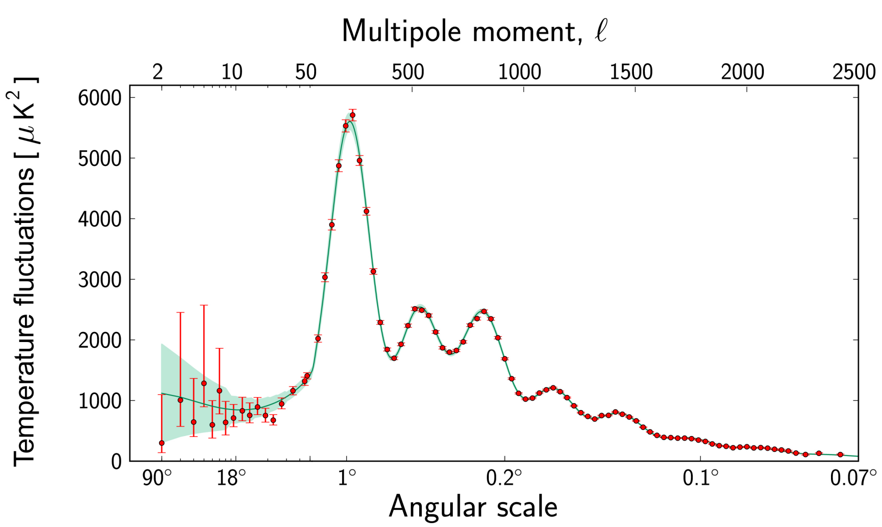

Planck Collaboration

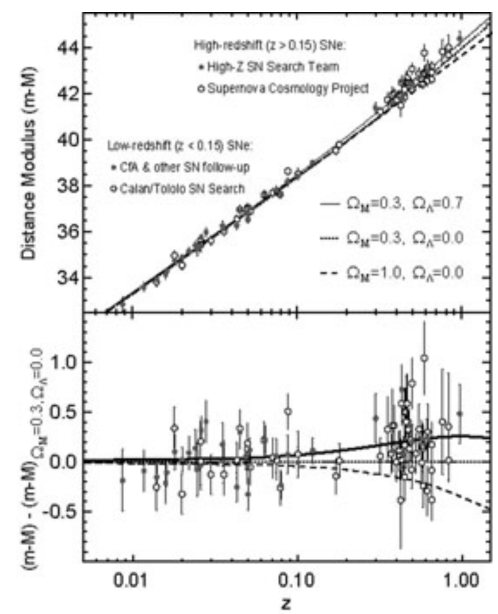

Riess et al., 1998, Perlmutter et al. 1999

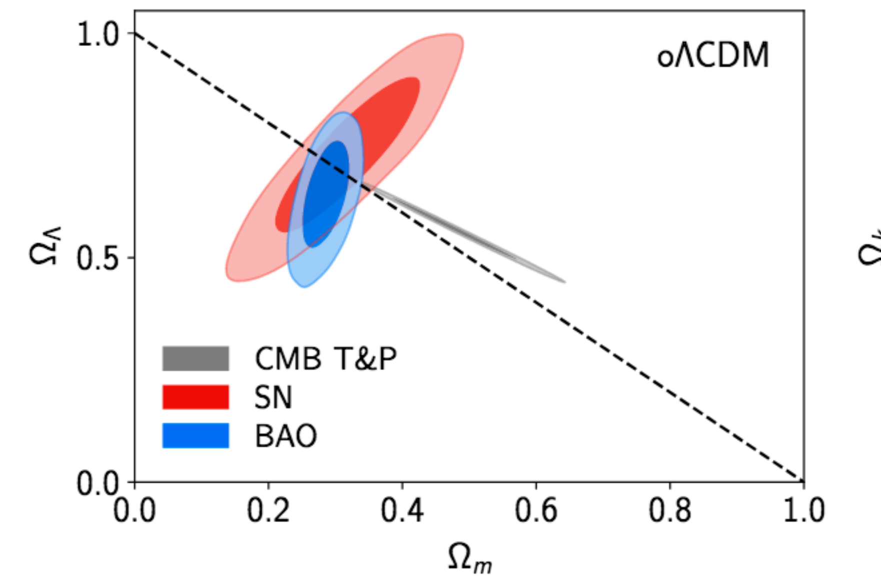

eBOSS Collaboration

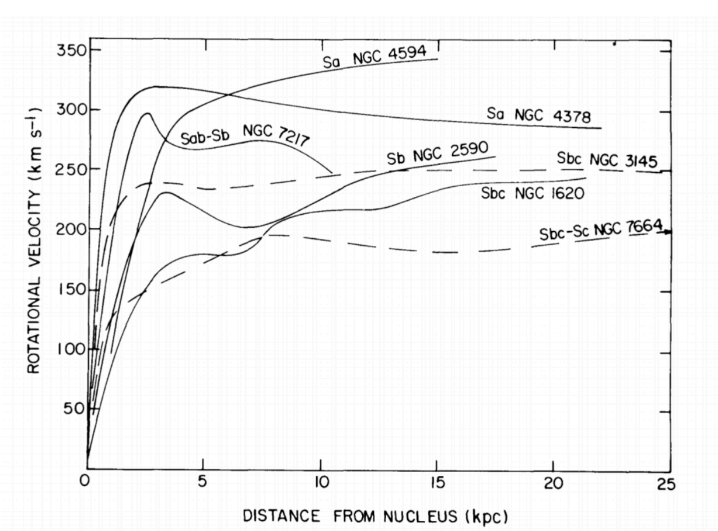

V. Rubin et al. 1978

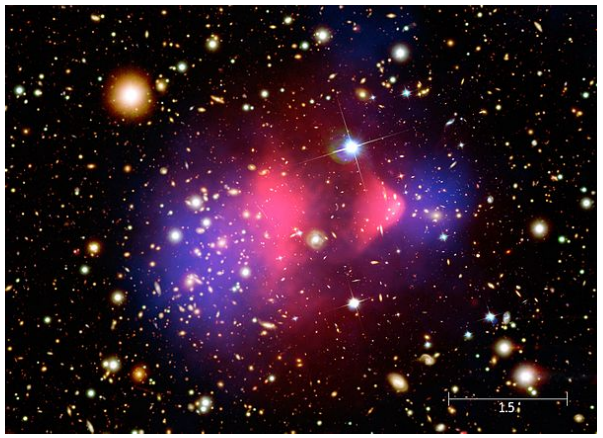

Bullet Cluster

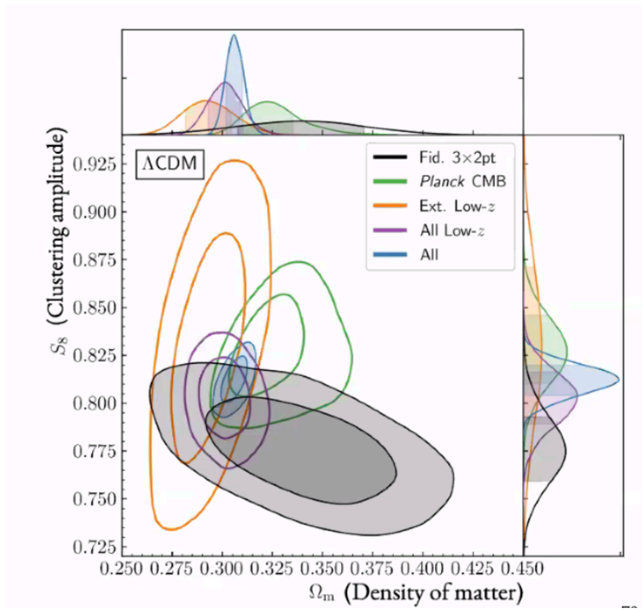

3x2pt (DES Collaboration 2021)

Latest results and anomalies

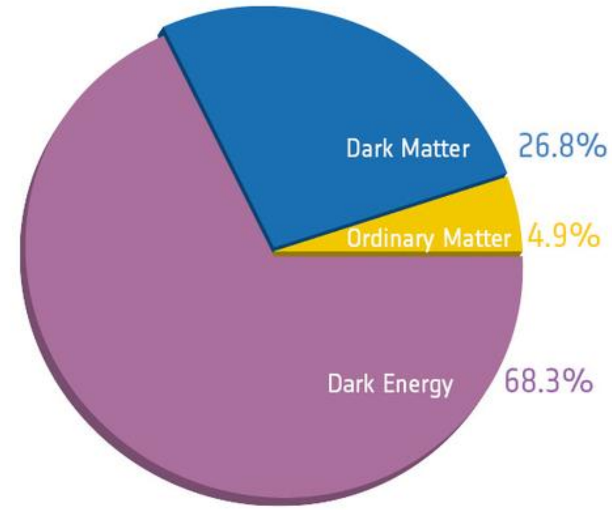

- Up to here we have shown the most relevant probes establishing the ΛCDM model.

- But there are some problems regarding some of the observations.

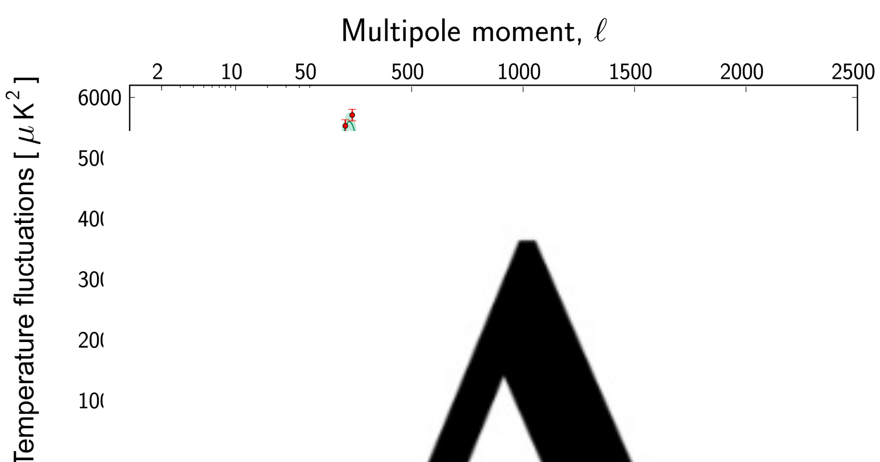

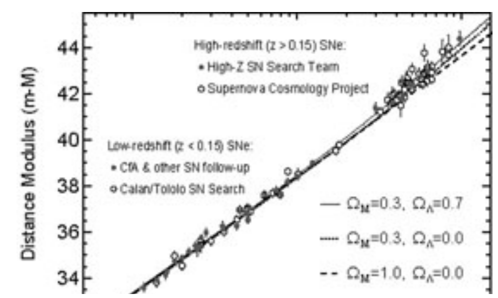

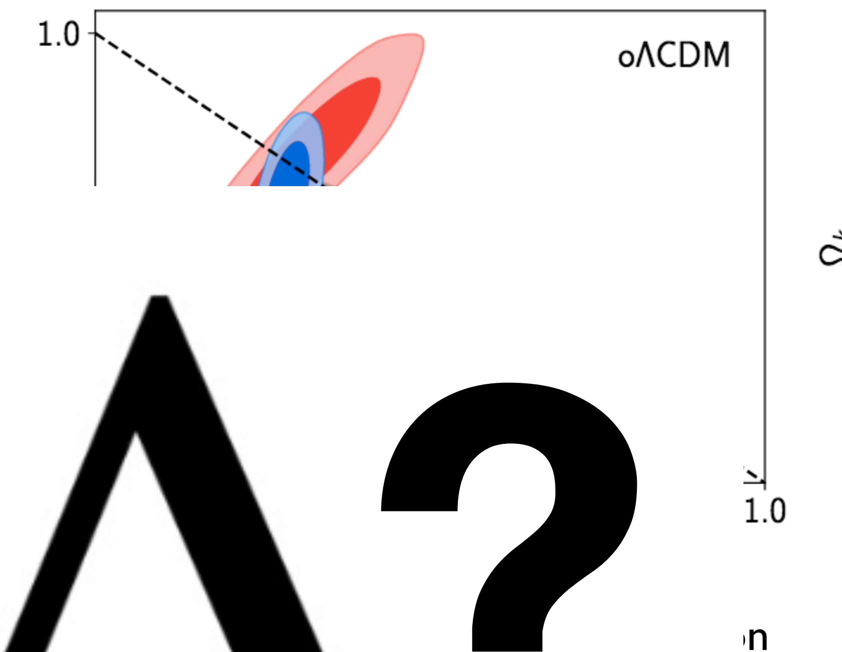

Λ or not Λ?

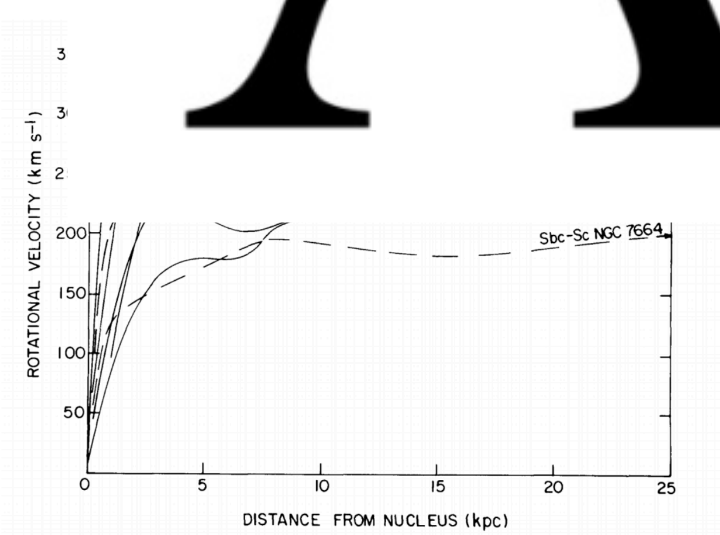

V. Rubin et al. 1978

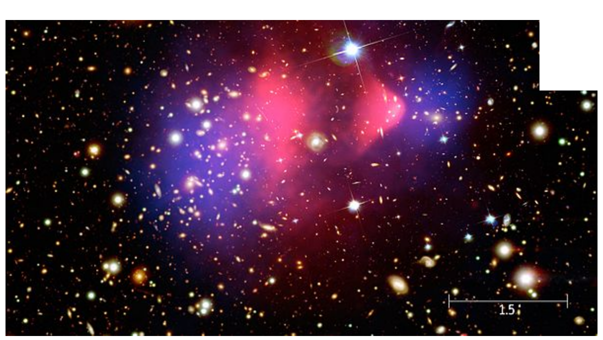

Bullet Cluster

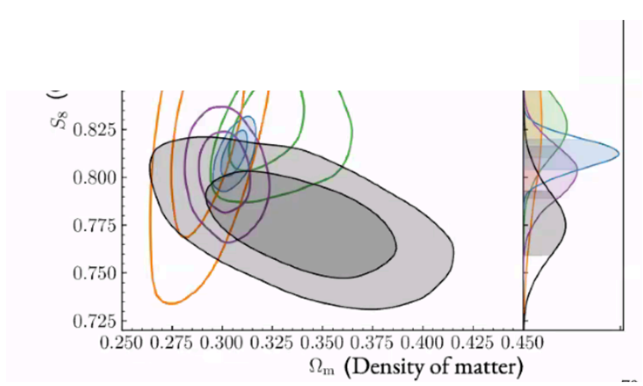

3x2pt (DES Collaboration 2021)

Latest results and anomalies

- Up to here we have shown the most relevant probes establishing the ΛCDM model.

- But there are some problems regarding some of the observations.

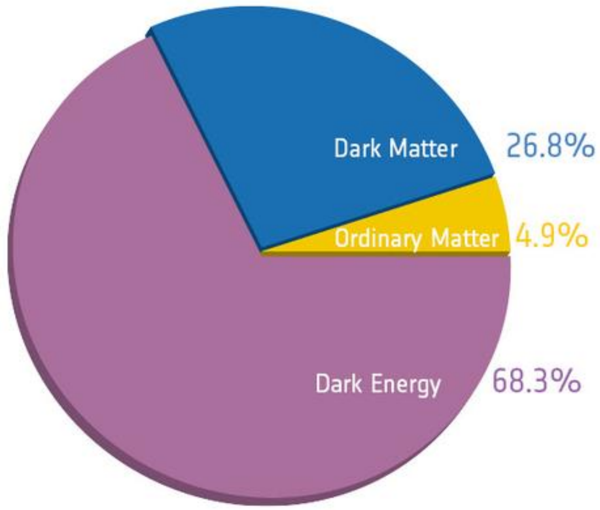

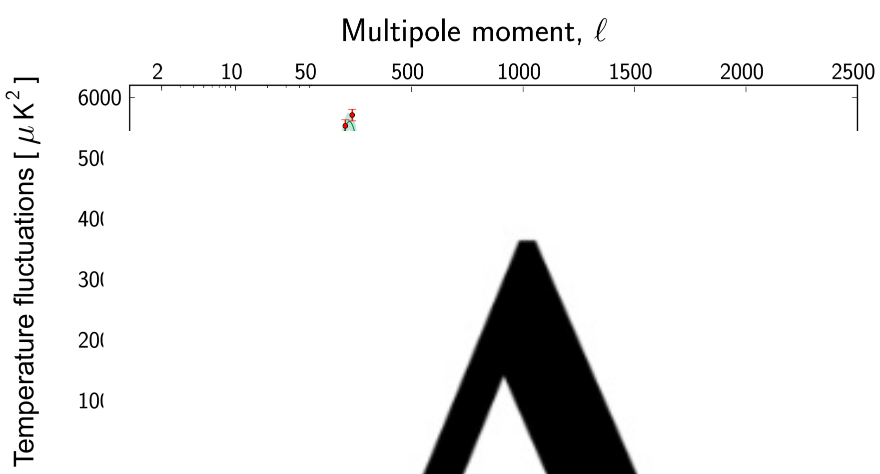

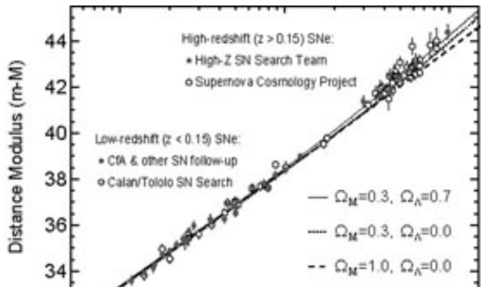

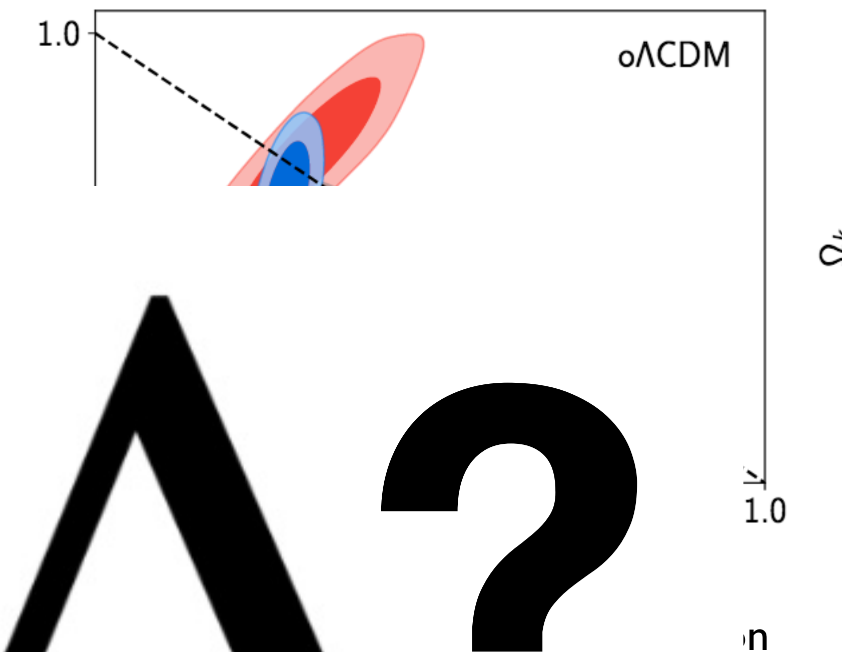

Λ or not Λ?

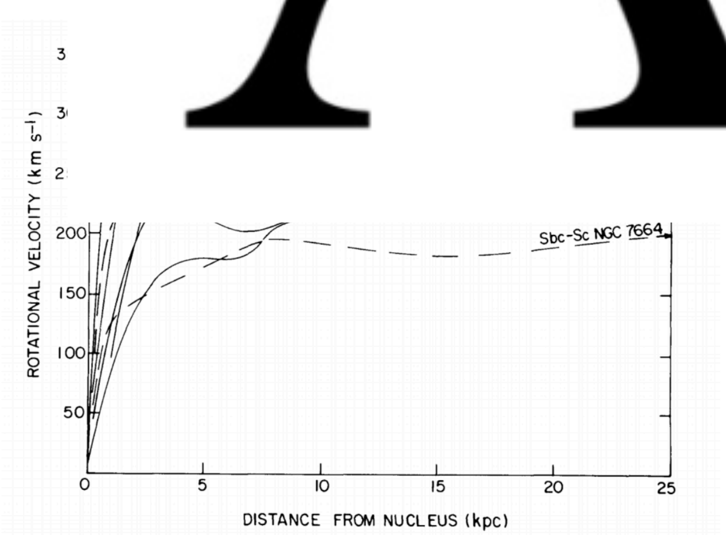

V. Rubin et al. 1978

Bullet Cluster

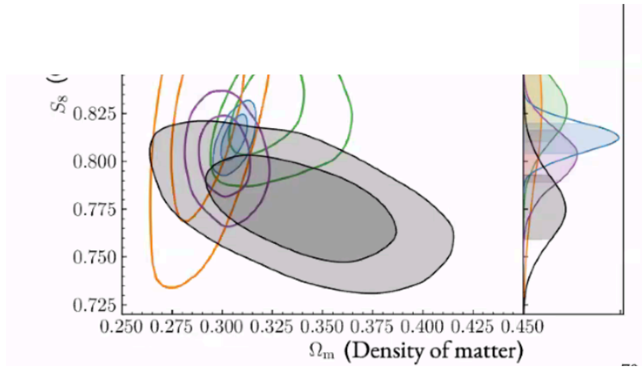

3x2pt (DES Collaboration 2021)

Dark Energy Spectroscopic Instrument (DESI)

DESI survey (2019 -) (@ 4m Mayall telescope, Kitt Peak Observatory, Arizona, USA):

- 5000 fibre multi-object
- Footprint of 14000 sq. degs:
  - 35 million ELGs
  - 4 million LRGs
  - 2.4 million QSOs

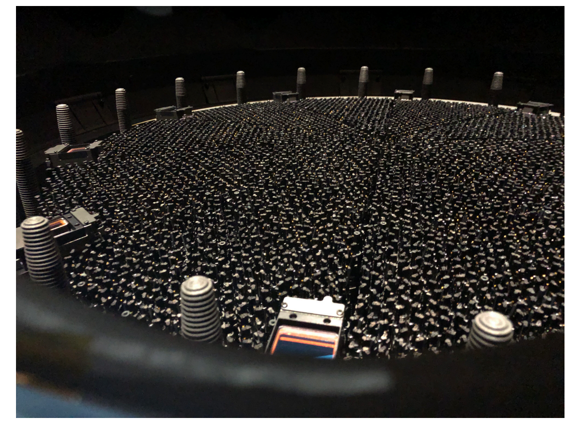

Credit: R. Lafever

Will produce the most precise BAO and RSD measurements up to date

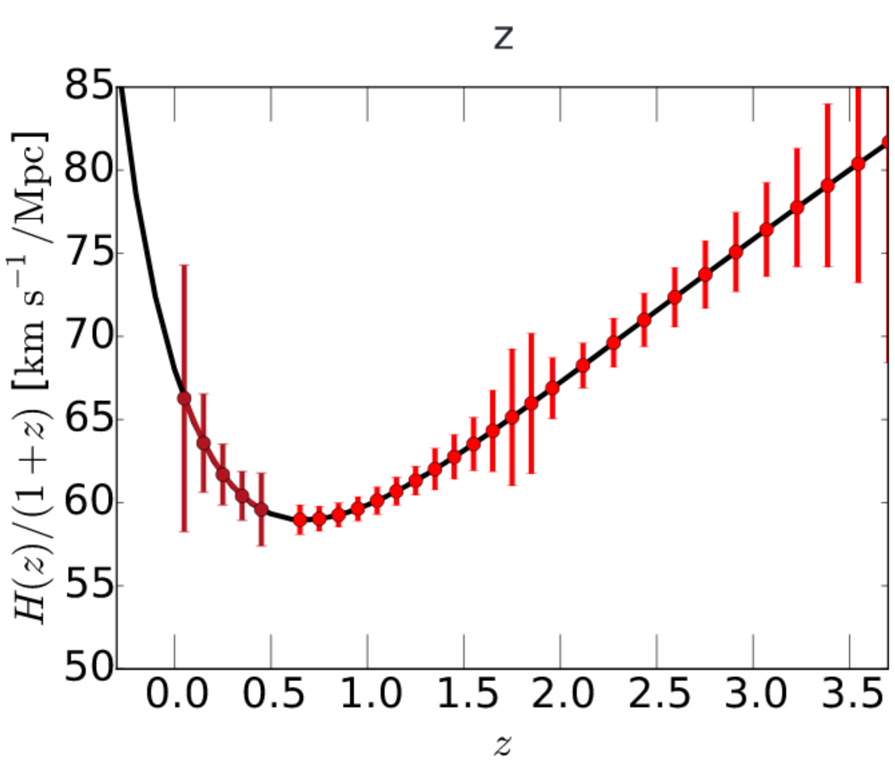

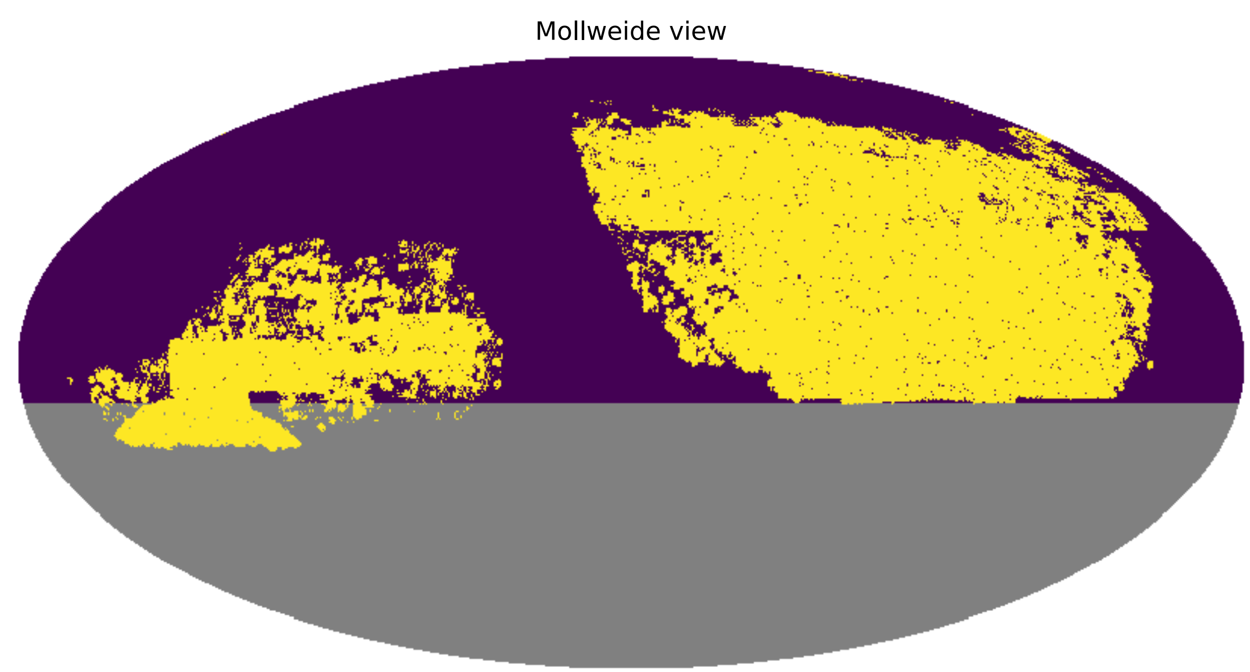

DESI Cosmological results

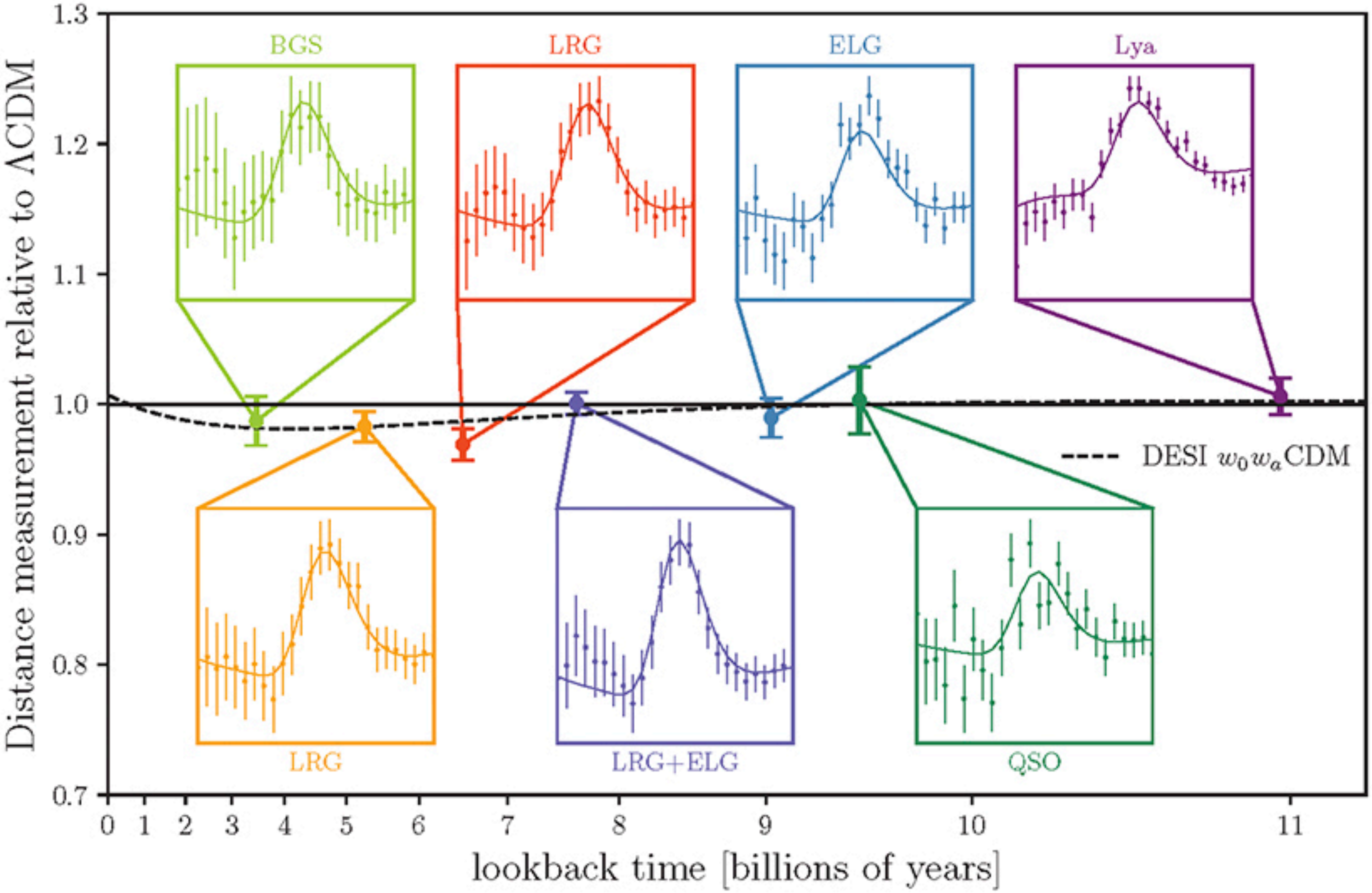

Dark Energy Survey Collaboration, 2024

DESI Cosmological results (LCDM)

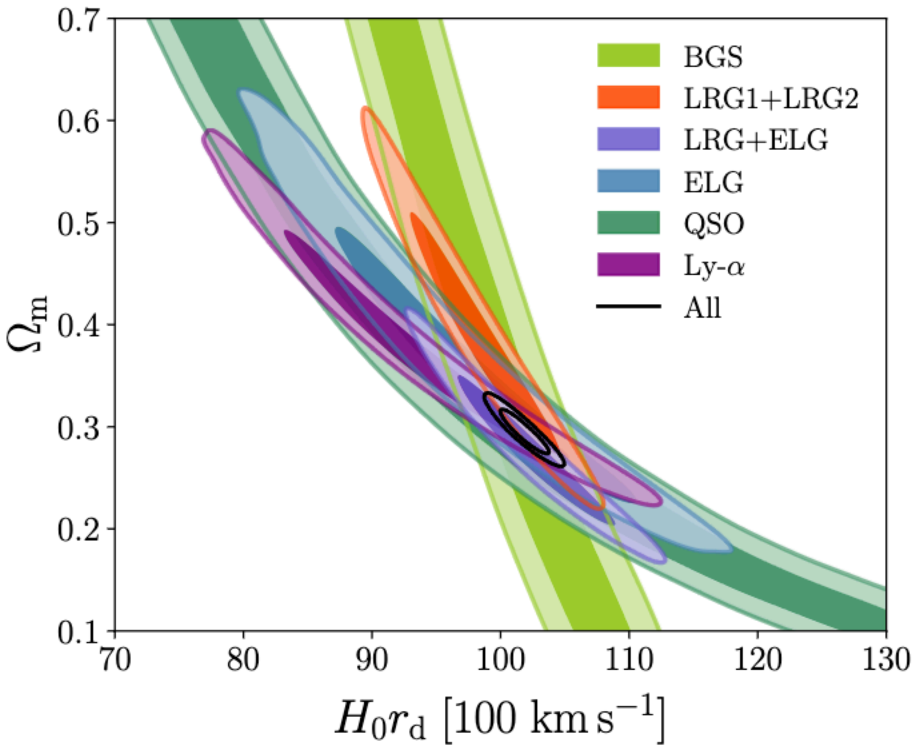

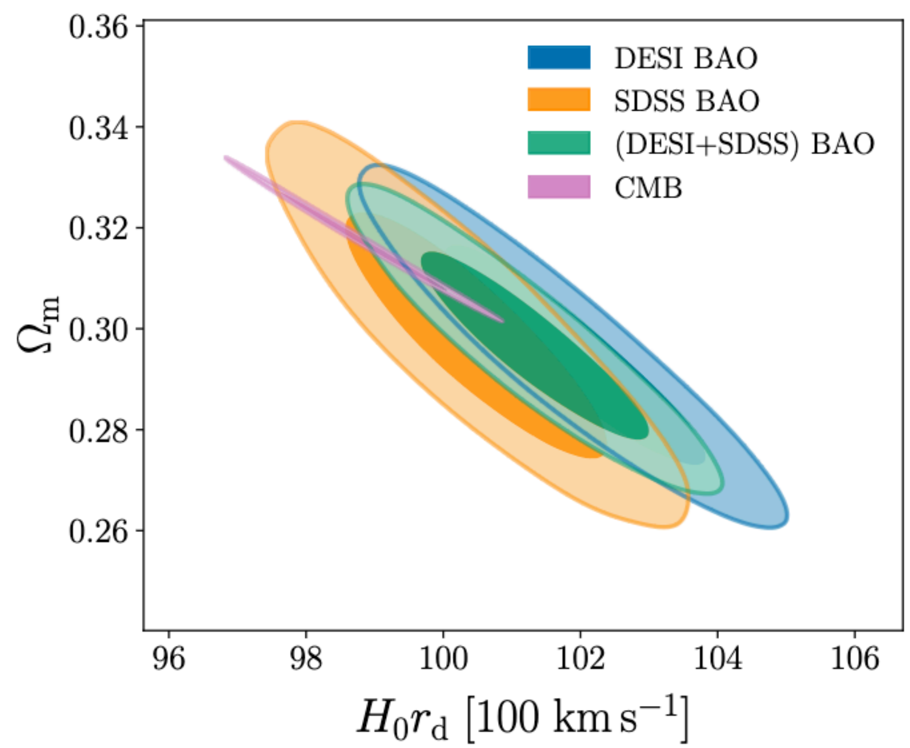

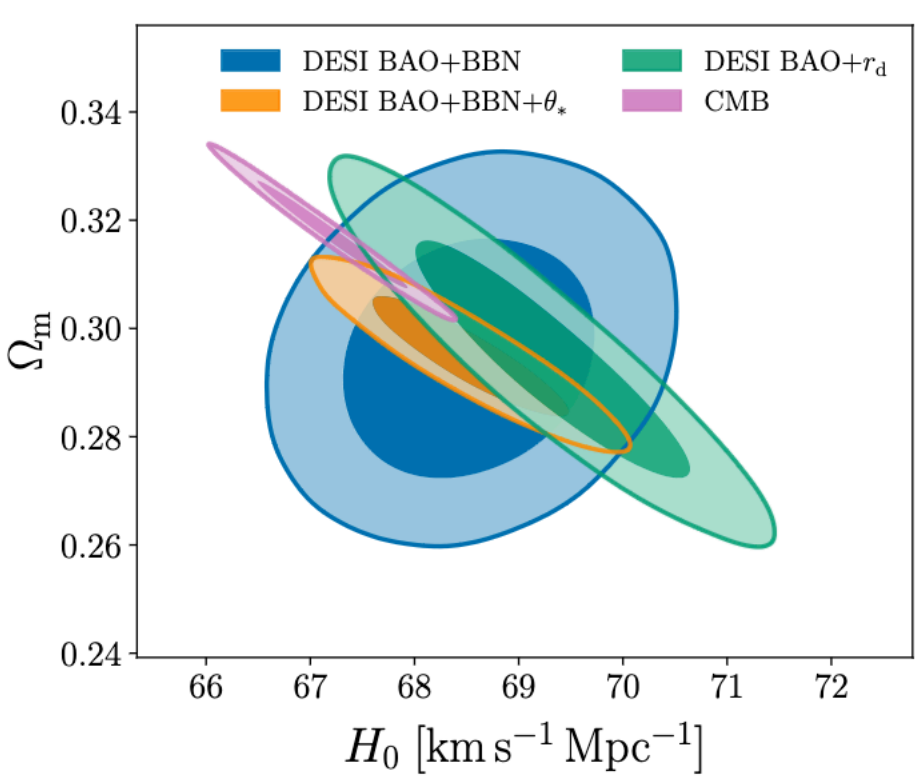

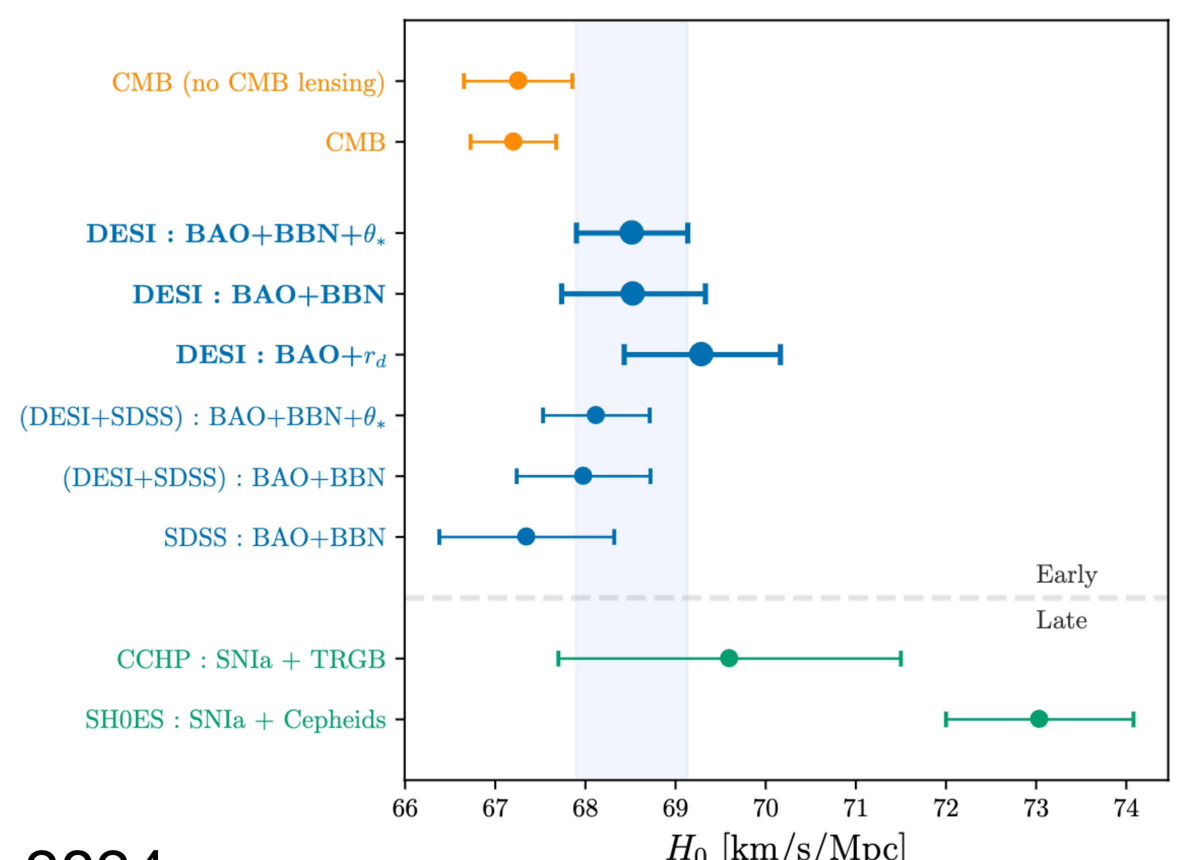

Dark Energy Survey Collaboration, 2024

DESI Cosmological results (wCDM)

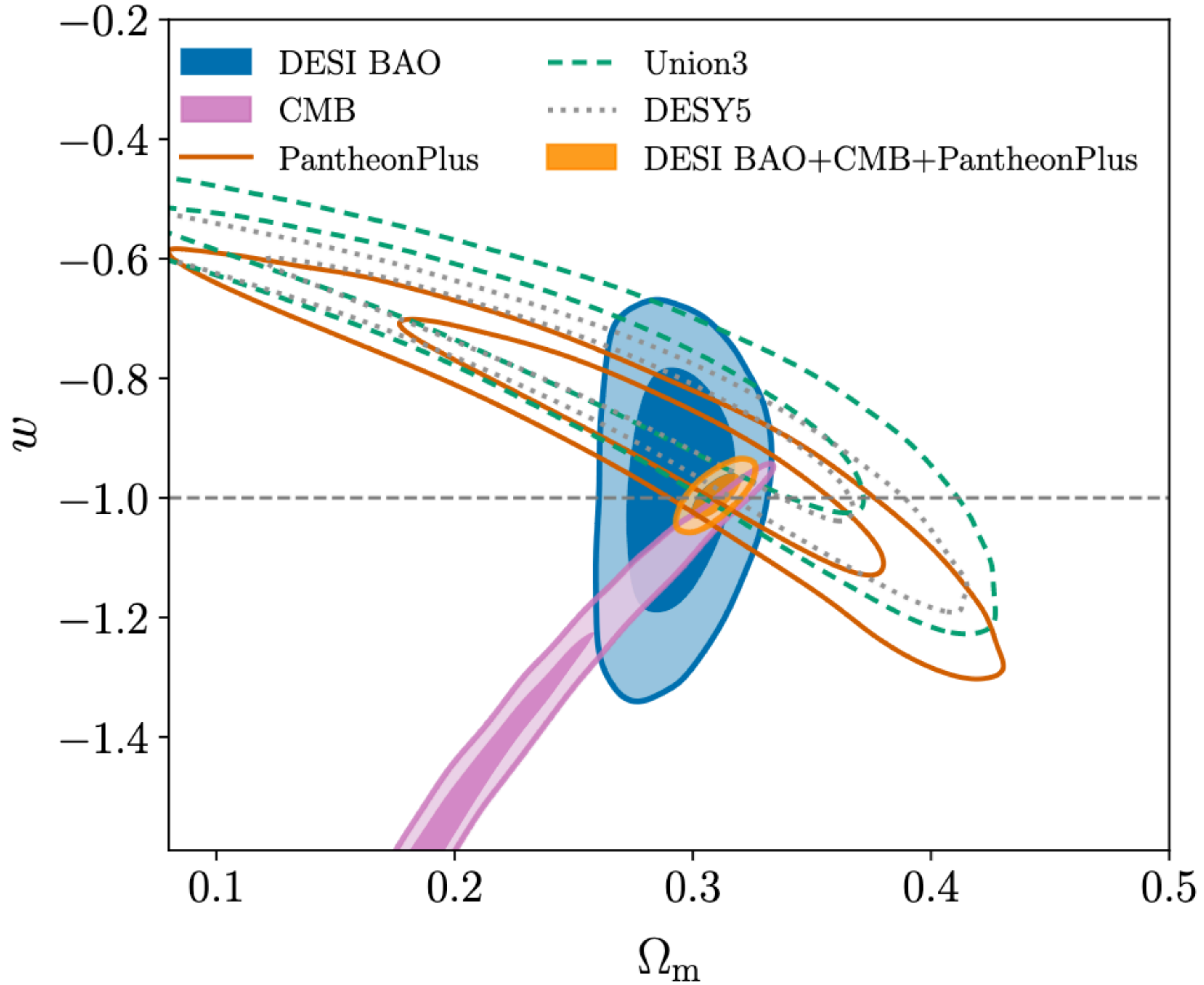

Dark Energy Survey Collaboration, 2024

DESI Cosmological results ($w_0 w_a$CDM) [time varying DE]

DE equation of state parametrisation:

$$w = w_0 + w_a(1 - a)$$

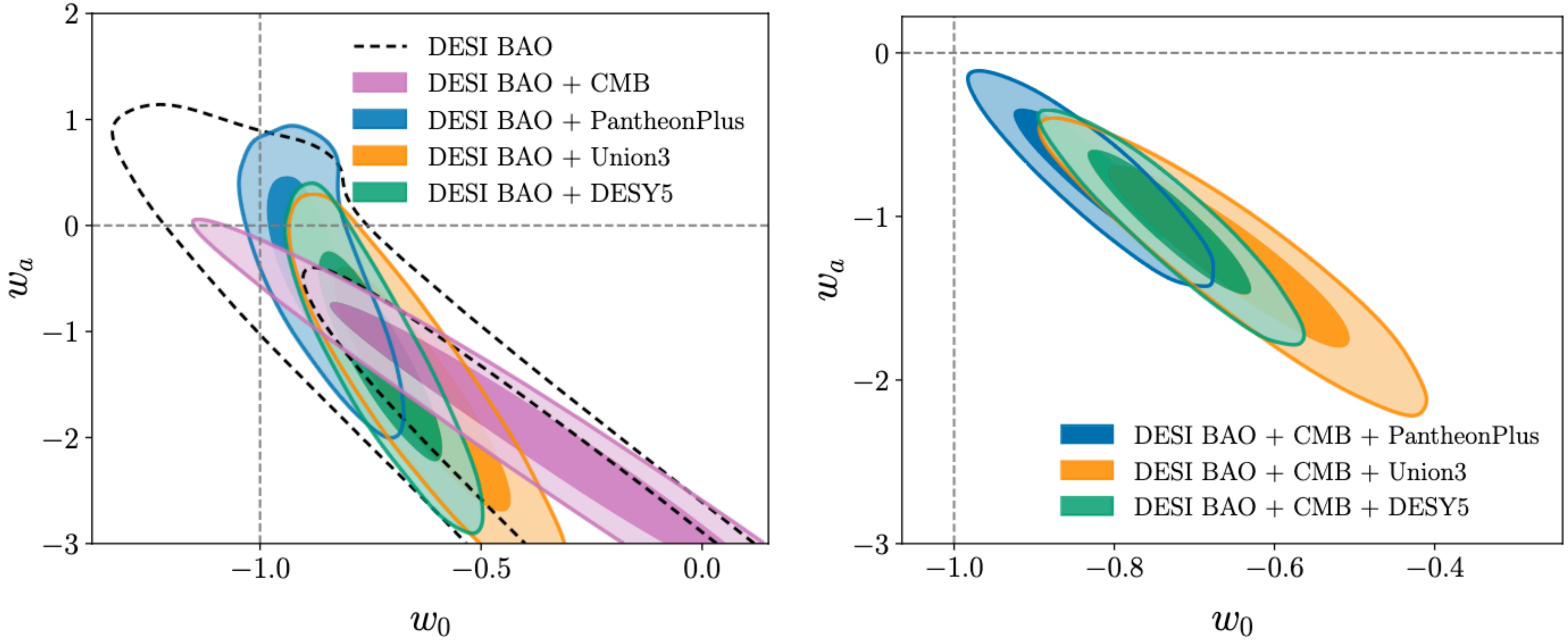

Dark Energy Survey Collaboration, 2024

Cosmic dipole

There are contradictory measurements regarding the cosmic dipole from CMB and radio surveys (both in position and amplitude)

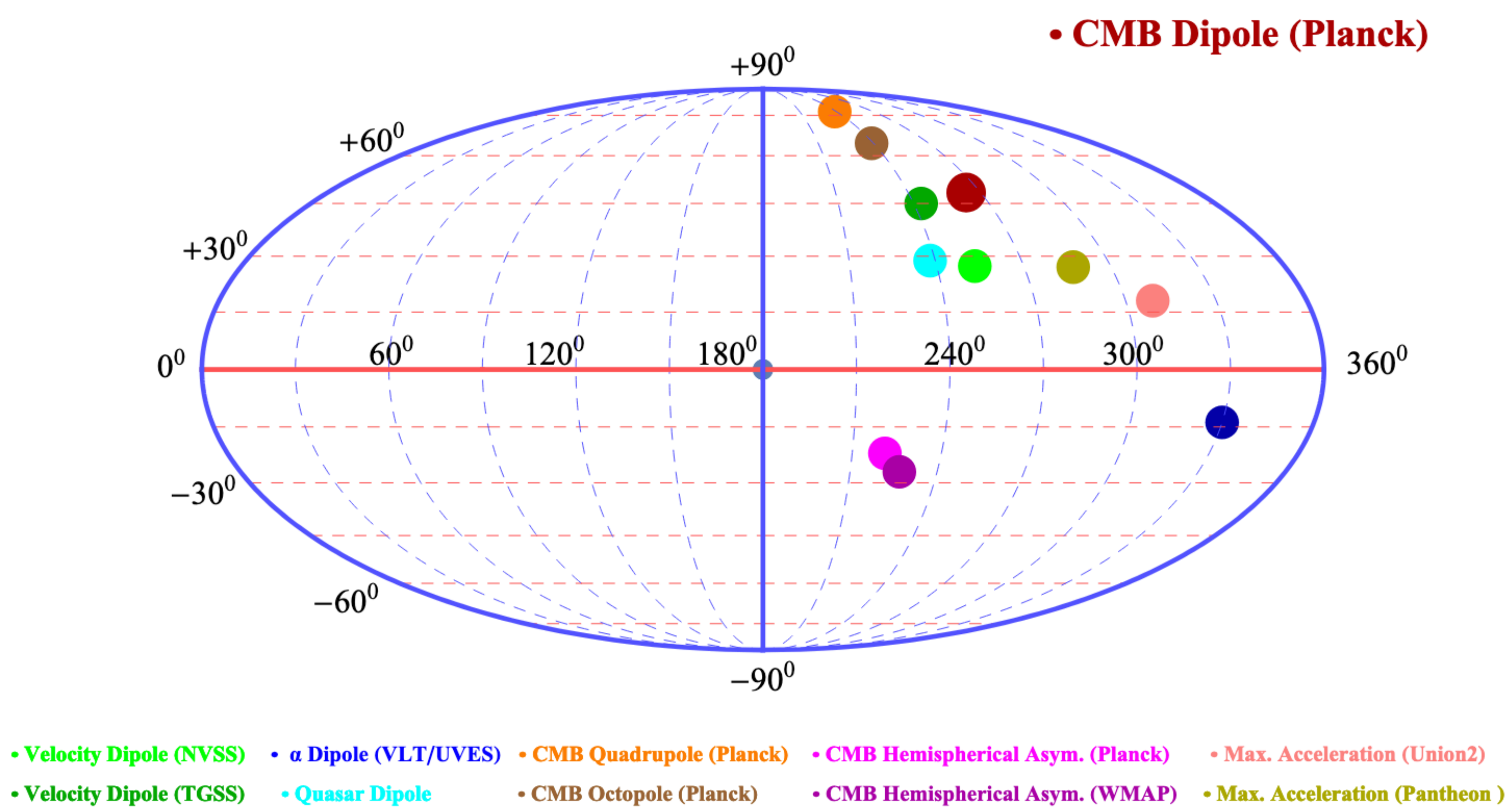

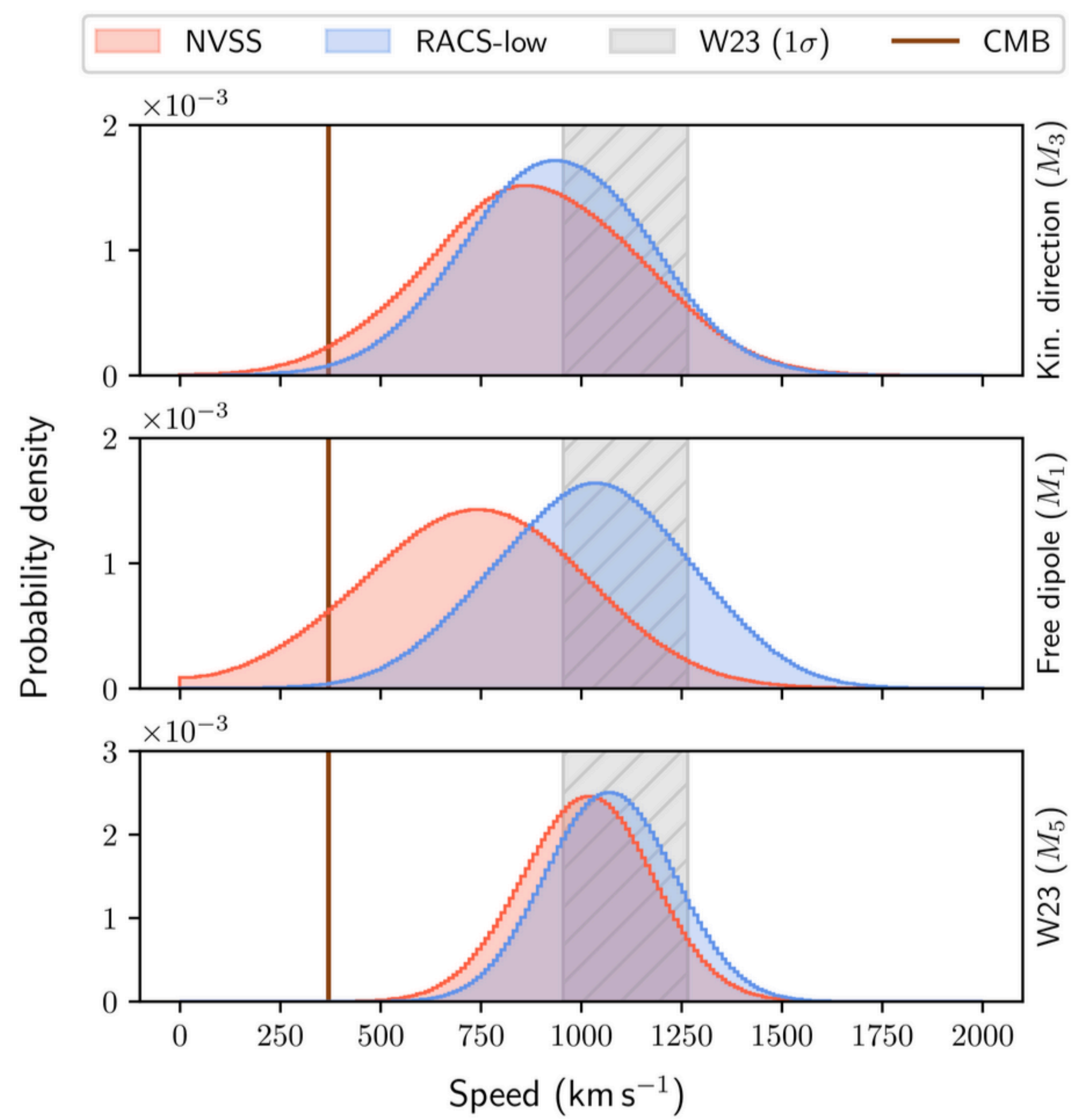

Perivolaropoulos & Skara 2022

Oayda et al. 2024

How to measure H_0 (with type Ia SN)

Most famous measurements are coming from cepheids and TRGB

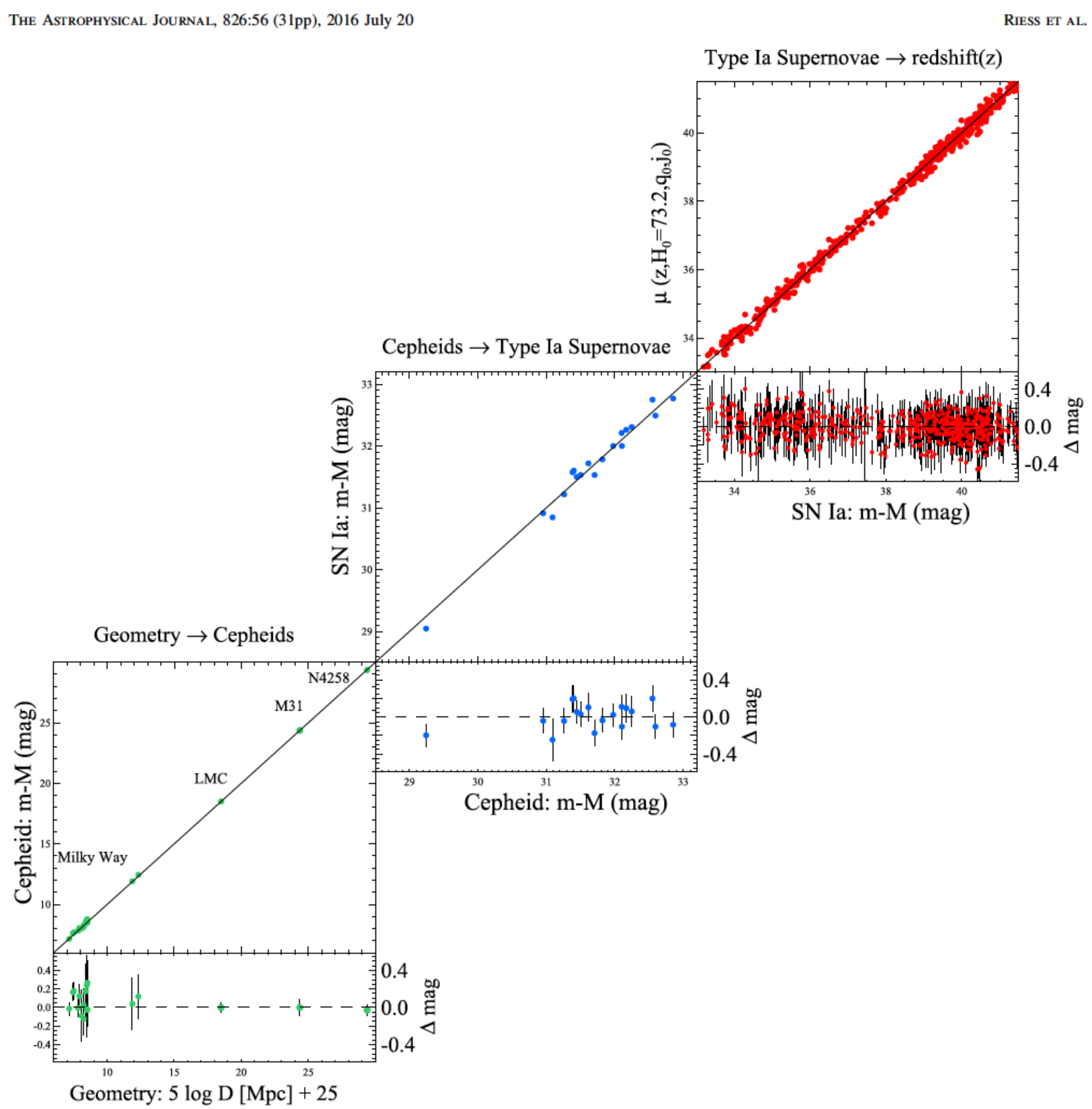

Figure 10. Complete distance ladder. The simultaneous agreement of pairs of geometric and Cepheid-based distances (lower left), Cepheid and SN Ia-based distances (middle panel) and SN and redshift-based distances provides the measurement of the Hubble constant. For each step, geometric or calibrated distances on the *x*-axis serve to calibrate a relative distance indicator on the *y*-axis through the determination of *M* or H_0. Results shown are an approximation to the global fit as discussed in the text.

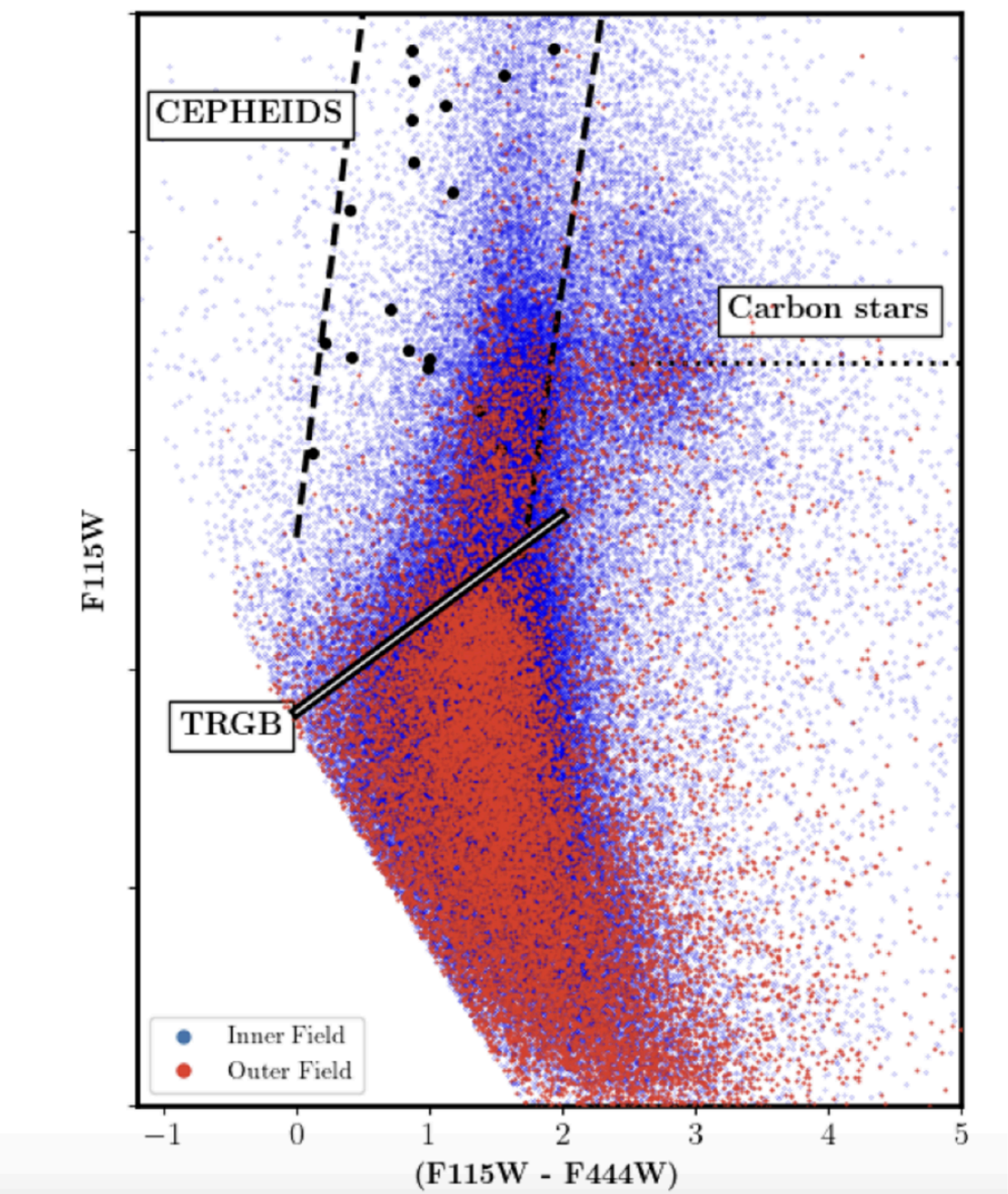

A. Riess 2016

W. Freedman et al. 2024

How to measure H_0 (with CMB)

1) Measure the angular scale of the acoustic wages: $\theta_s = \dfrac{r_s}{d_A(z_*)}$

2) Determine the drag scale at z_* from the parameters inferred from the peaks of the CMB:
$$r_s = \int_{z_*}^{\infty} \frac{c_s^2(\omega_b, \omega_\gamma)}{\sqrt{(w_b + w_c)(1+z)^3 + w_r(1+z)^4}}$$

3) Get $d_A(z_*)$ and get the remaining part from $d_A(z_*) = \displaystyle\int_0^{z_*} \frac{cdz}{\sqrt{w_\Lambda + w_m(1+z)^3 + w_r(1+z)^4}}$

4) Finally $H(z=0) = H_0$

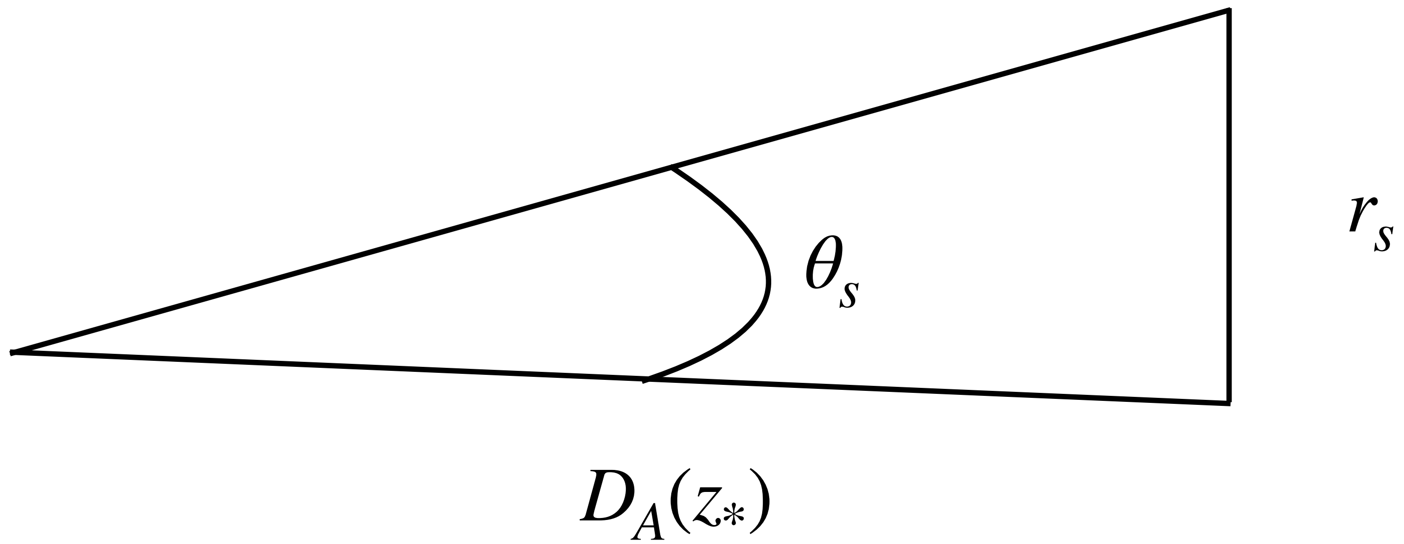

How to measure H_0 (with strong lenses)

We can measure the Hubble constant using the time delay between images of strong lensing. We can define the Fermat potential that depends on the projected potential of the lens.

$$\tau(\vec{\theta};\vec{\beta}) = \frac{1}{2}(\vec{\theta}-\vec{\beta})^2 - \psi(\vec{\theta})$$

Then, the time delay depends on the difference of the Fermat potentials and the Hubble constant. This method depends strongly on the mass modelling of the lease.

$$\begin{aligned} \Delta t &= \frac{D_d^{ang} D_s^{ang}}{c D_{ds}^{ang}}(1+z_d)\left[\tau(\vec{\theta^1;}\beta) - \tau(\vec{\theta^2;}\beta)\right] \\ &= \frac{D_d D_s}{c D_{ds}}\left[\tau(\vec{\theta^1;}\beta) - \tau(\vec{\theta^2;}\beta)\right] \end{aligned}$$

$\longrightarrow \Delta t \propto H_0^{-1}\Delta\tau$

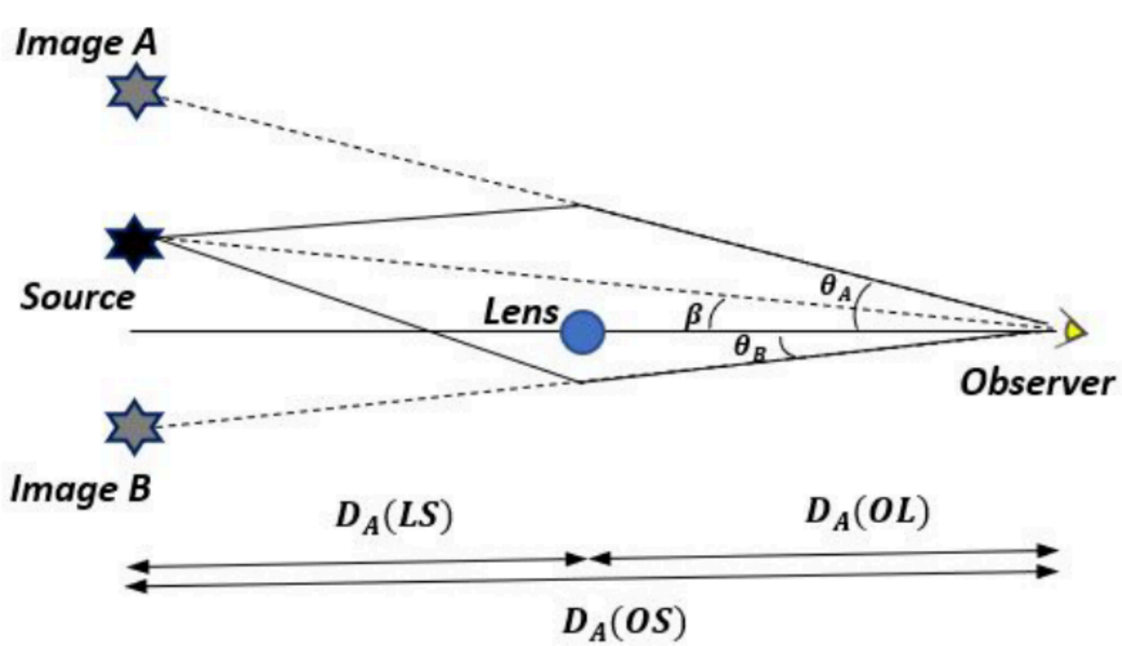

Perivolaropoulos & Skara 2022

How to measure H_0 (with GW)

With gravitational wave mergers we can estimate the distance to an object. If we have an electromagnetic counterpart, we have a bright siren (like the GW170817 kilonova) while some statistical methods using information from galaxy surveys can help us get some constraints (dark sirens)

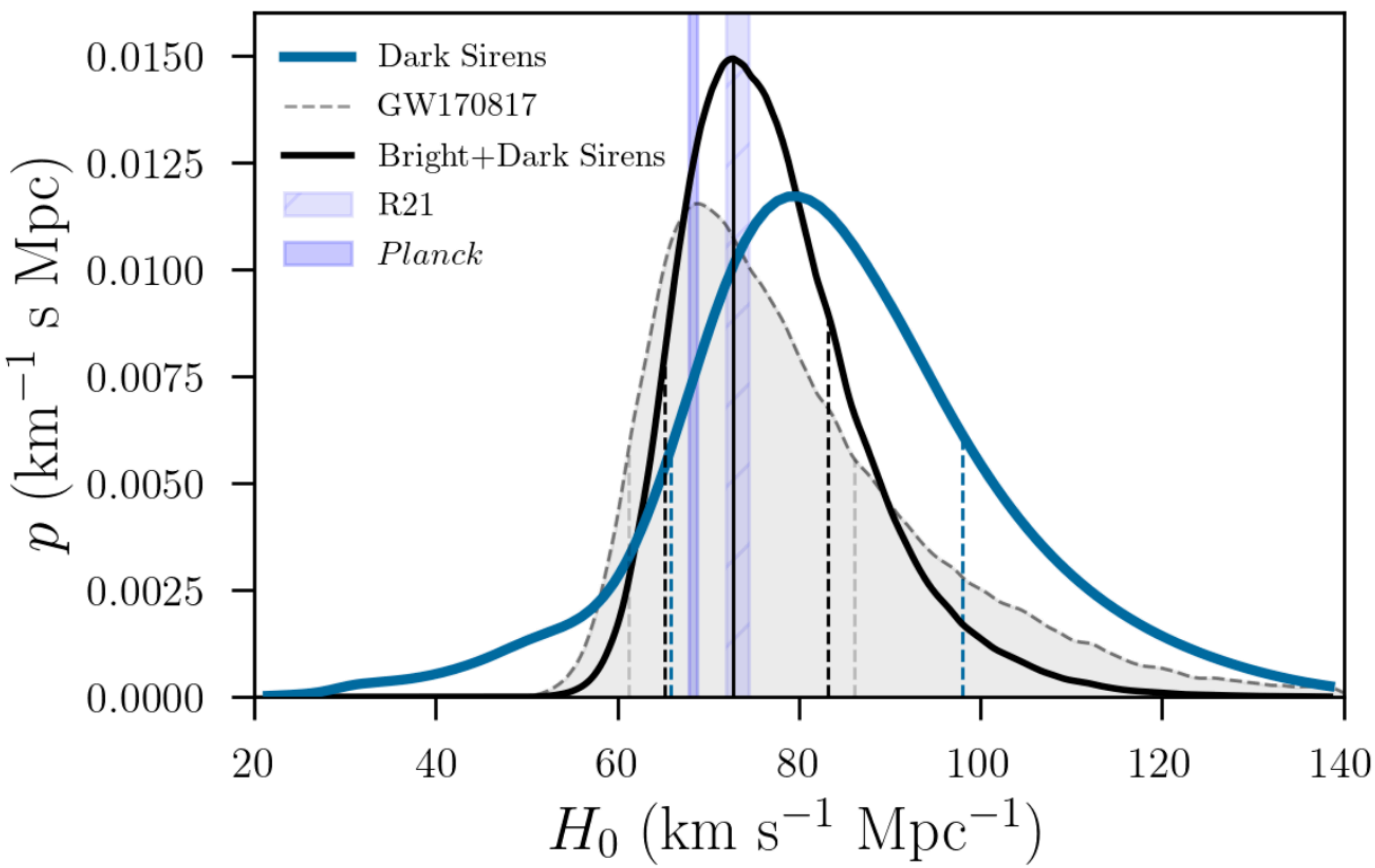

Palmese et al. 2022

H_0 tension

Tension between some measurements can reach the 6-σ level

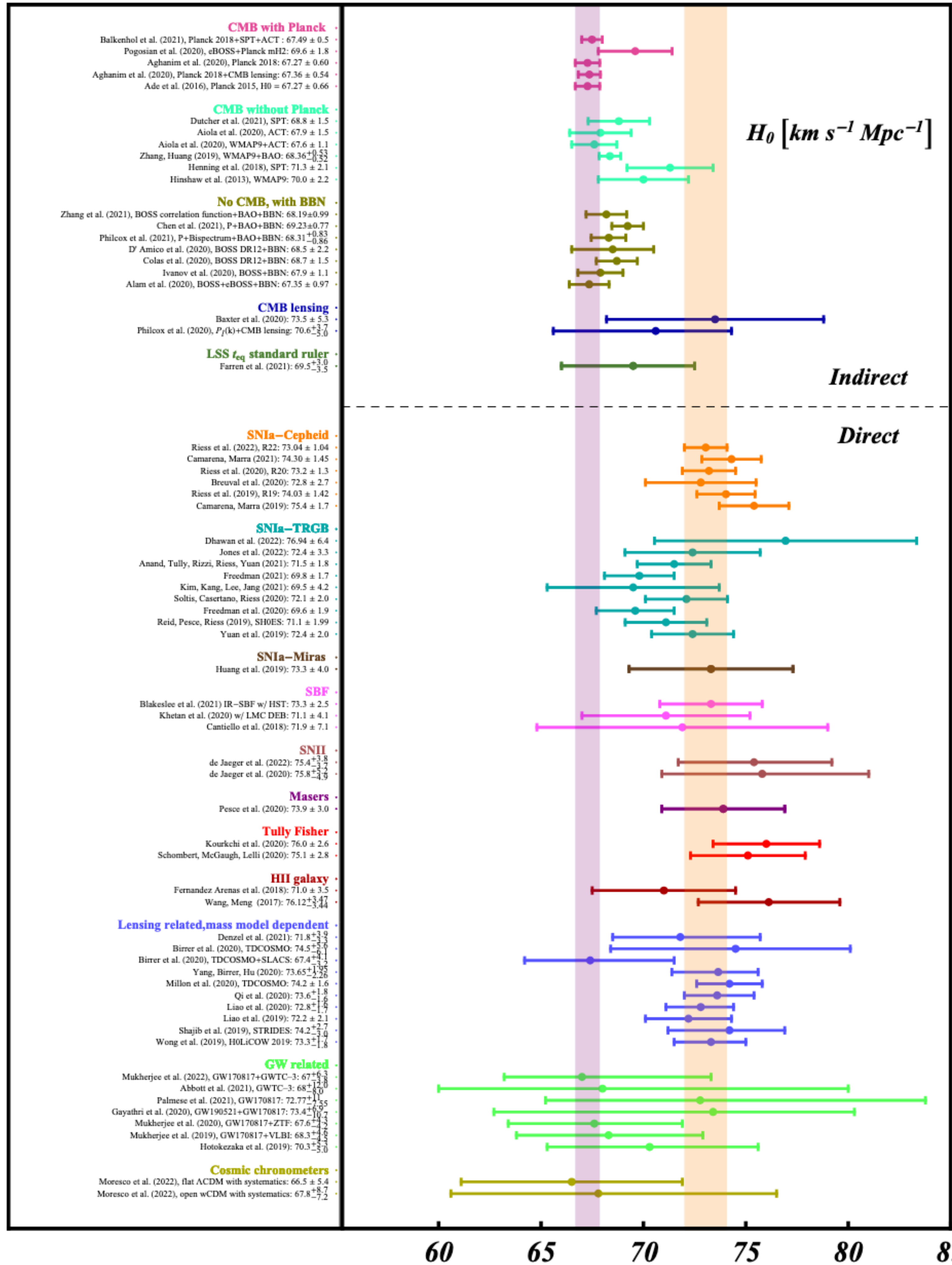

Snowmass (2022)

σ_8 tension

Another not that big tension arises from different measurements on the clustering amplitude.

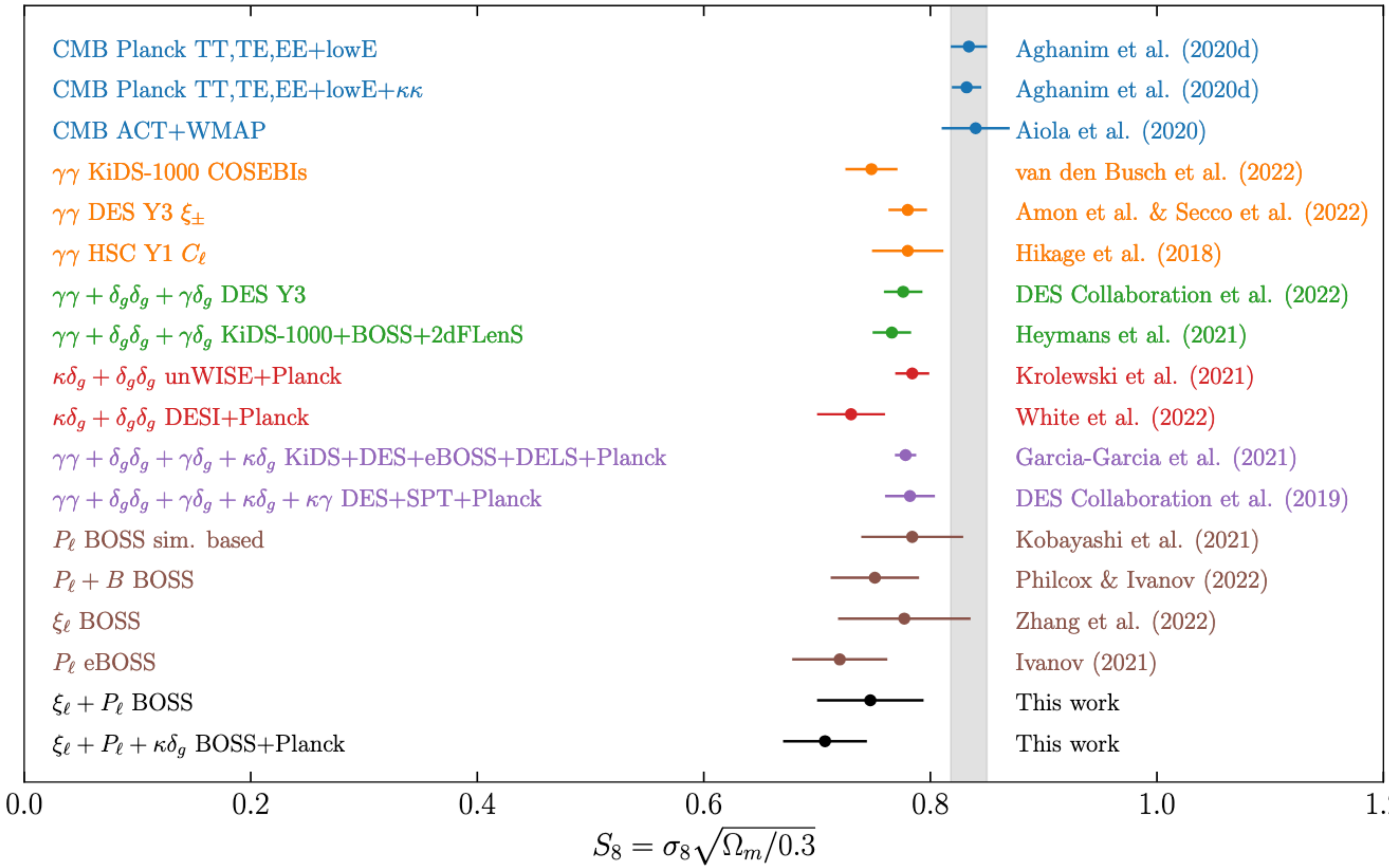

Chen et al. JCAP 2207 (2022)

New physics or systematics?

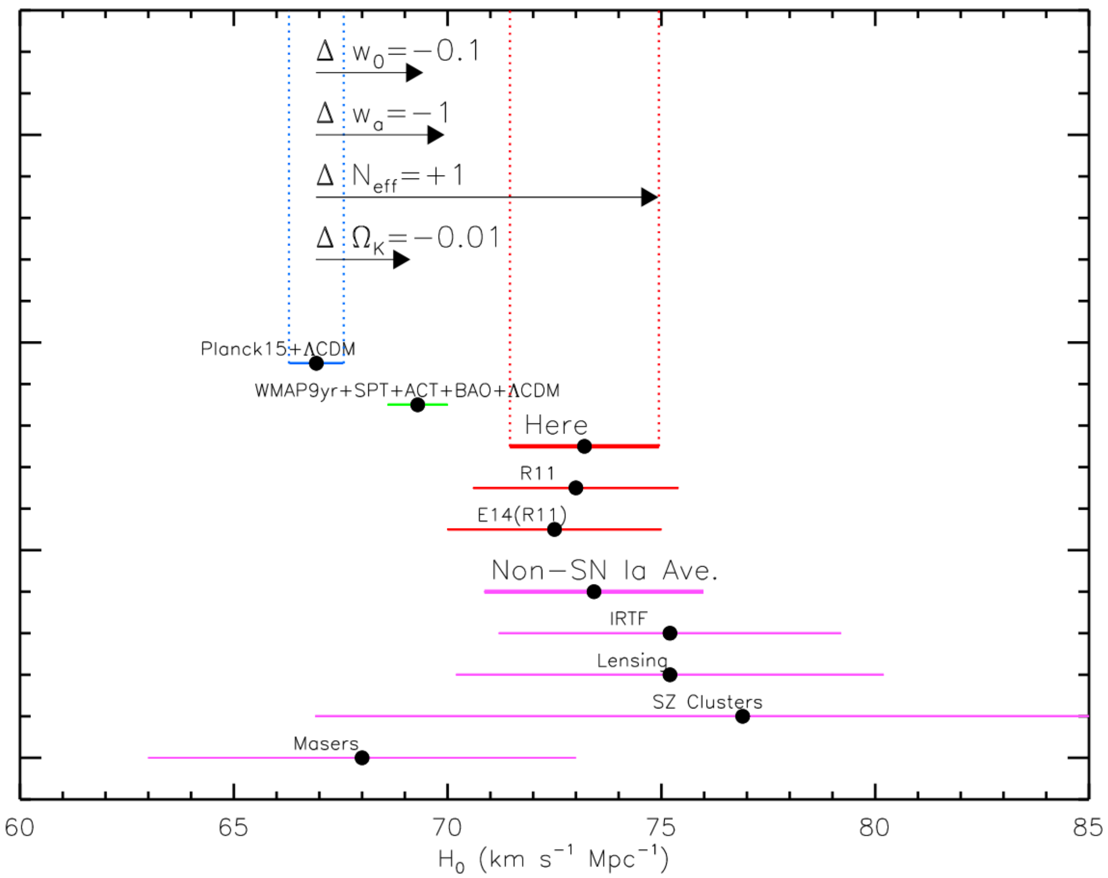

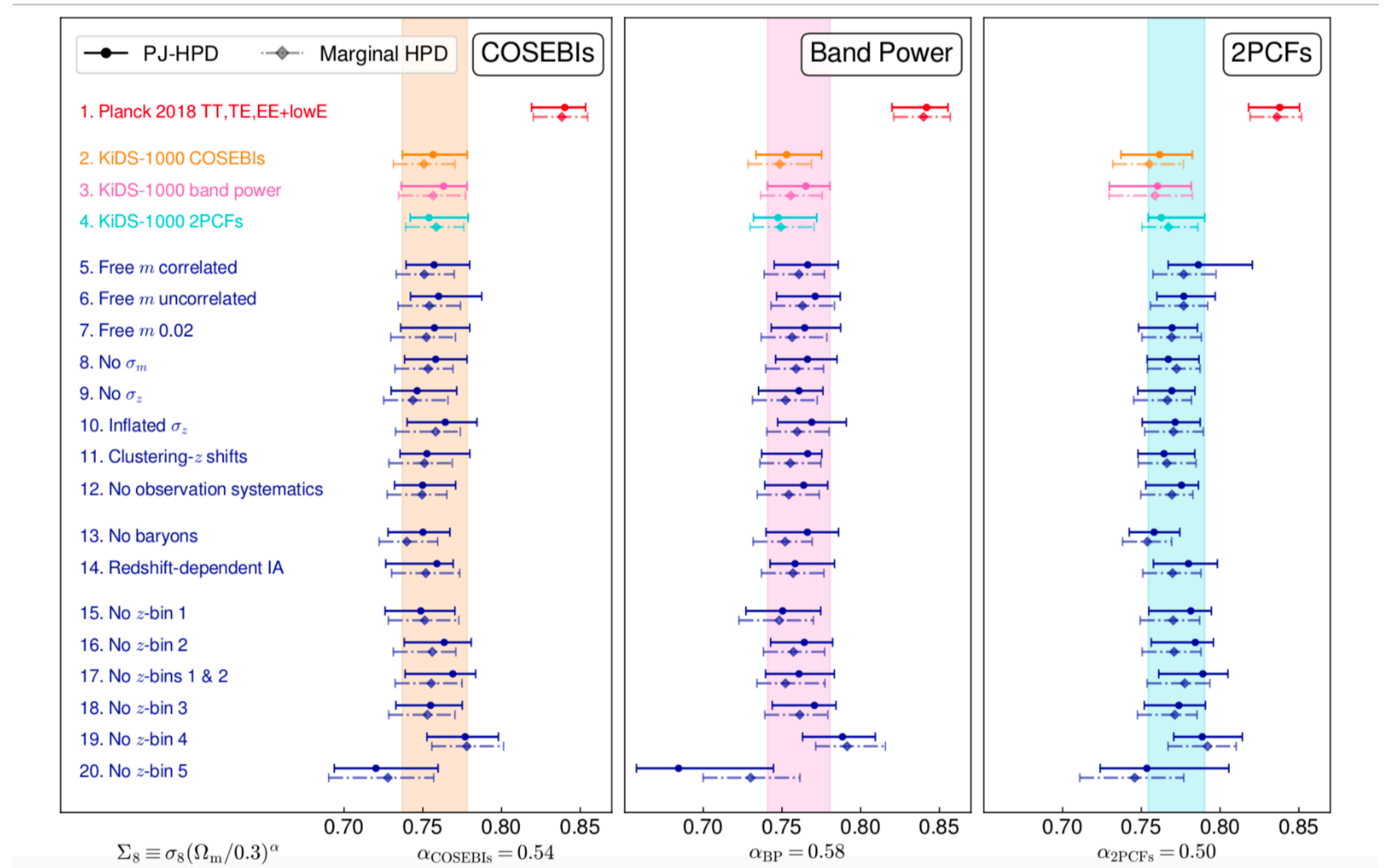

Riess et al. (2016)

Asgari et al. (2020)

Should we change the model?

Is this explained by systematics?

CMB lensing

- On top of the other effects, the temperature maps (and the polarisation of the CMB) are lensed by the matter in the path.
- This can be modelled by convolving the unlensed power spectrum with the lensing potential C_ℓ^ψ.

$$\tilde{C}_l^\Theta \approx (1 - l^2 R^\psi) C_l^\Theta + \int \frac{d^2\mathbf{l}'}{(2\pi)^2} \left[\mathbf{l}' \cdot (\mathbf{l} - \mathbf{l}')\right]^2 C^\psi_{|\mathbf{l}-\mathbf{l}'|} C^\Theta_{l'}.$$

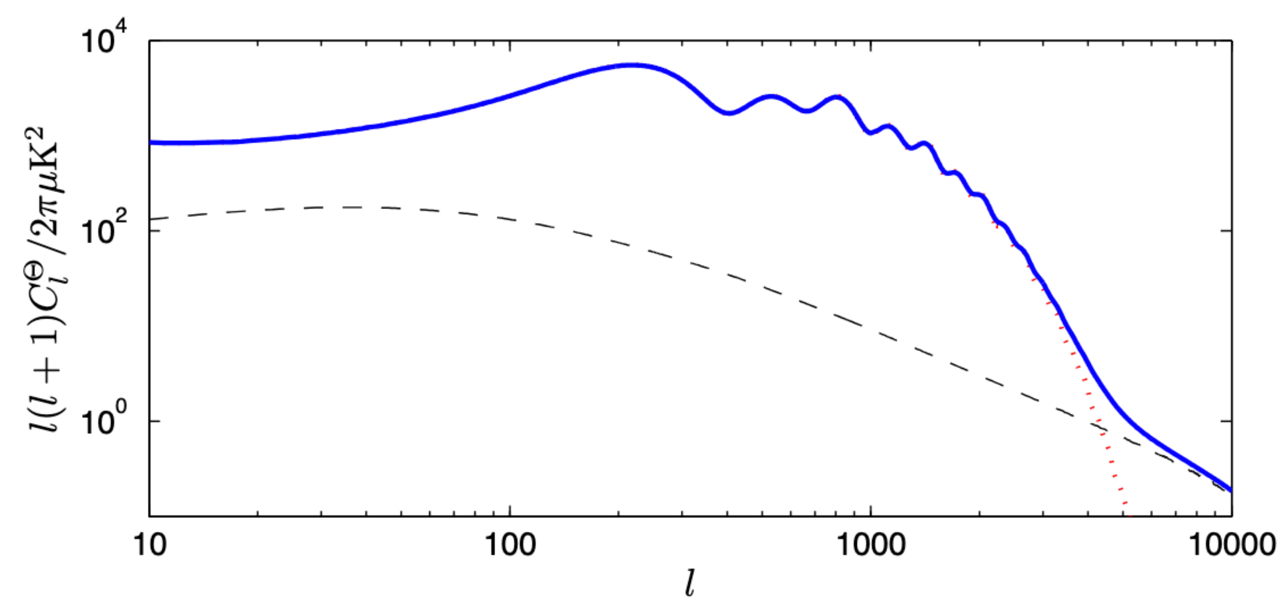

- The effect is mostly smoothing the acoustic peaks

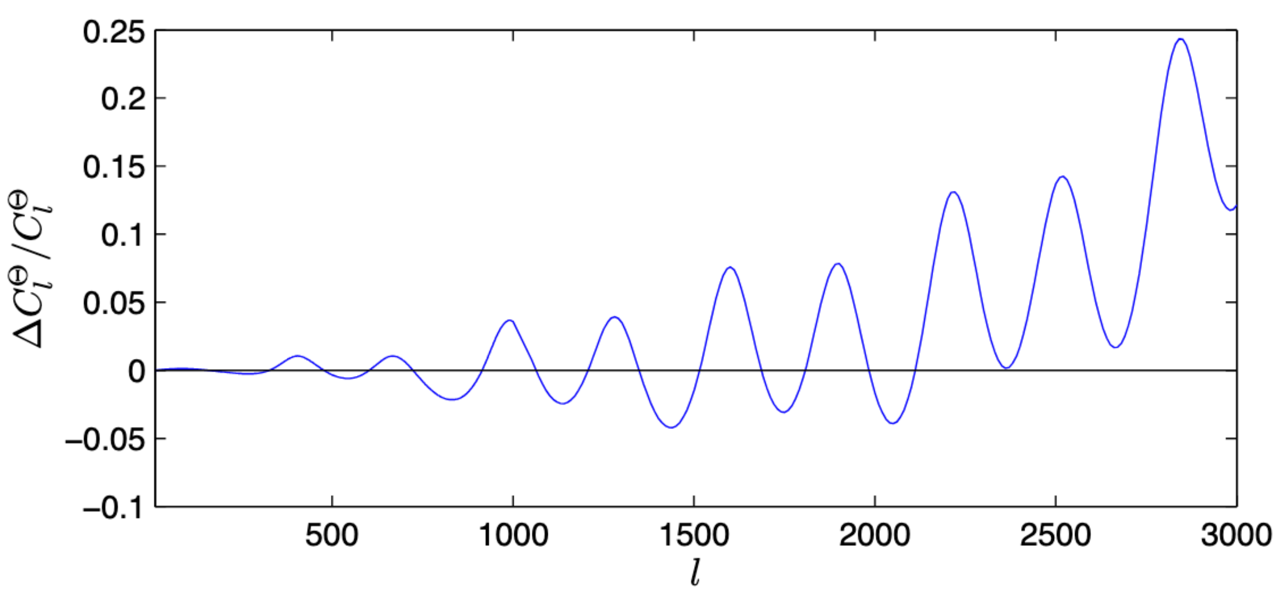

Challinor & Lewis, 2006

Lensing anomaly

- In order to test ΛCDM, a mock parameter was introduced A_L. If the model is correct $A_L = 1$. The lensing potential is multiplied by it in the theoretical modelling:

$$C_\ell^\Psi \rightarrow A_L C_\ell^\Psi$$

- Planck official 2018 data release shows a significant deviation of A_L from standard model

A_L

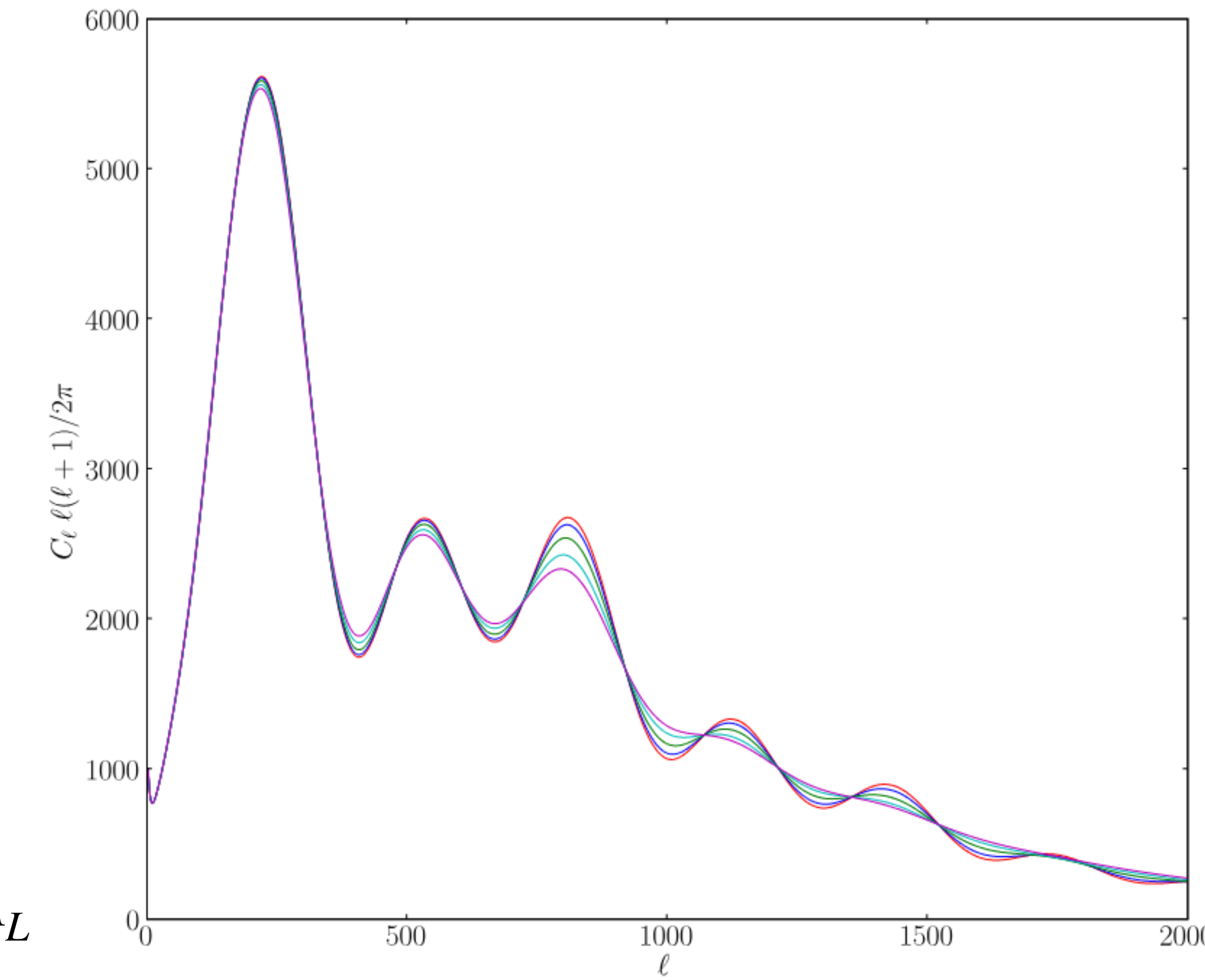

Calabrese et al., 2008

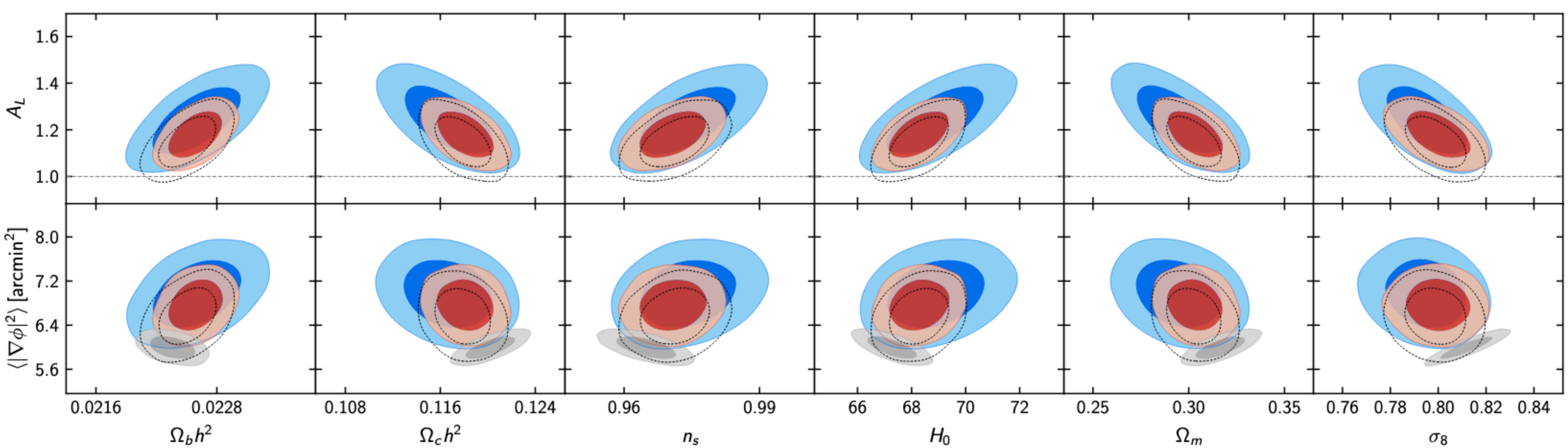

Aghanim et al., 2008

Lensing anomaly & closed Universe

- Planck alone has a 2-σ deviation in favour of a closed Universe. When combining with late Universe probes, the flatness becomes more robust.
- The lensing anomaly and the spatial curvature anomalies are degenerated.

$$\Omega_K = -0.056^{+0.028}_{-0.018} \quad (68\,\%,\ \textit{Planck}\ \mathrm{TT+lowE}),$$

$$\Omega_K = -0.044^{+0.018}_{-0.015} \quad (68\,\%,\ \textit{Planck}\ \mathrm{TT,TE,EE+lowE}),$$

$$\Omega_K = 0.0007 \pm 0.0019 \quad (68\,\%,\ \mathrm{TT,TE,EE+lowE+lensing+BAO}).$$

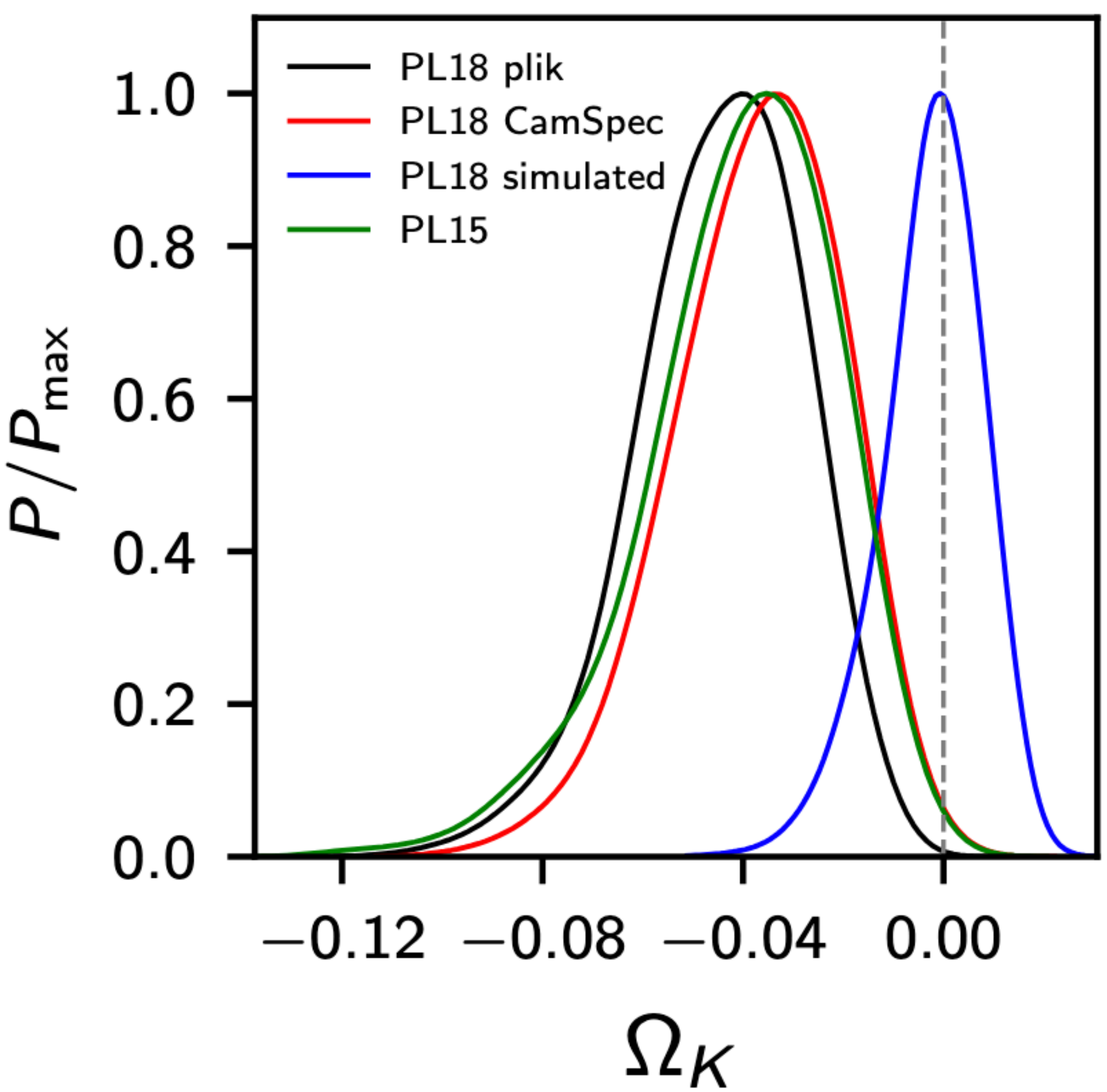

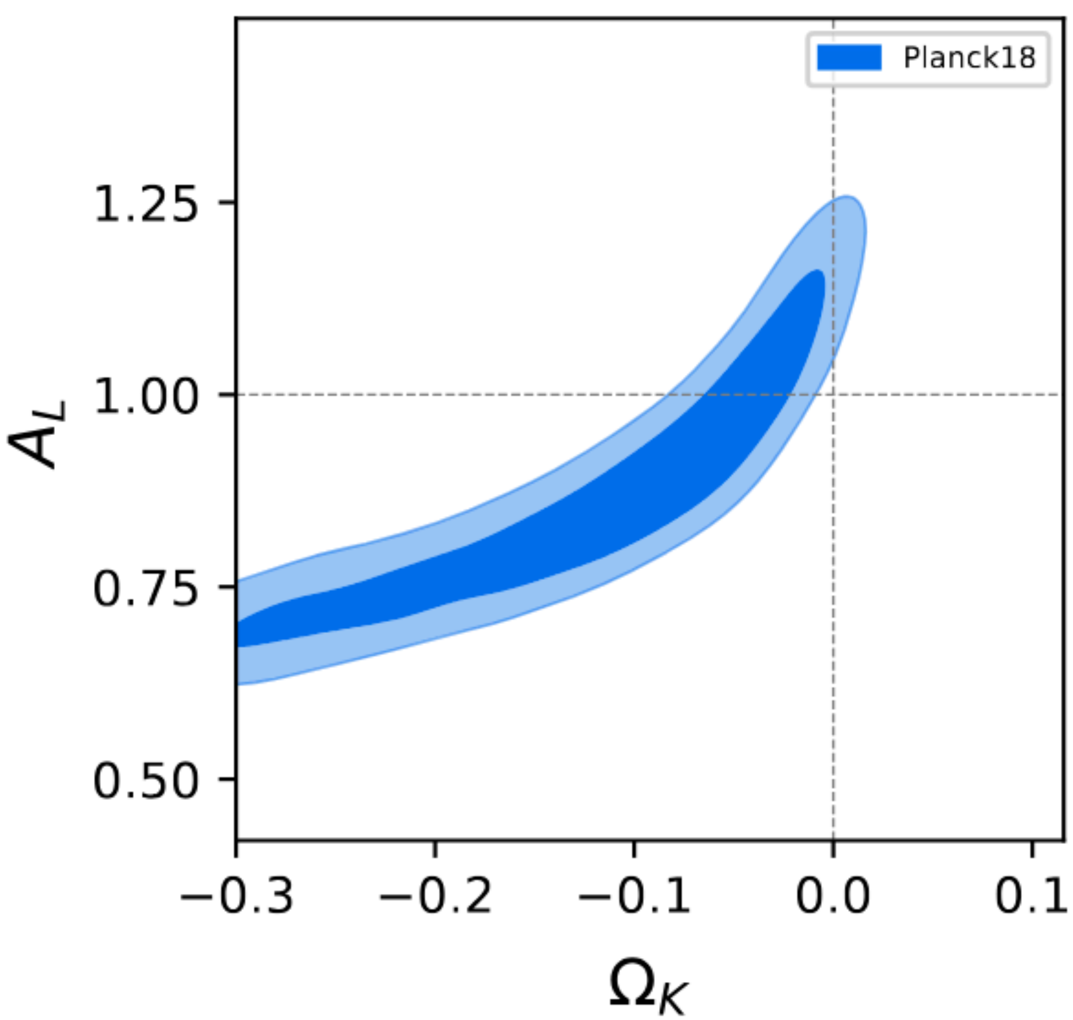

di Valentino et al., 2019, Handley et al, 2020

Reanalyzing Planck data: PR4 (NPIPE 2020)

- In 2020, new re-analysis of Planck data with unified framework (NPIPE, Planck Collaboration LVII 2020) produced maps with lower levels of noise and systematics.
- From this re-analysis, 2 different likelihoods for PR4: CamSpec (Rosenberg, Gratton, Efstathiou 2022) and Plik (Tristram et al. 2024)
- They hint at a change in tensions with respect to PR3

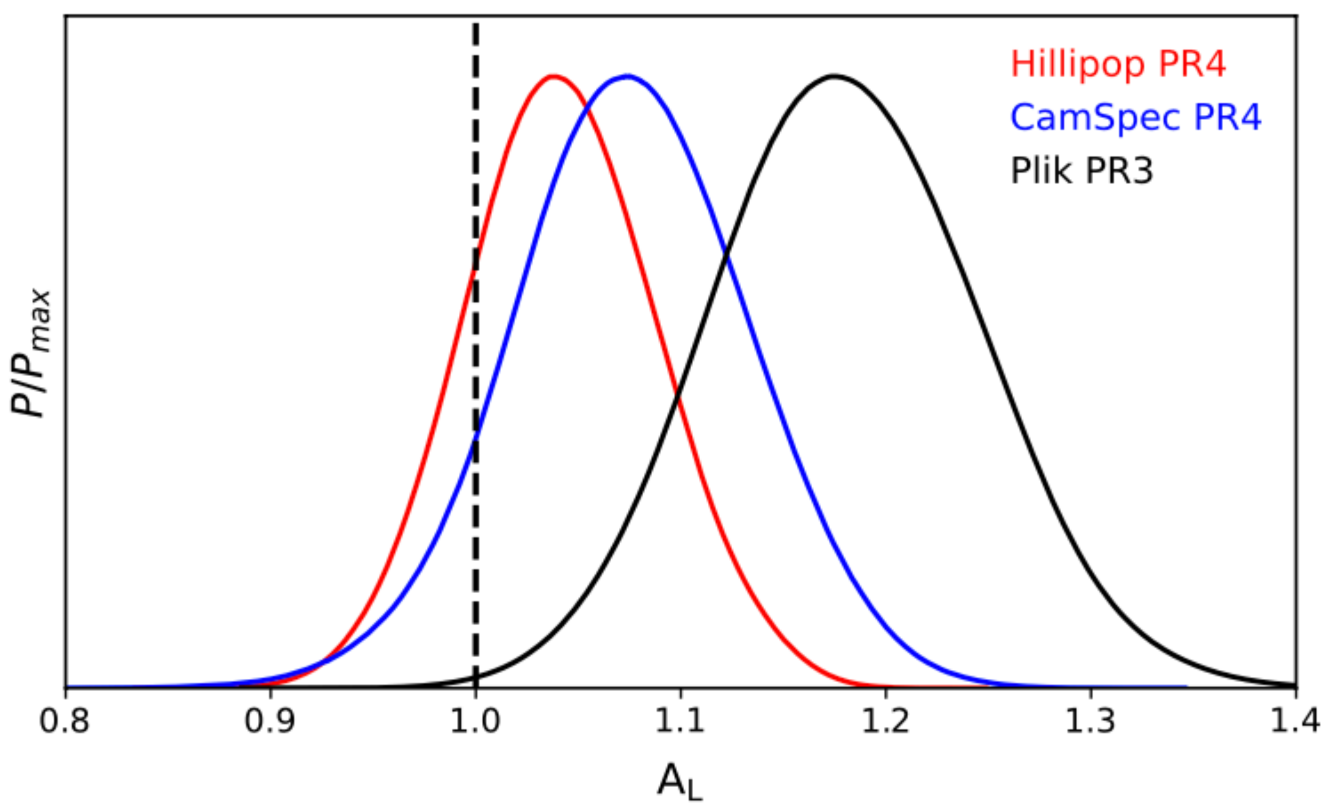

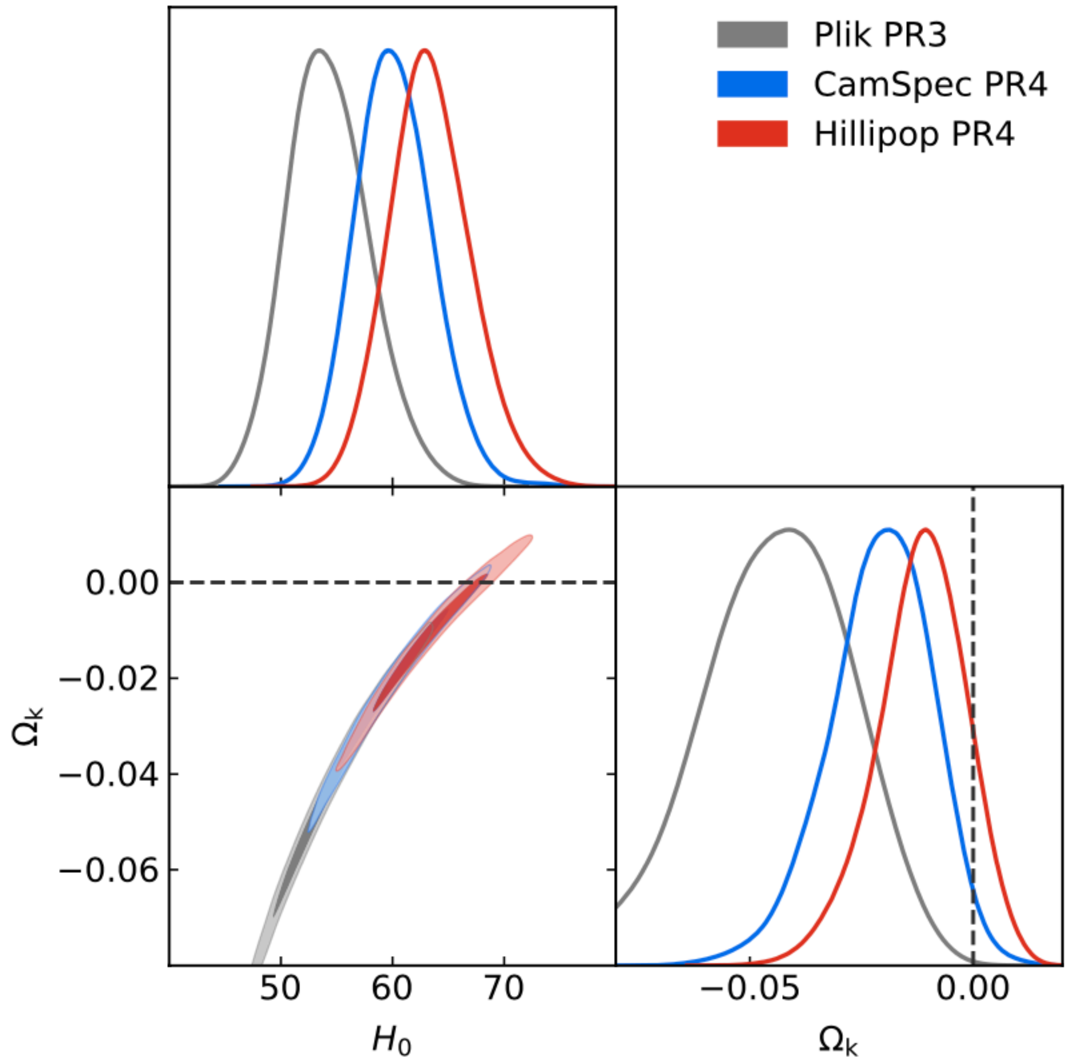

Rosenberg et al. 2022, Tristram et al. 2024

ΛCDM Extensions

- We consider 5 extensions of ΛCDM to evaluate the tensions:

1) $\Lambda CDM + A_L$: $C_\ell^\Psi \to A_L C_\ell^\Psi$

2) $\Lambda CDM + \Omega_k$ (given by Planck primordial power spectrum for non-flat Universe):

$$P_\delta(1) \propto \frac{(q^2 - 4K^2)^2}{q(q^2 - K)} \left(\frac{k}{k_0}\right)^{n_s - 1}$$

where $k_0 = 0.05 \mathrm{Mpc}^{-1}$ $\quad q = \sqrt{k^2 + K^2}$ $\quad K = -(H_0^2/c^2)\Omega_k$

3) $XCDM$: CDM model with constant equation of state for dark energy, w

4) CPL: $w = w_0 + w_a(1 - a)$

New PR4 (NPIPE) preliminary results

- We used the Planck PR4 Plik data (Tristan et al. 2024) with reduced level of noise and systematics of ΛCDM

Parameter	ΛCDM	ΛCDM + A_L	non-flat Planck $P(q)$	XCDM	CPL
Ω_m	0.3100 ± 0.0077	$0.3070^{+0.0081}_{-0.0094}$	0.354 ± 0.033	$0.215^{+0.022}_{-0.070}$	$0.218^{+0.028}_{-0.074}$
H_0 [km/s/Mpc]	67.63 ± 0.57	67.86 ± 0.65	$63.4^{+2.5}_{-3.1}$	83^{+10}_{-8}	83^{+10}_{-8}
A_L	-	1.035 ± 0.055	-	-	-
Ω_k	-	-	-0.011 ± 0.009	-	-
w_0	-	-	-	$-1.46^{+0.21}_{-0.38}$	-1.26 ± 0.42

If we include PR4 lensing maps, similar conclusions and lower errors (too preliminary)

Comparison with PR3

We decrease the lensing anomaly with the new dataset.

	PR3	PR4	σ
ΛCDM $+A_L$	$A_L = 1.181 \pm 0.067$	$A_L = 1.035 \pm 0.055$	1.68σ
non-flat Planck $P(q)$	$\Omega_k = -0.043^{+0.018}_{-0.015}$	$\Omega_k = -0.011 \pm 0.009$	1.59σ

PR3 data favoured non-flat Universe while PR4 does less.

New PR4 + DESI-BAO + SNIa

- When we add the late Universe probes, the conclusions change for some of the extensions

Parameter	ΛCDM	ΛCDM + A_L	non-flat Planck $P(q)$	XCDM	CPL
Ω_m	0.3043 ± 0.0052	0.3025 ± 0.0054	0.3028 ± 0.0054	0.3081 ± 0.0068	0.3073 ± 0.0068
H_0 [km/s/Mpc]	68.05 ± 0.39	68.19 ± 0.41	68.45 ± 0.55	67.54 ± 0.71	67.85 ± 0.72
A_L	-	1.049 ± 0.050	-	-	-
Ω_k	-	-	0.0018 ± 0.0016	-	-
w_0	-	-	-	-0.978 ± 0.026	-0.858 ± 0.067

JA, J. de Cruz-Pérez, in preparation

Contours for $\Lambda CDM + A_L$ case

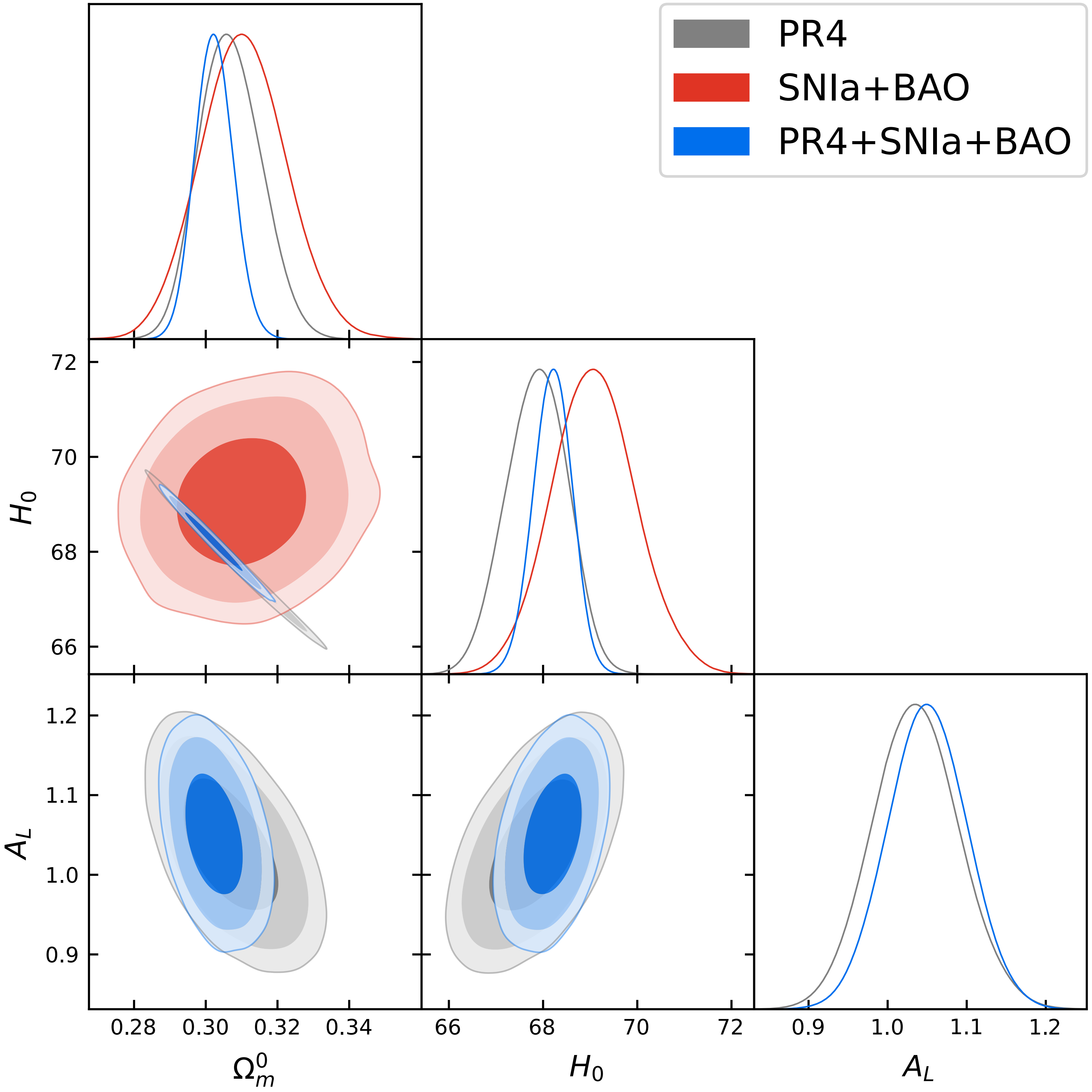

Contours for the non flat Planck P(q) case

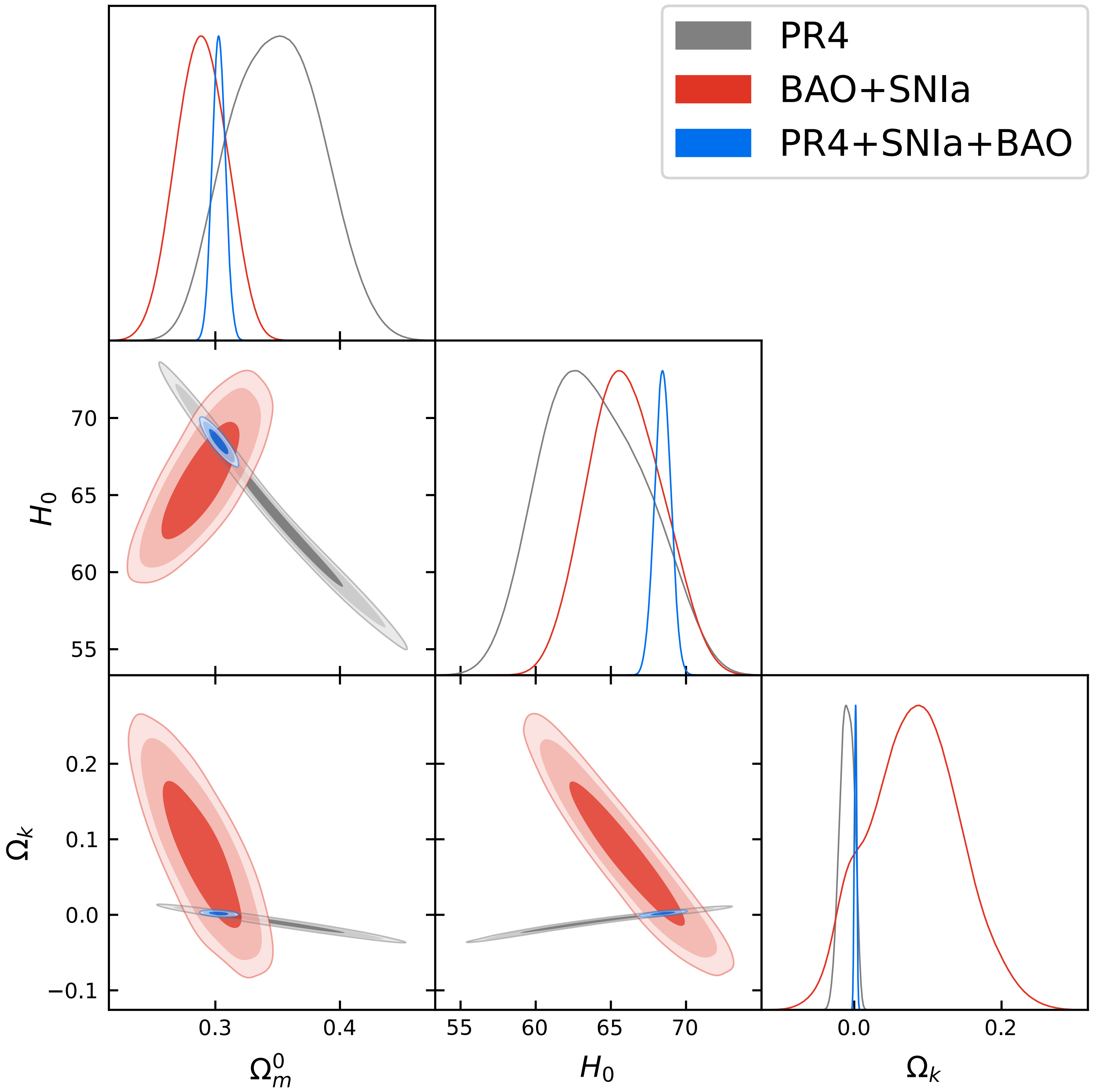

Contours for the XCDM and CPL cases

- The results when including BAO and SN are consistent with DESI recent results

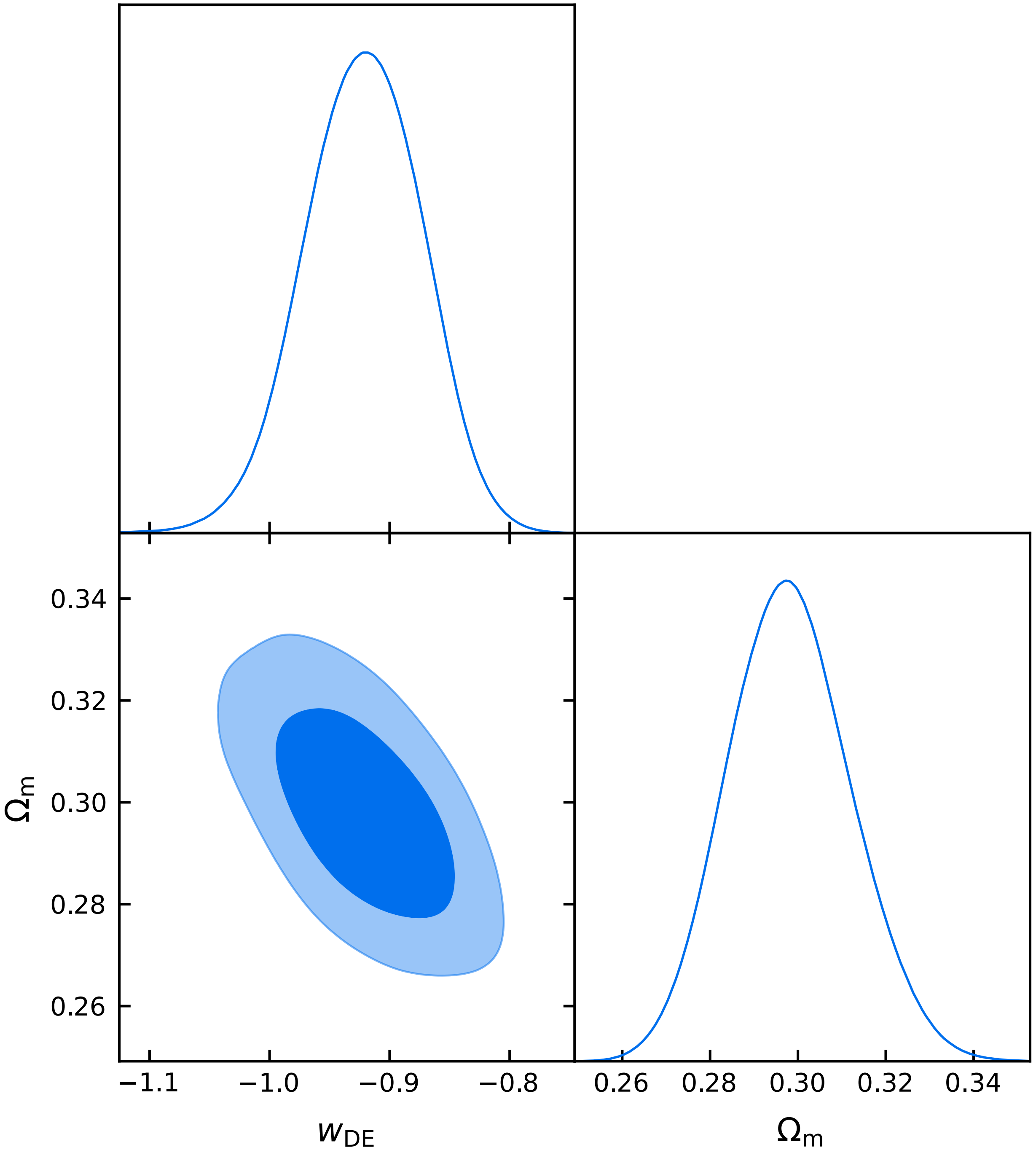

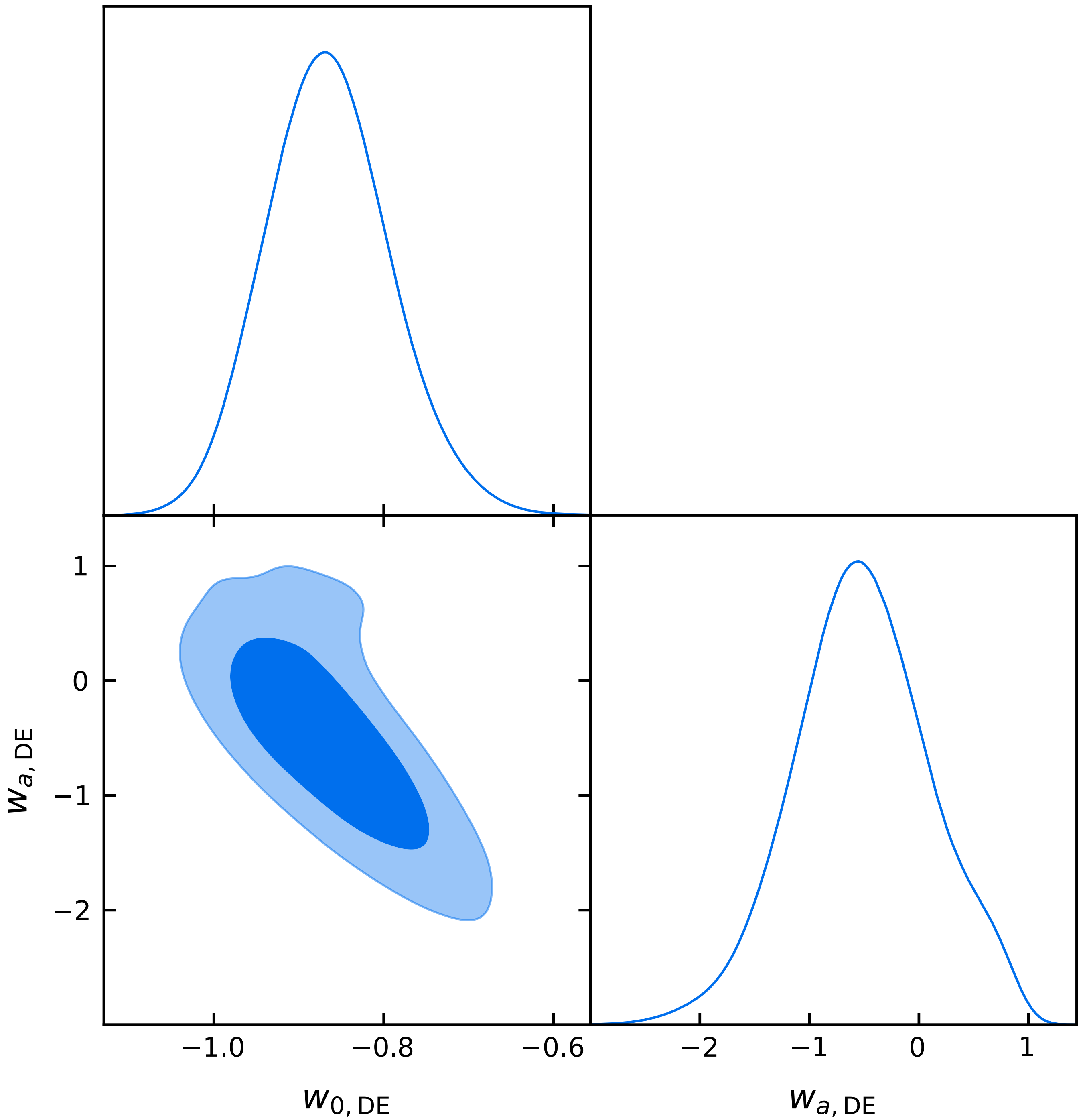

Neutrino cosmology

- Neutrinos participate as relativistic particles first and then as part of the matter component where their contribution is related with the sum of masses of neutrino families.

$$\Omega_\nu = \frac{\rho_\nu}{\rho_c^0} = \frac{\sum_i m_i}{93.14\, h^2\ \mathrm{eV}}\ .$$

- Main effect in the power spectrum is the suppression of the growth of structures for scales beyond the free streaming scale (similar to radiation domination effect on the growth of structures). The suppression of growth depends on the masses of the neutrinos.

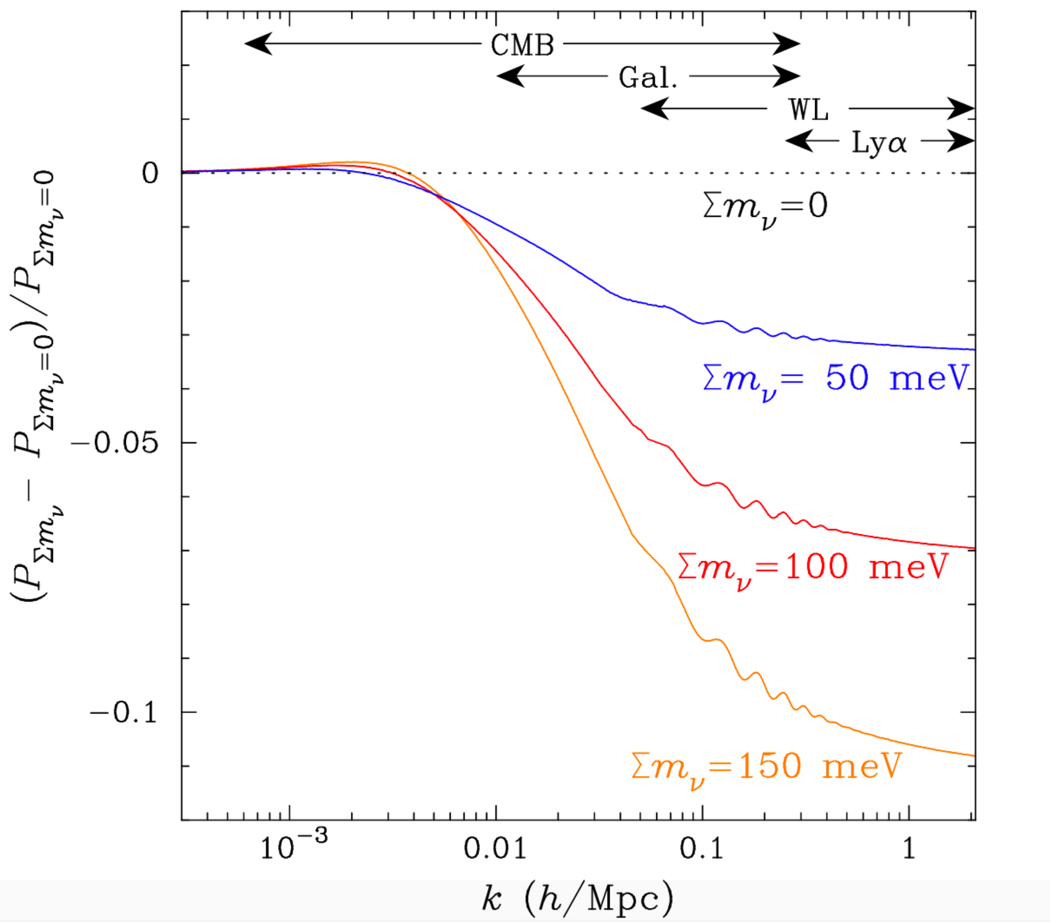

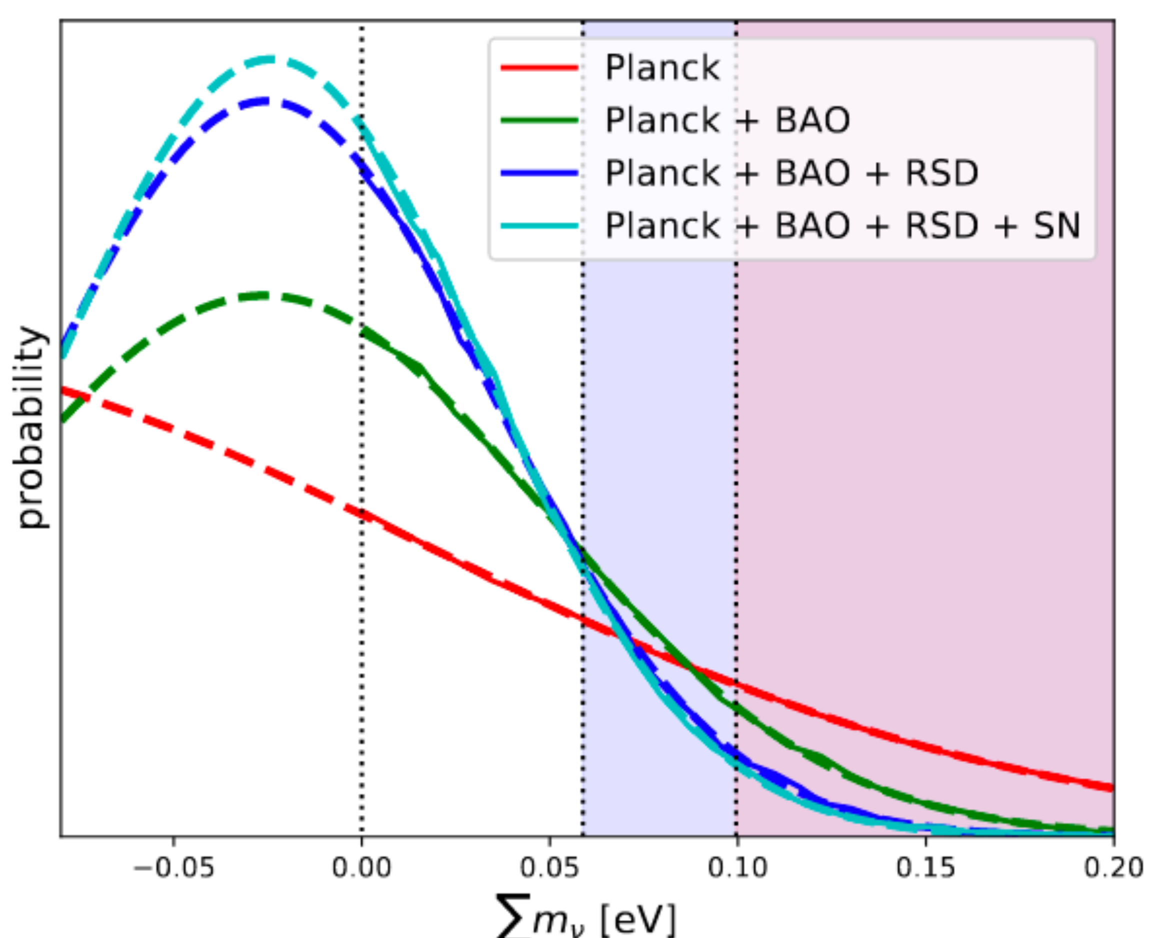

eBOSS Collaboration 2020

Neutrino cosmology with DESI

- DESI has reached the lowest limit on the mass of neutrinos

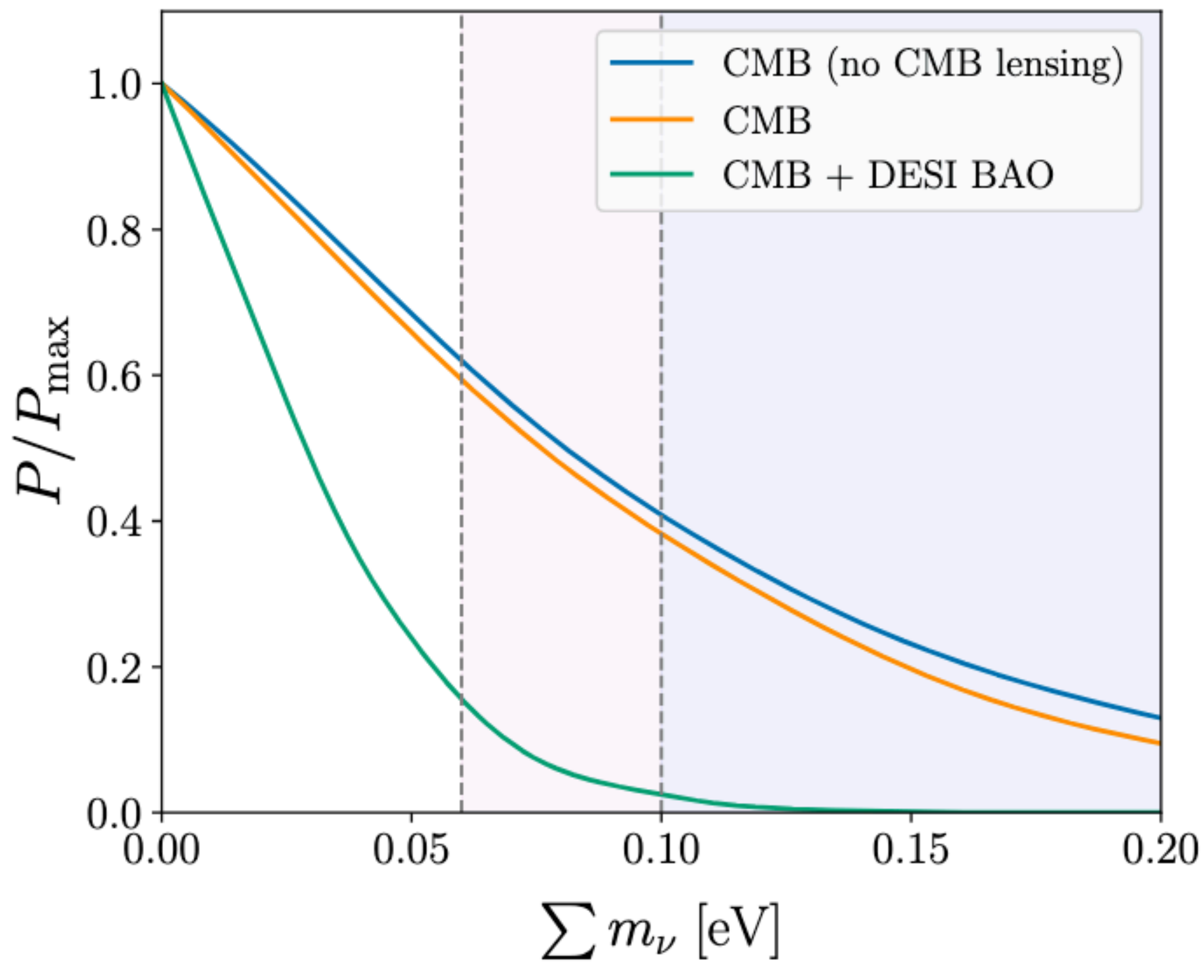

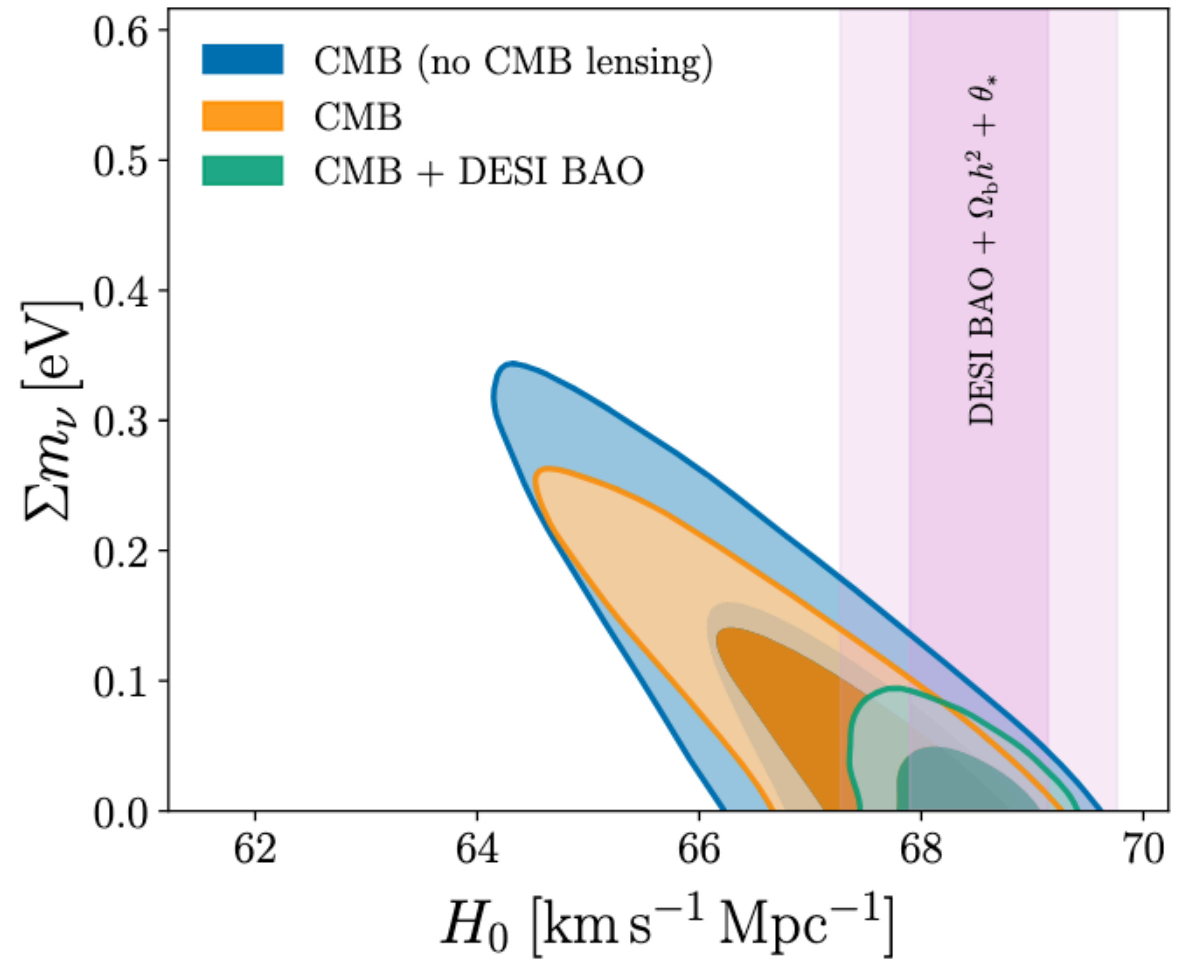

DESI Collaboration (2024)

“The redshift desert”

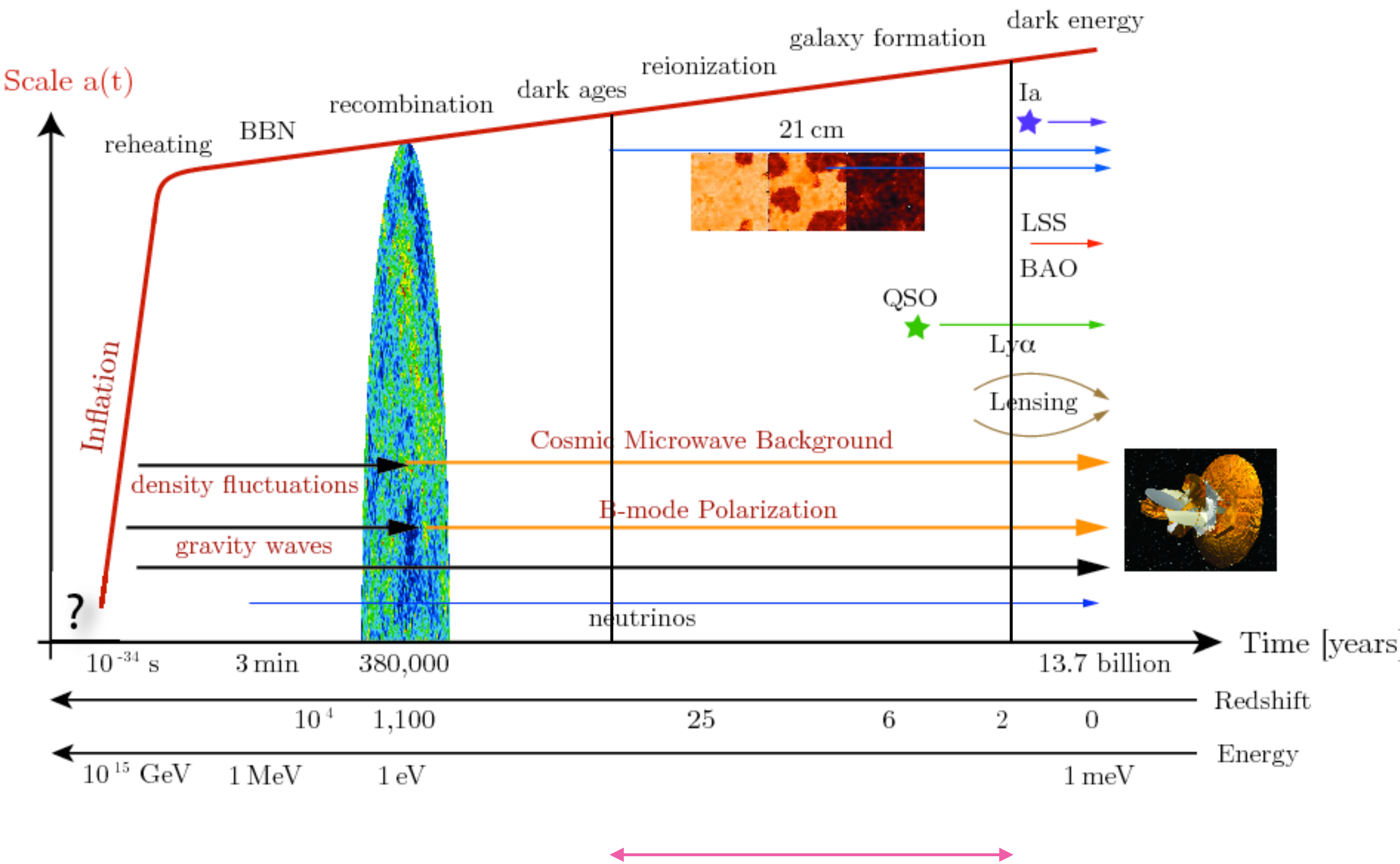

Redshift desert

Present and future

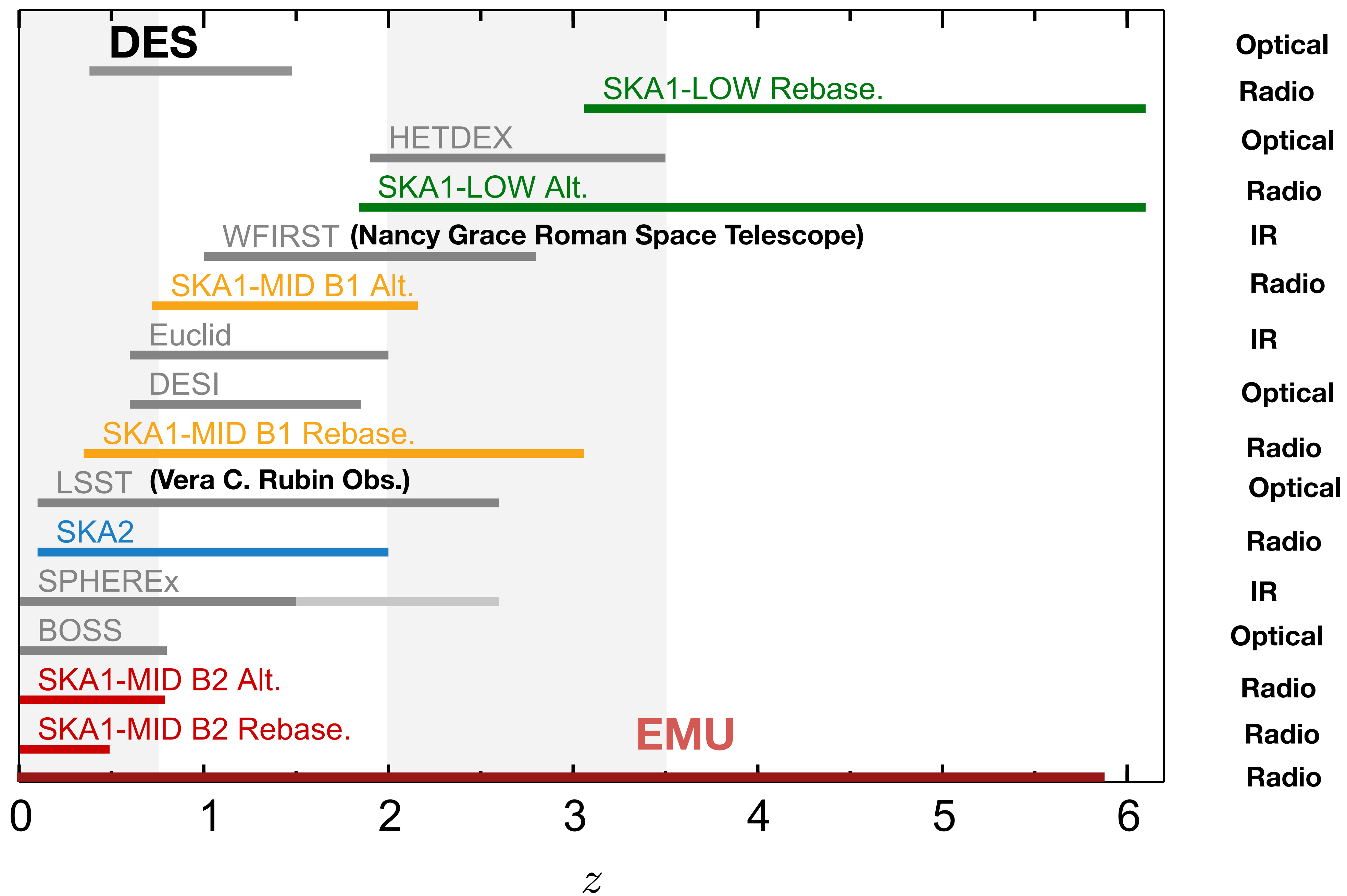

P. Bull (2016)

Radiocosmology

Radio Cosmology

HI galaxy

(like spectroscopic surveys)

[e.g., HIPASS, ALFALFA]

Continuum galaxy

(like photometric) surveys)

[e.g., EMU]

HI intensity mapping

(like 3D CMB)

[e.g., CHIME, TIANLAI]

Radio Cosmology

HI galaxy
(like spectroscopic surveys)
[e.g., HIPASS, ALFALFA]

Continuum galaxy
(like photometric) surveys)
[e.g., EMU]

HI intensity mapping
(like 3D CMB)
[e.g., CHIME, TIANLAI]

Radio Cosmology

HI galaxy

(like spectroscopic surveys)

[e.g., HIPASS, ALFALFA]

Continuum galaxy

(like photometric) surveys)

[e.g., EMU]

HI intensity mapping

(like 3D CMB)

[e.g., CHIME, TIANLAI]

Radio Cosmology

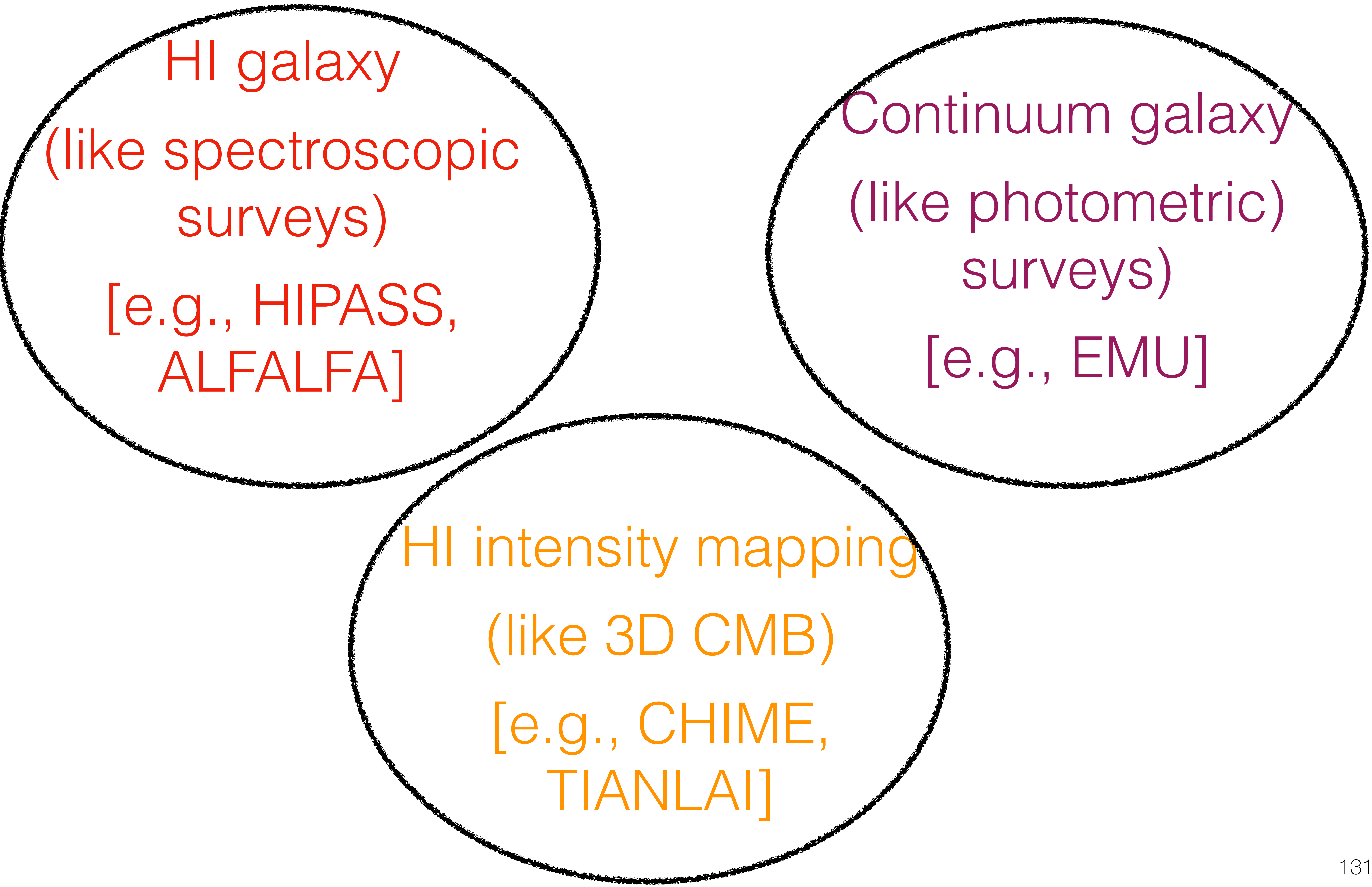

ASKAP overview

- 36 12-metre antennas spread over a region 6 km in diameter
- frequency band of 700–1800 MHz, with an instantaneous bandwidth of 300 MHz.
- 75% of the time: Survey projects

EMU: Continuum

WALLABY: Spectroscopy 21cm

DINGO: HI evolution

POSSUM: MW magnetic fields

FLASH: HI absorption

CRAFT: Fast transients

COAST: PTA

VAST: Slow transients

VLBI: long baseline

ASKAP-EMU

- Already analysing pilot data
- Almost 300 sq. deg
- 10 pointings (field). 1 field per scheduling block (SB)
- 10 hours per SB. Total integration time: 100 hours
- July-November 2019
- Synthesized bandwidth: 13'' x 11'' FWHM
- Frequency: 800 - 1088 MHz

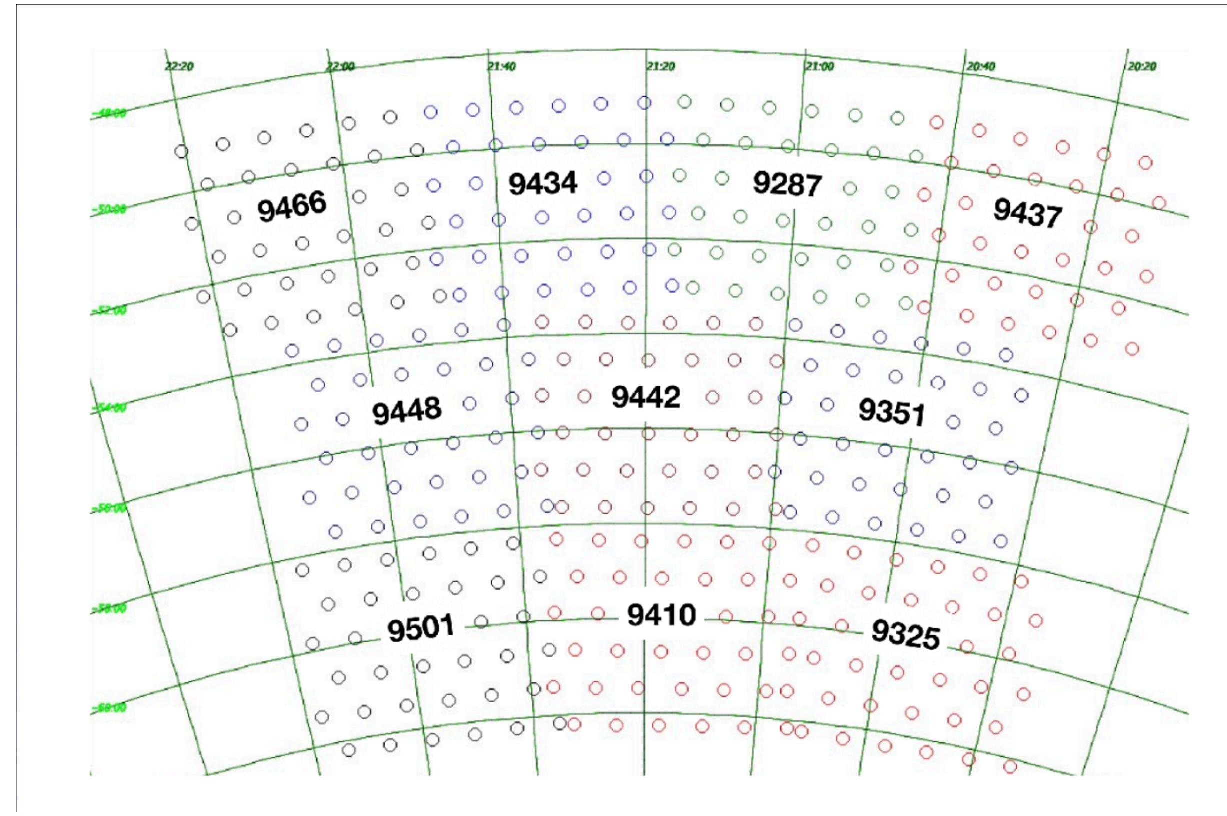

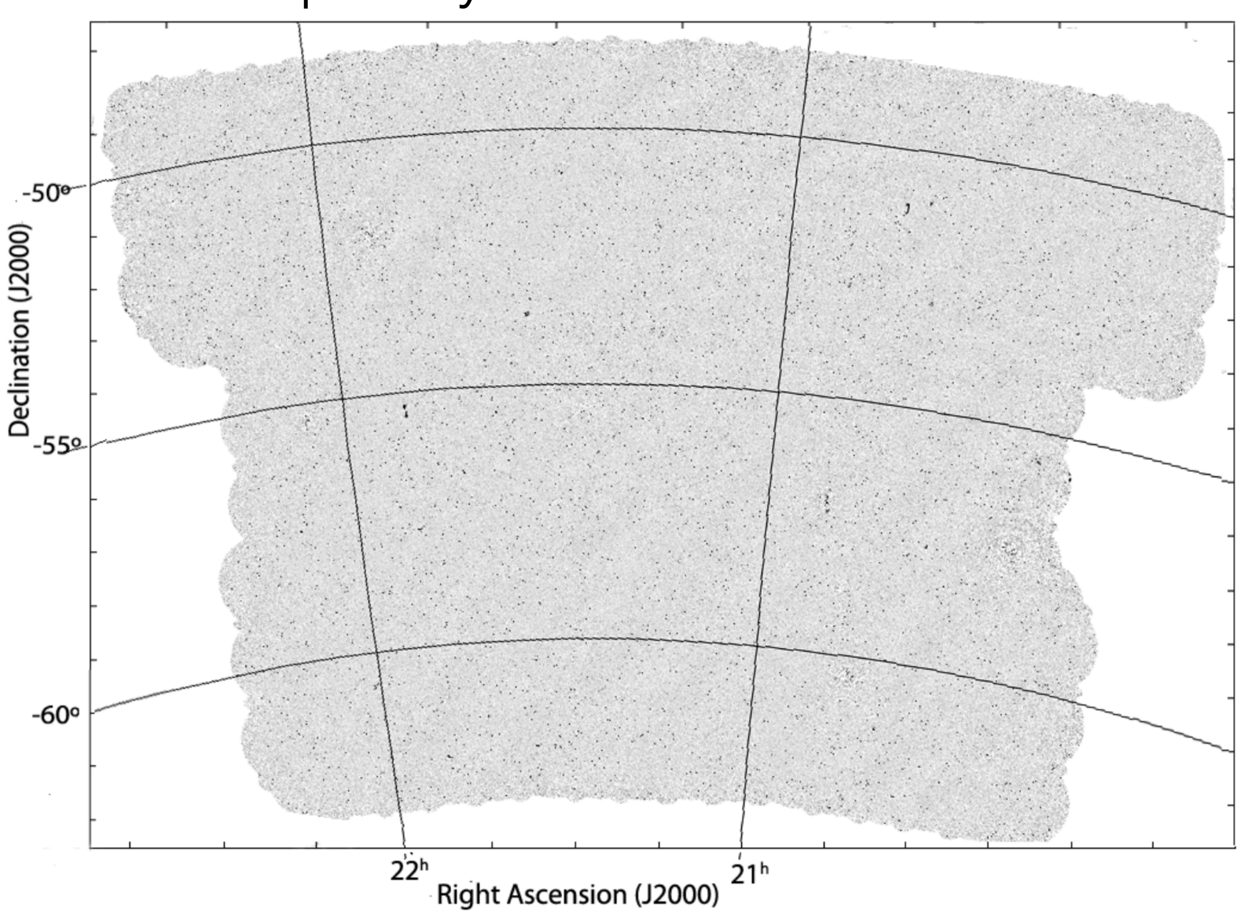

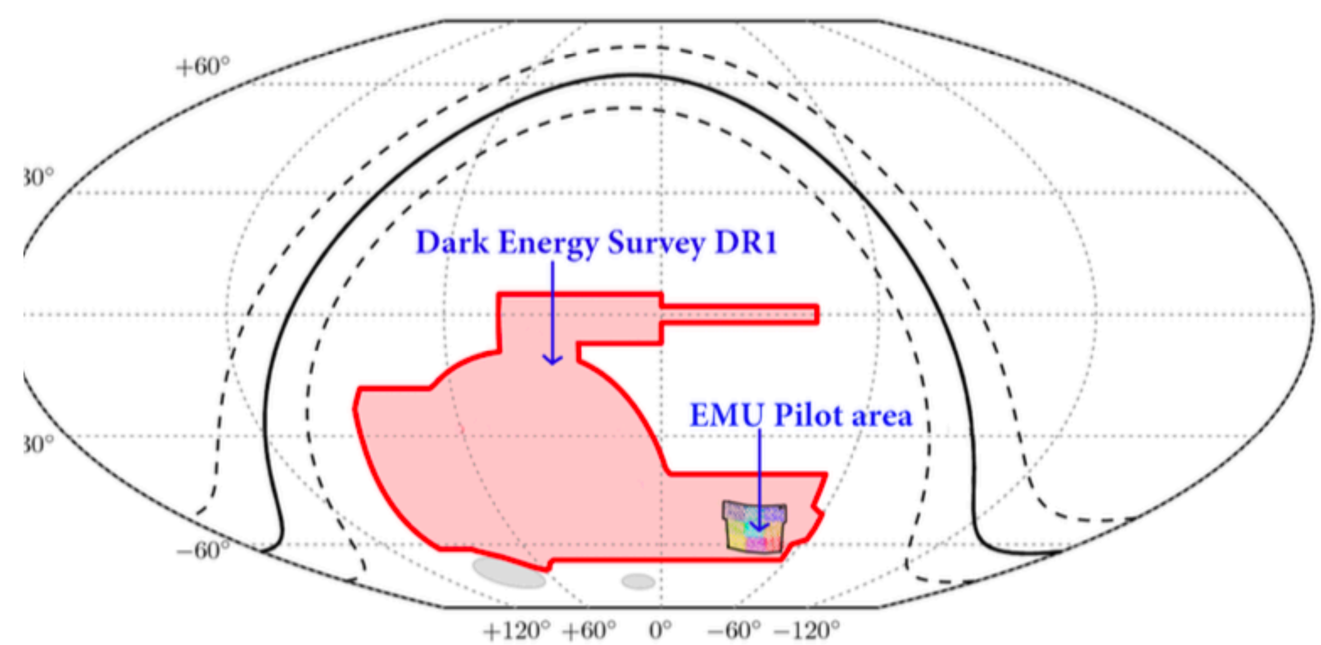

R. Norris et al, 2021, PASA

RACS x Planck SMICA R3

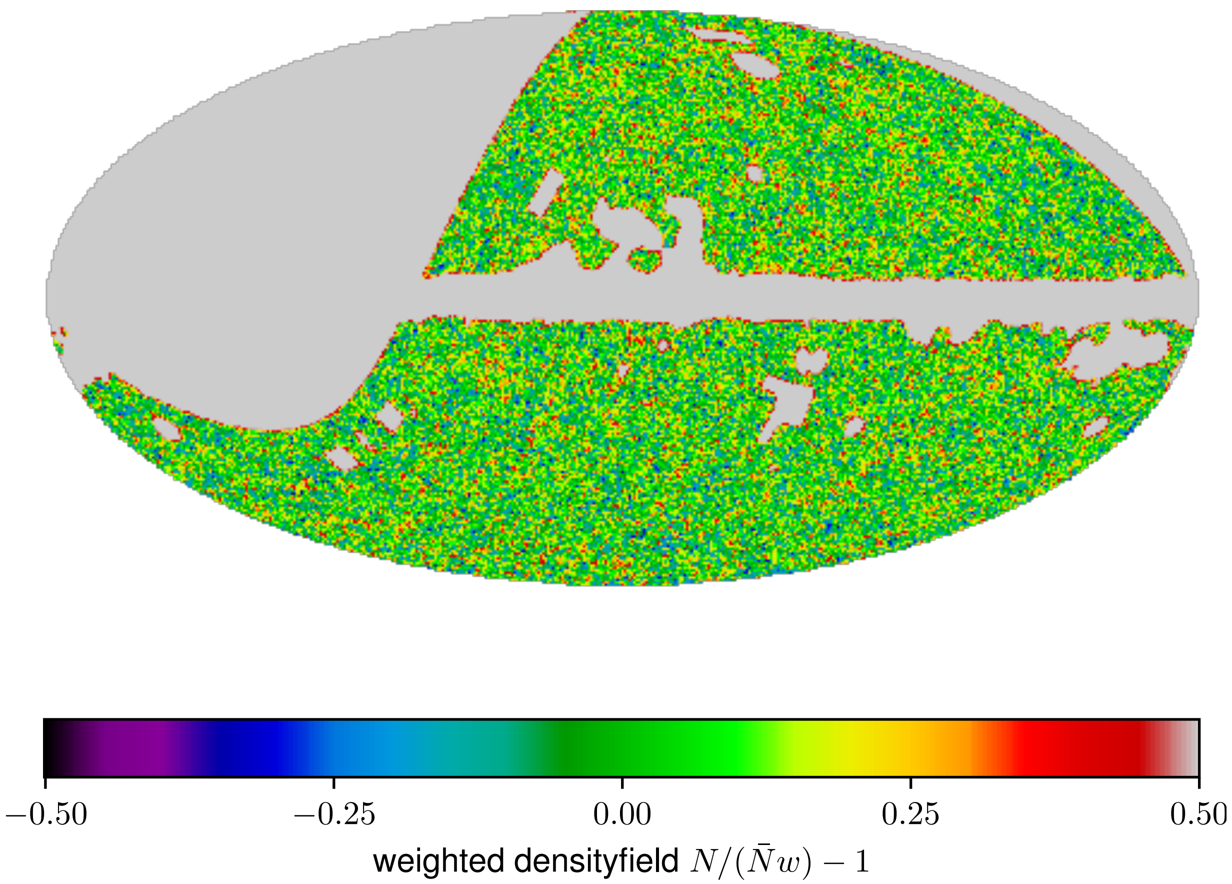

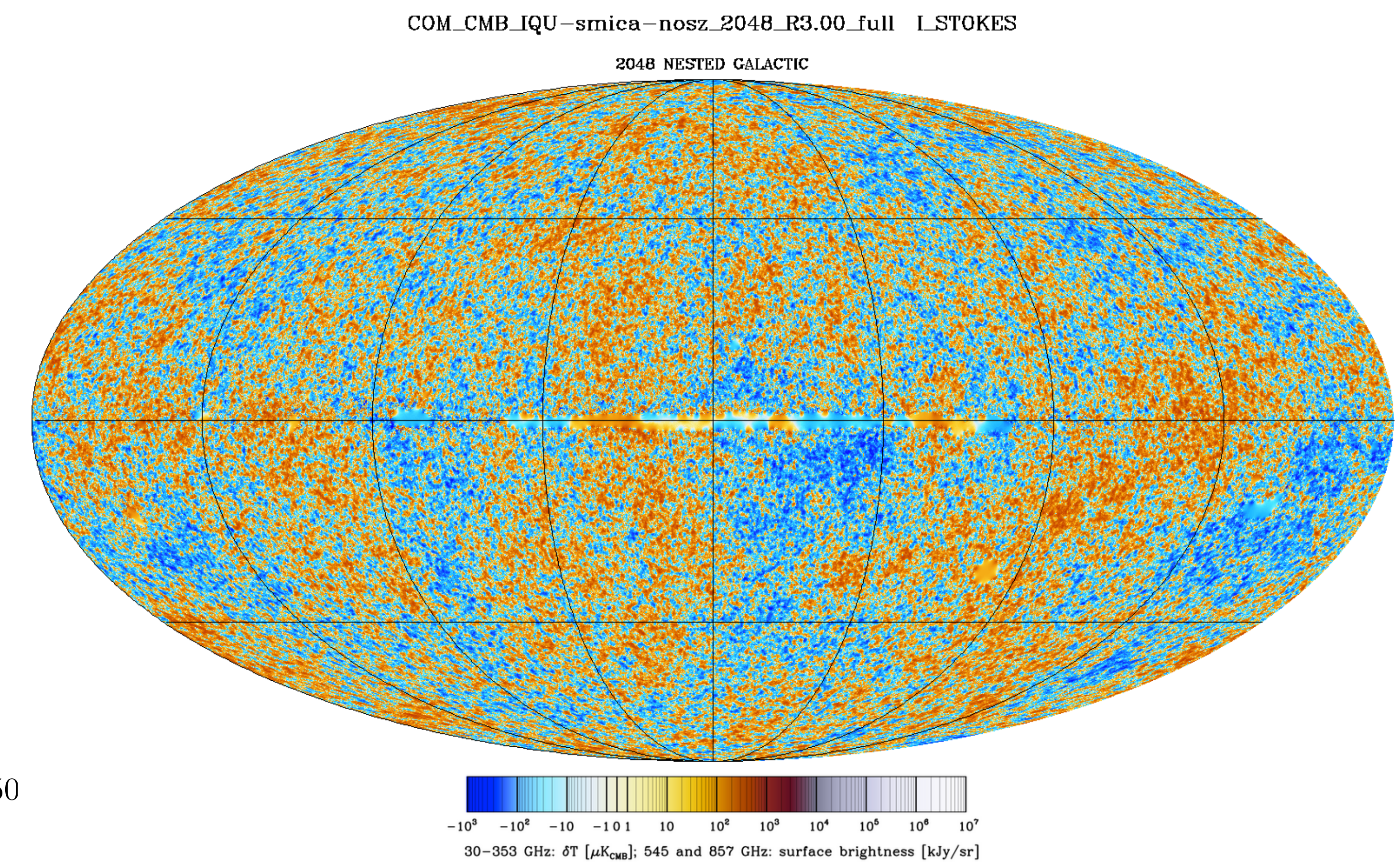

- Removed Galactic plane ($|b| < 5°$)
- Flux cut of 4 mJy
- Construct weight map w using SKADS simulations
- Apply Planck mask
- Cut regions with w < 0.5
- Apply weights to number count and obtain over-density field

B. Bahr-Kalus, D. Parkinson D., JA, S. Camera, C. Hale, F. Qin, 2022, MNRAS

RACS measurements

gg

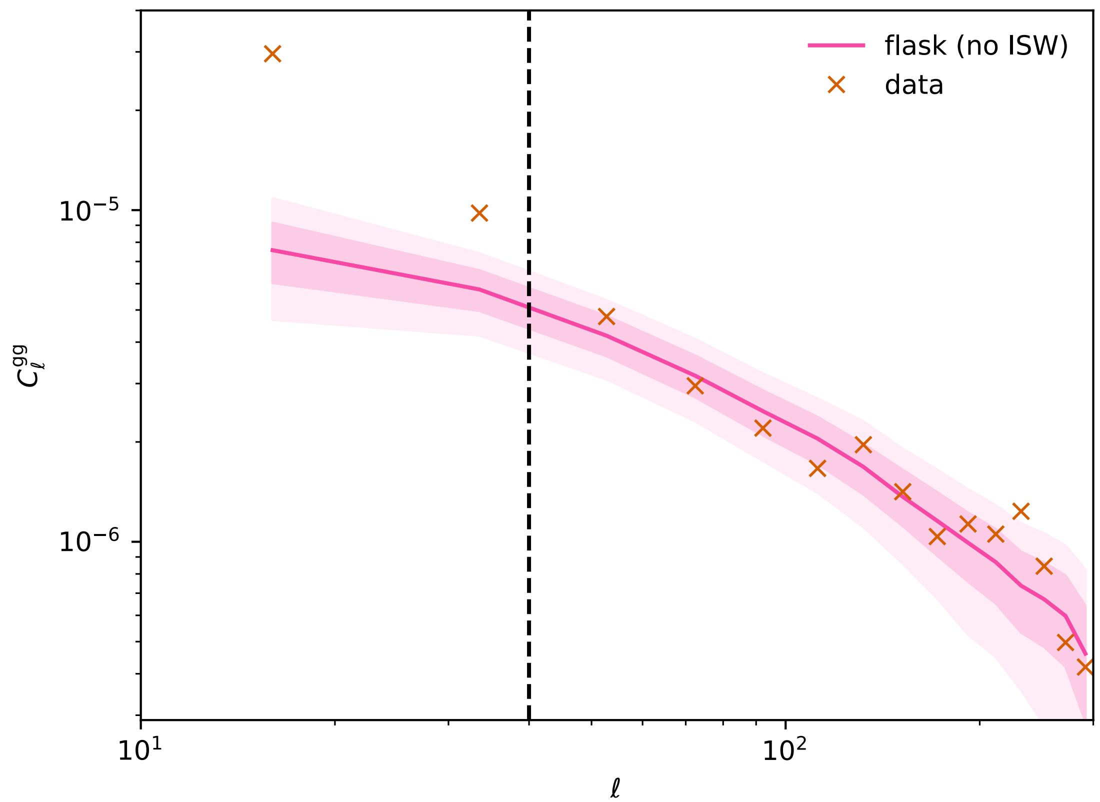

gT

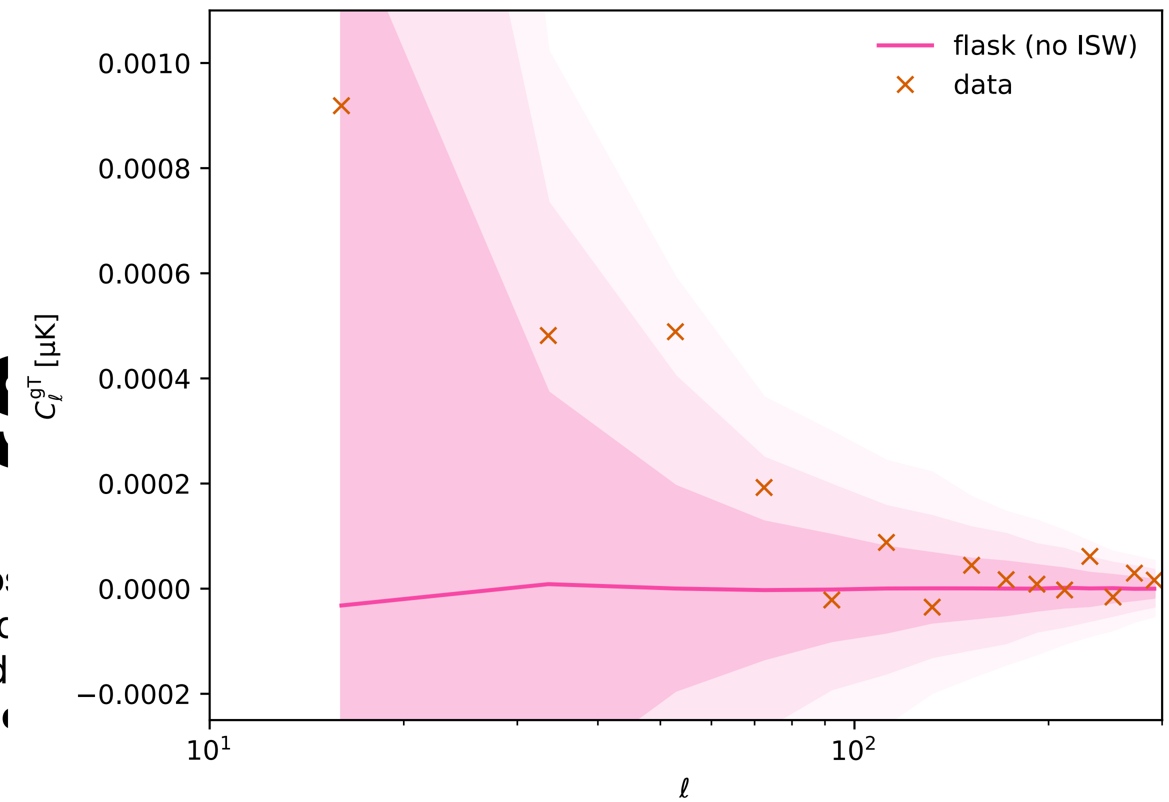

Good agreement at small scales,
Large scale power offset
(Galaxy power spectra information at $\ell >$ 40 not included in analysis)

$$\frac{S}{N} = \frac{\sum_{\ell,\ell'} C_\ell^{(\mathrm{data})} \mathbf{K}_{\ell\ell'} C_{\ell'}^{(\mathrm{model})}}{\sqrt{\sum_{\ell,\ell'} C_\ell^{(\mathrm{model})} \mathbf{K}_{\ell\ell'} C_{\ell'}^{(\mathrm{model})}}} \approx 2.8$$

relative to null hypothesis of no correlation

RACS measurements

gg

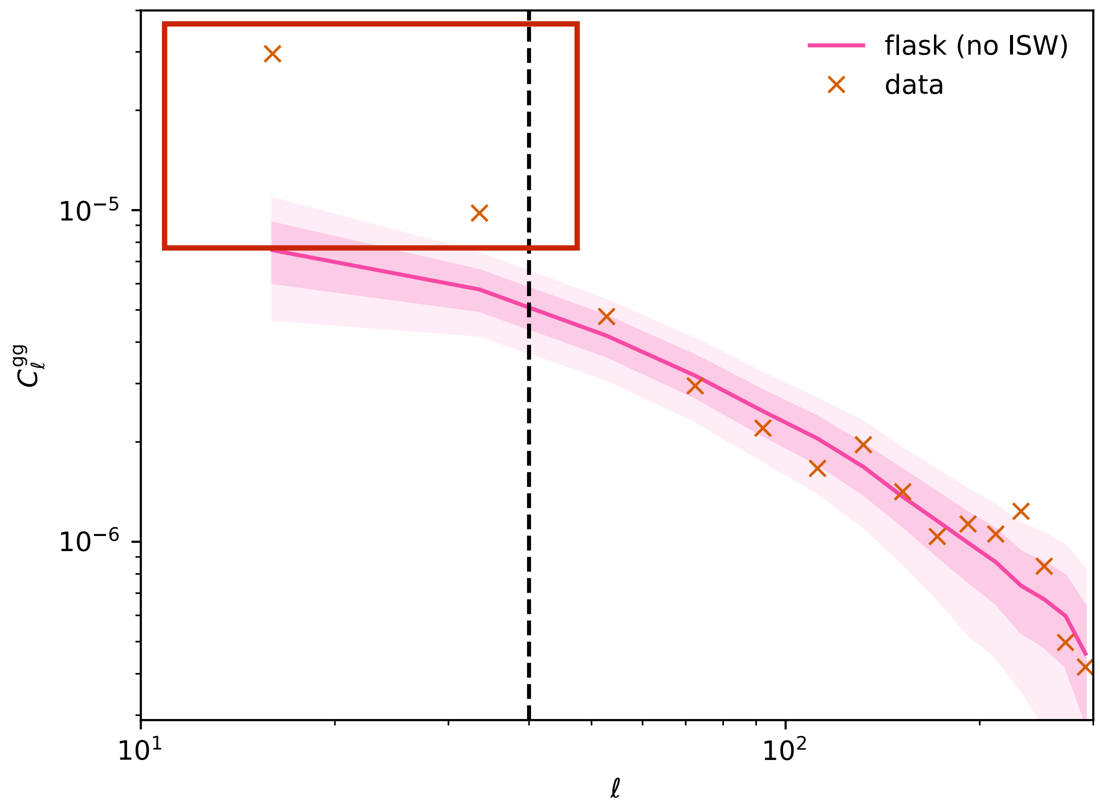

as
SKA co
e data, c
nd rand
bright s

gT

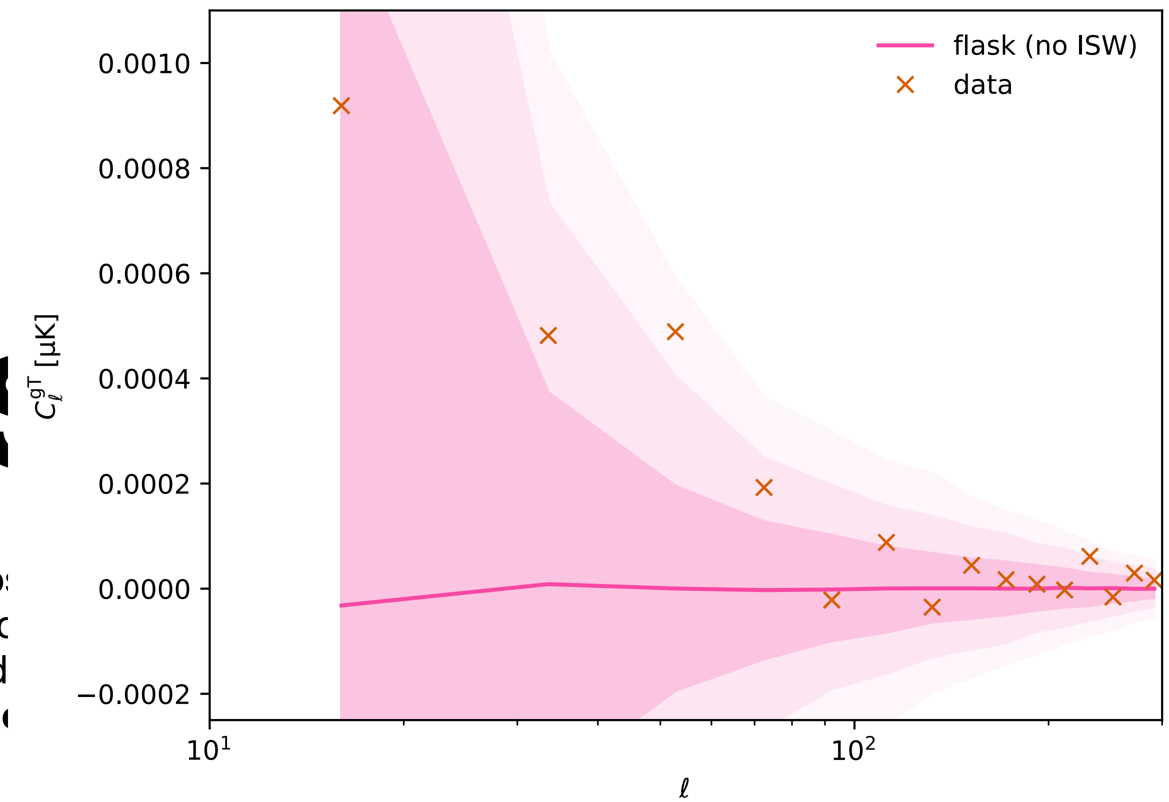

Good agreement at small scales,
Large scale power offset
(Galaxy power spectra information at $\ell >$ 40 not included in analysis)

$$\frac{S}{N} = \frac{\sum_{\ell,\ell'} C_\ell^{(\mathrm{data})} \mathbf{K}_{\ell\ell'} C_{\ell'}^{(\mathrm{model})}}{\sqrt{\sum_{\ell,\ell'} C_\ell^{(\mathrm{model})} \mathbf{K}_{\ell\ell'} C_{\ell'}^{(\mathrm{model})}}} \approx 2.8$$

relative to null hypothesis of no correlation

Some systematics

- Large scale power excess seems to be correlated with declination
  - Close to south pole errors smaller, and mean close to predicted value
  - Close to equator number of counts smaller and sky noise large, power is higher than expected
- Hypothesis is that power excess is **not** non-Gaussianity causing scale-dependent bias, but a systematic caused by data reduction procedure

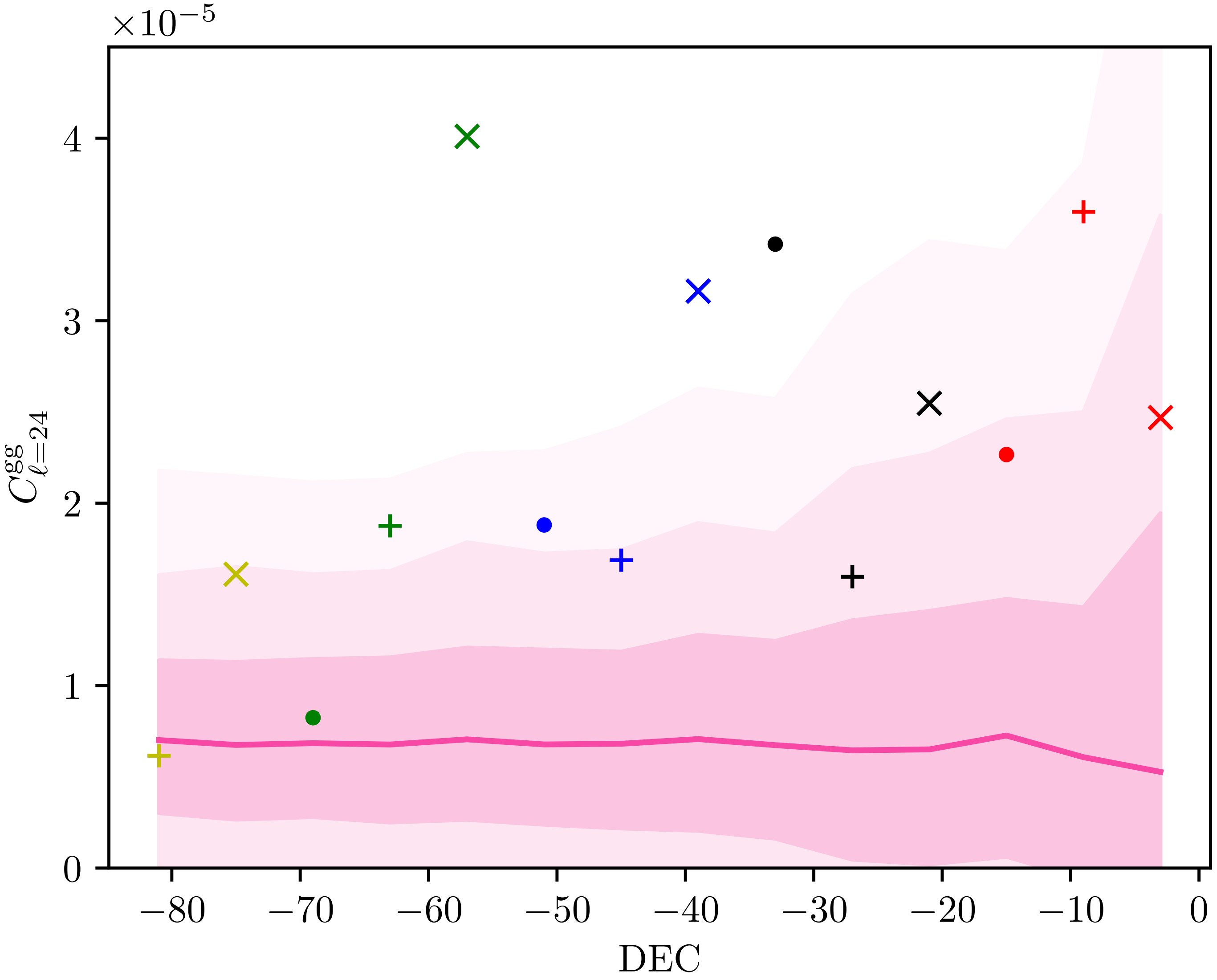

HI intensity mapping

Radio Cosmology allows us to reach higher redshifts opening gates to new probes of large-scale structure.

The newest technique is the use of 21cm line intensity mapping

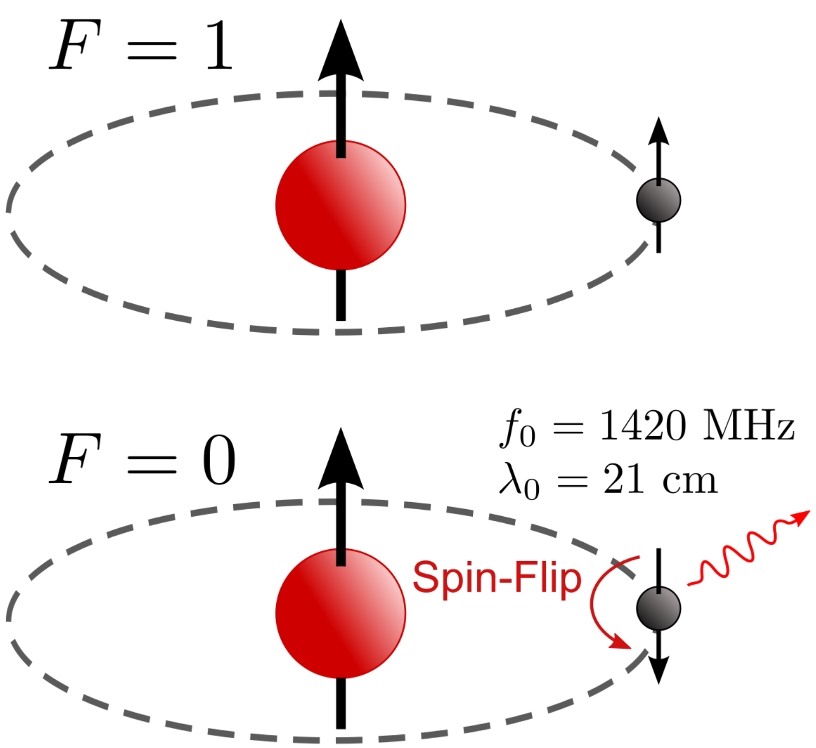

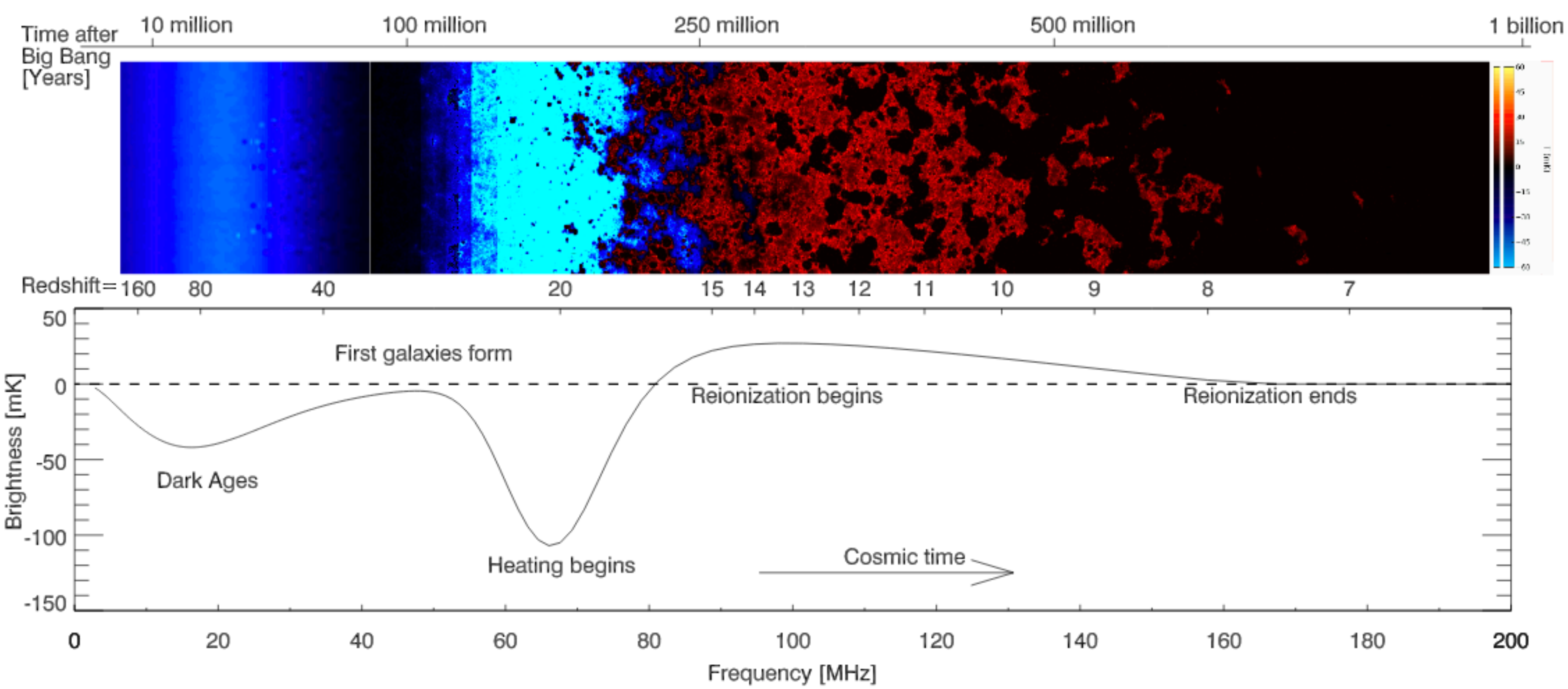

21cm line emission surveys

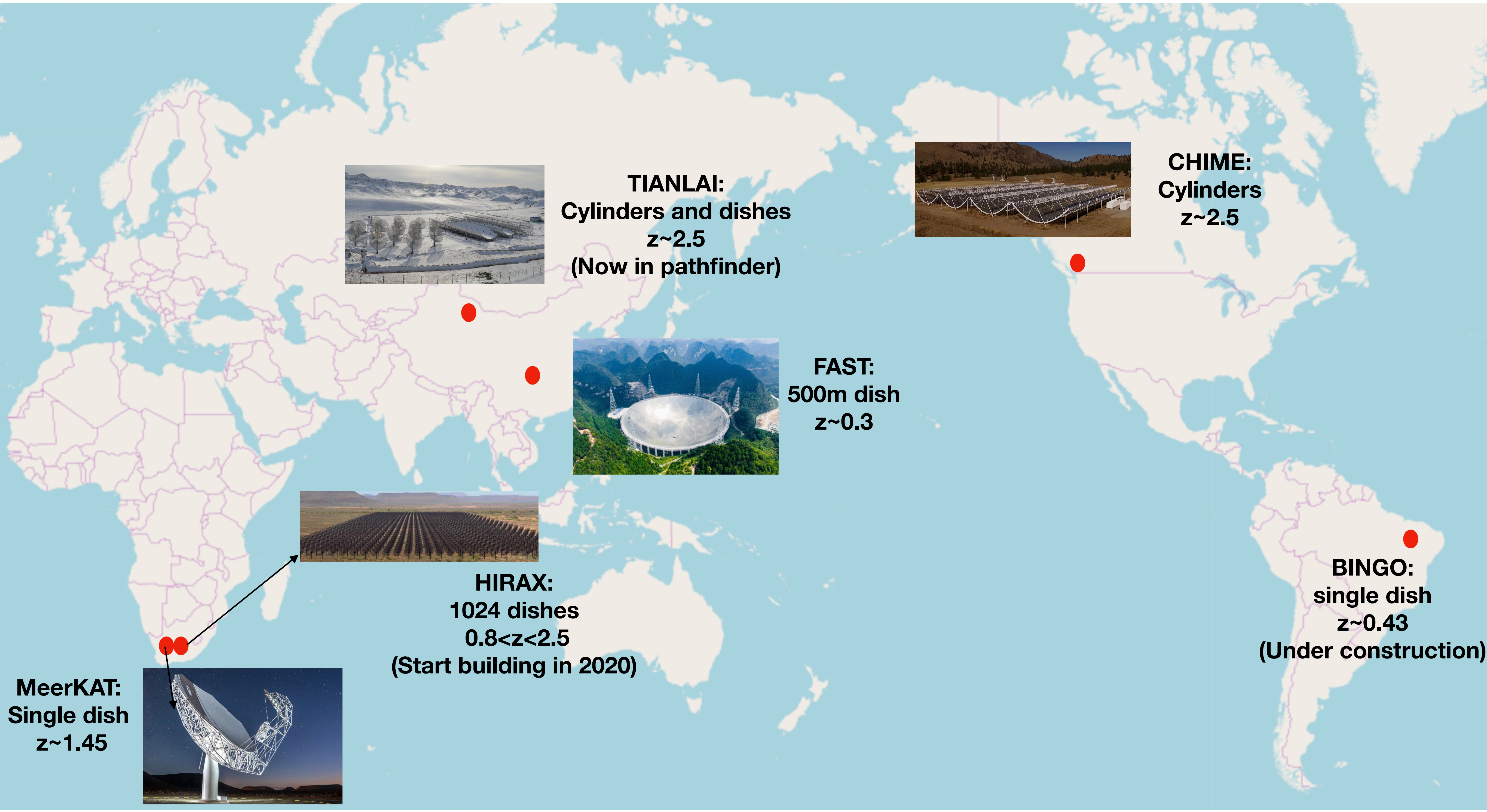

SKA Observatory (SKAO)

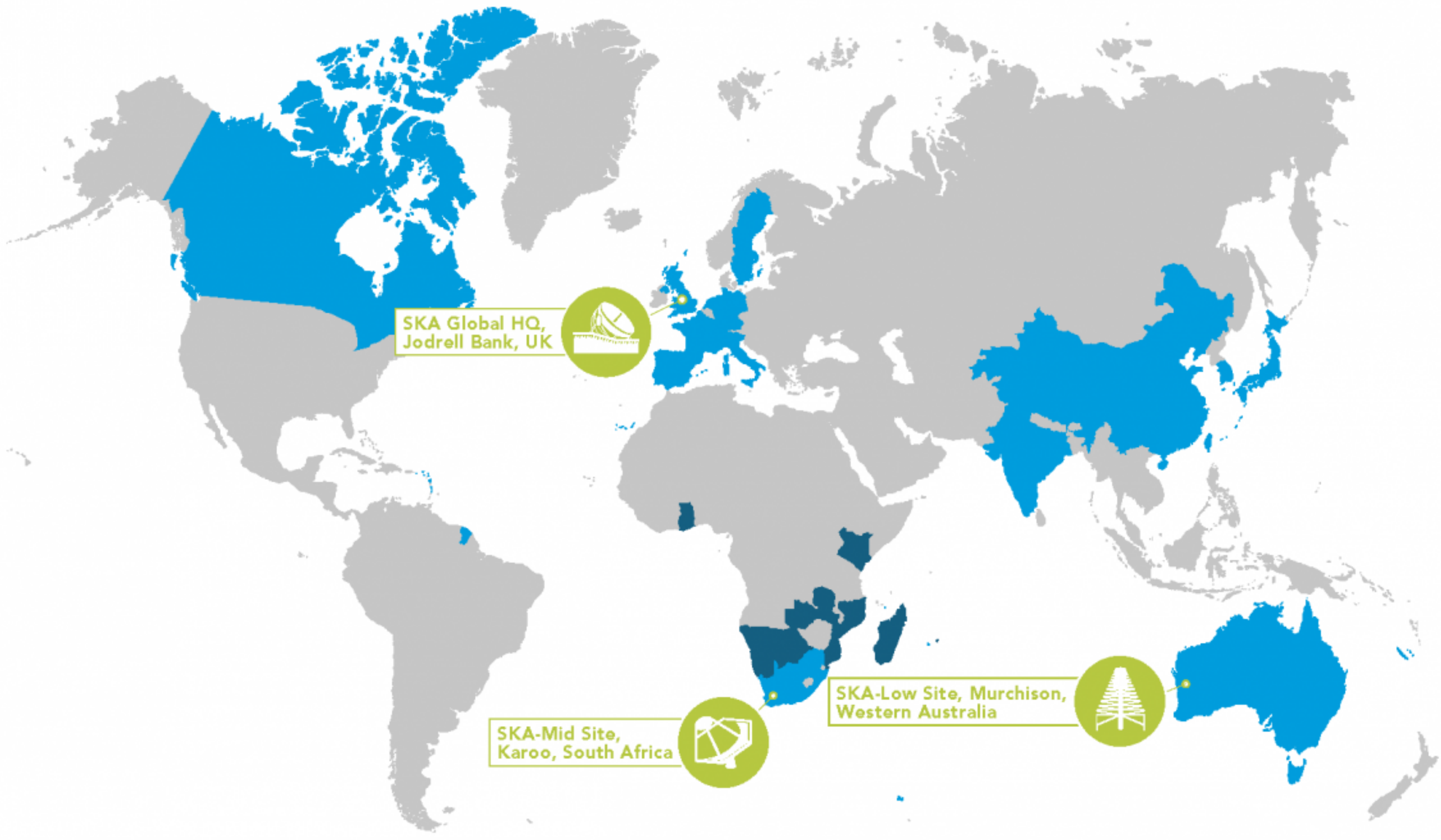

SKA Partners – includes Members of the SKA Organisation – precursor to the SKAO –, current SKAO Member States*, and SKAO Observers (as of June 2021)

African Partner Countries

SKA Observatory

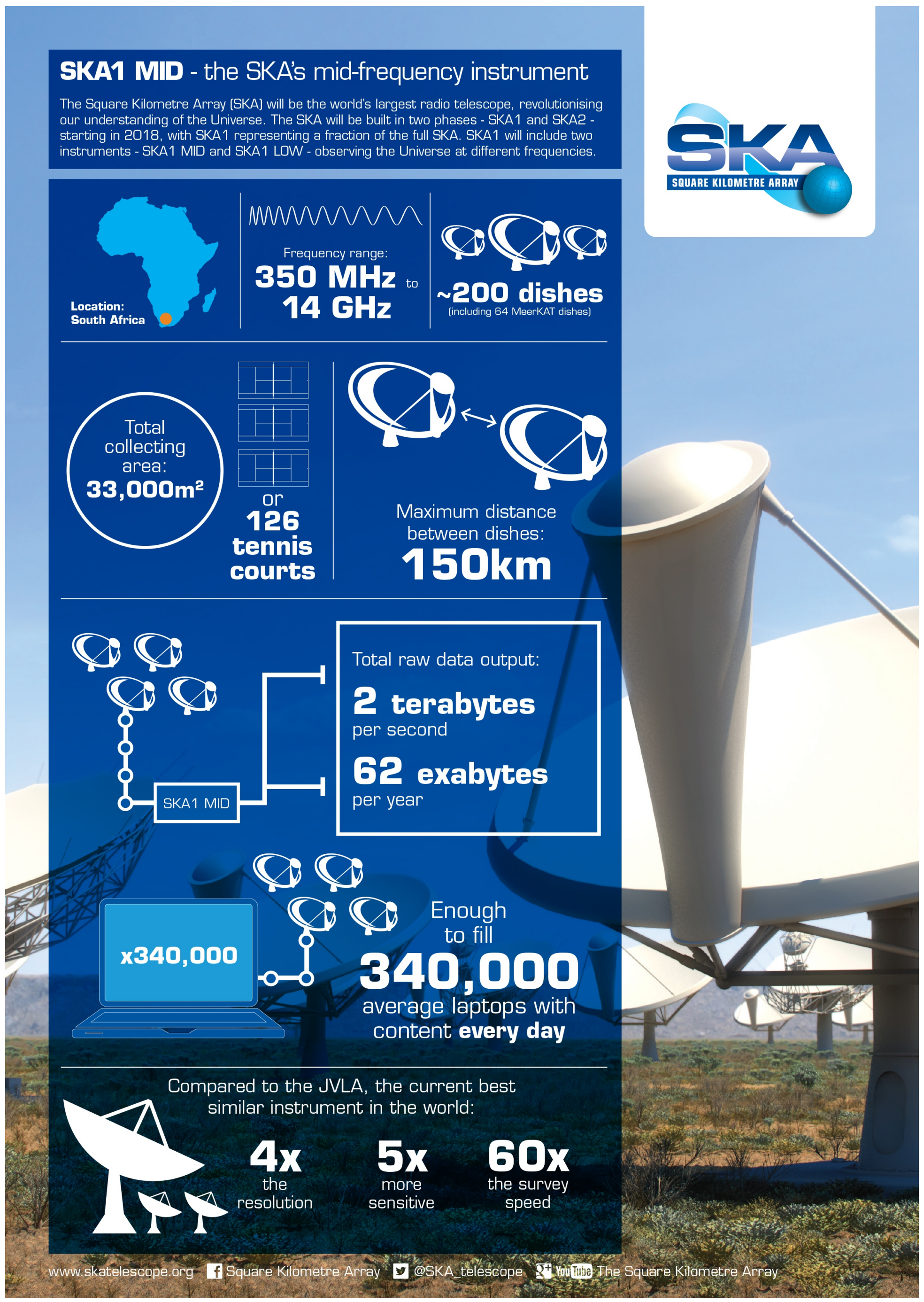

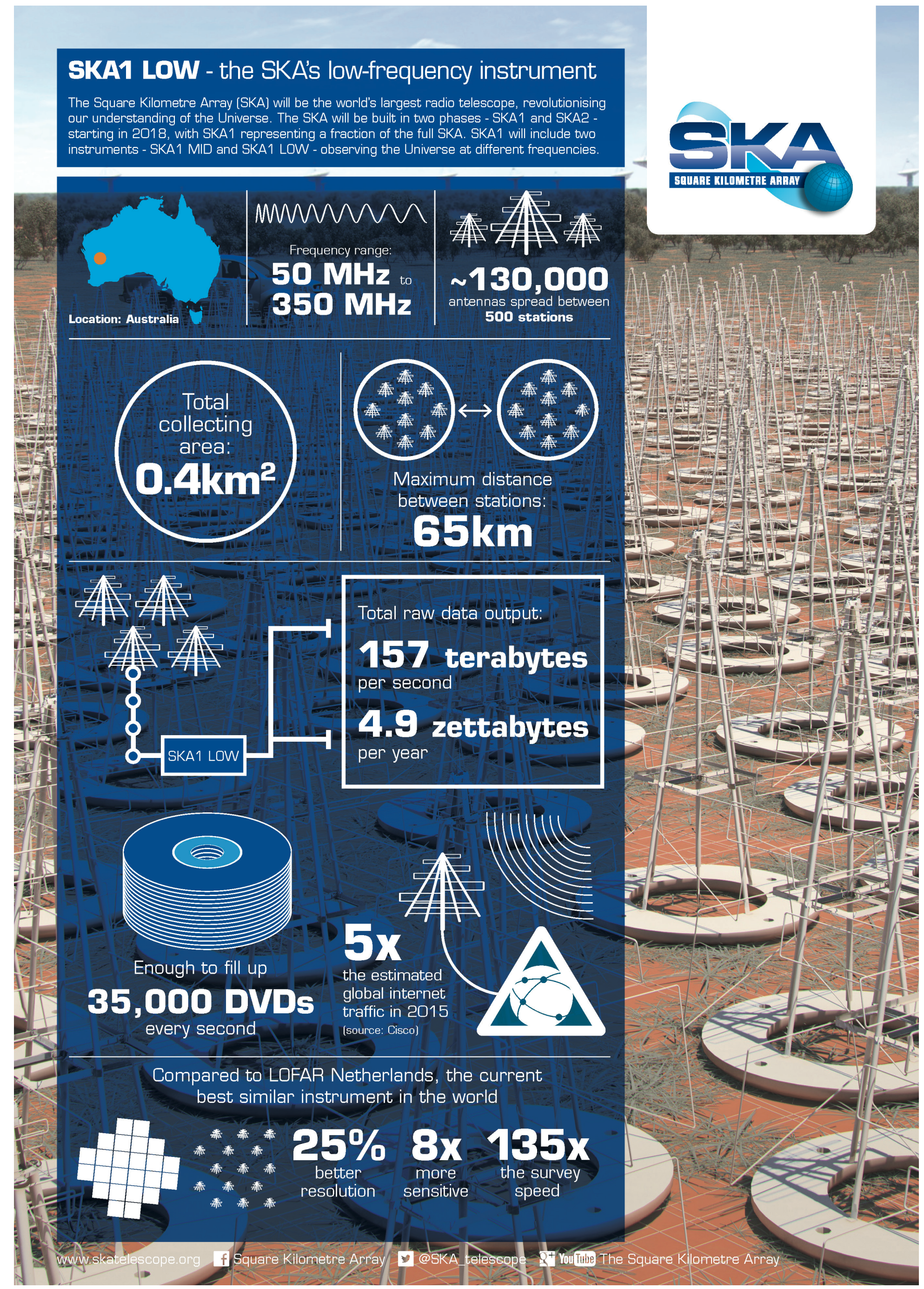

CMB future

If we can measure the primordial B-modes, that is a direct check in the tensor perturbations of the metric and directly linked with gravitational waves produced during inflation

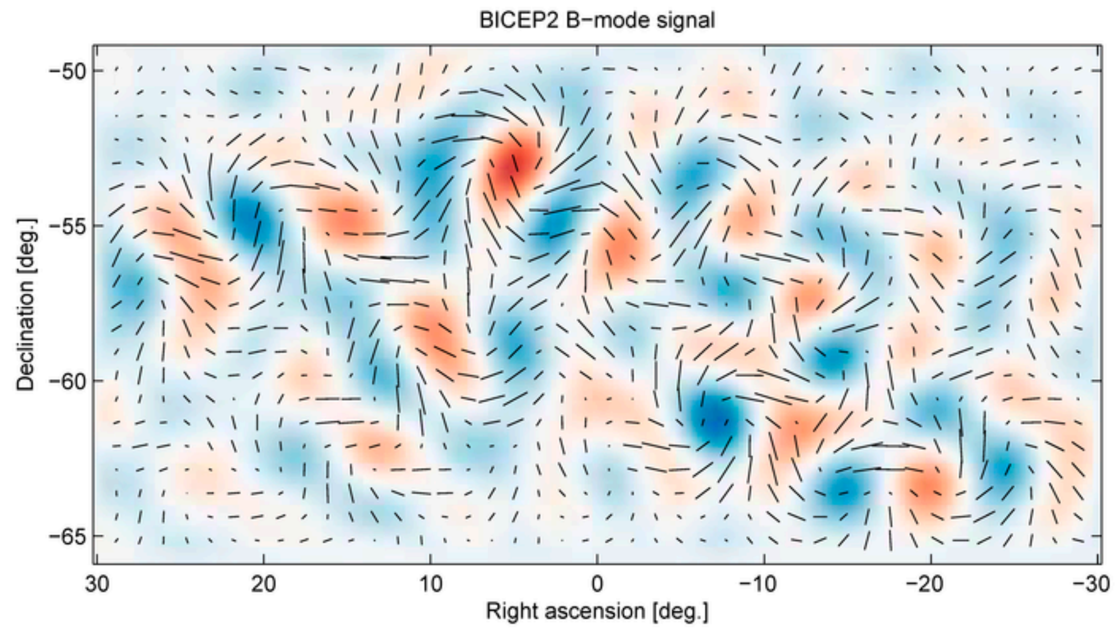

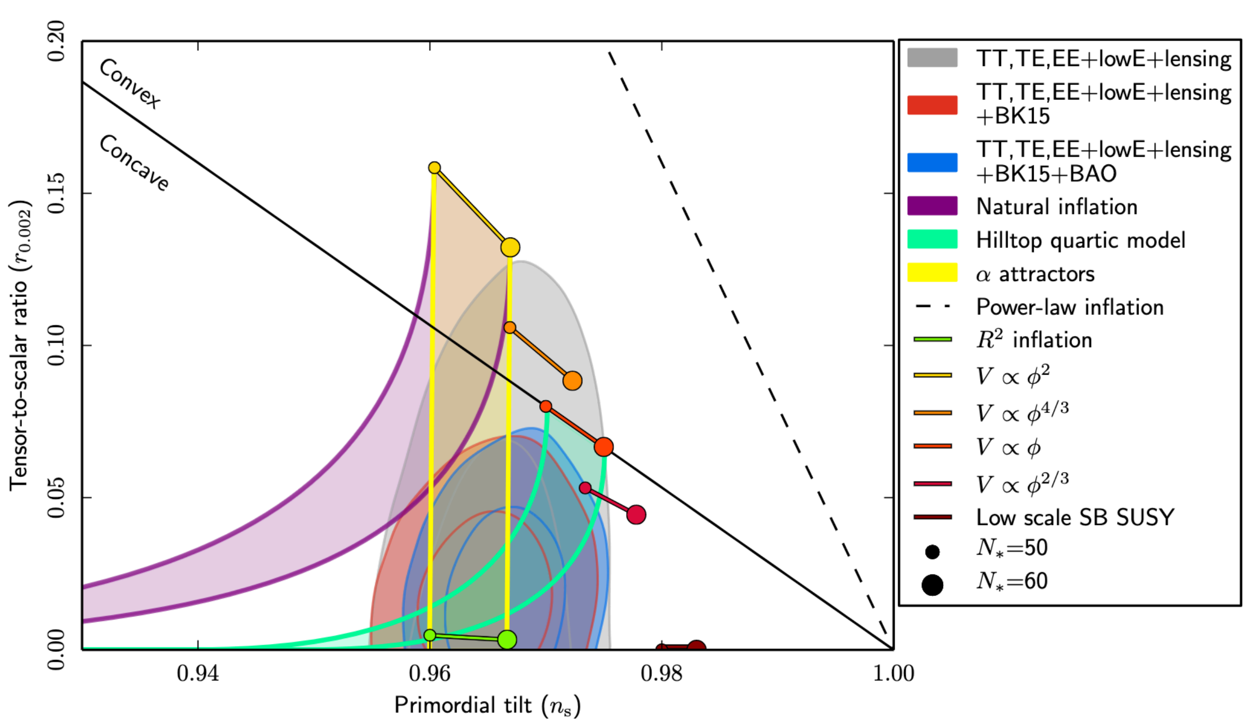

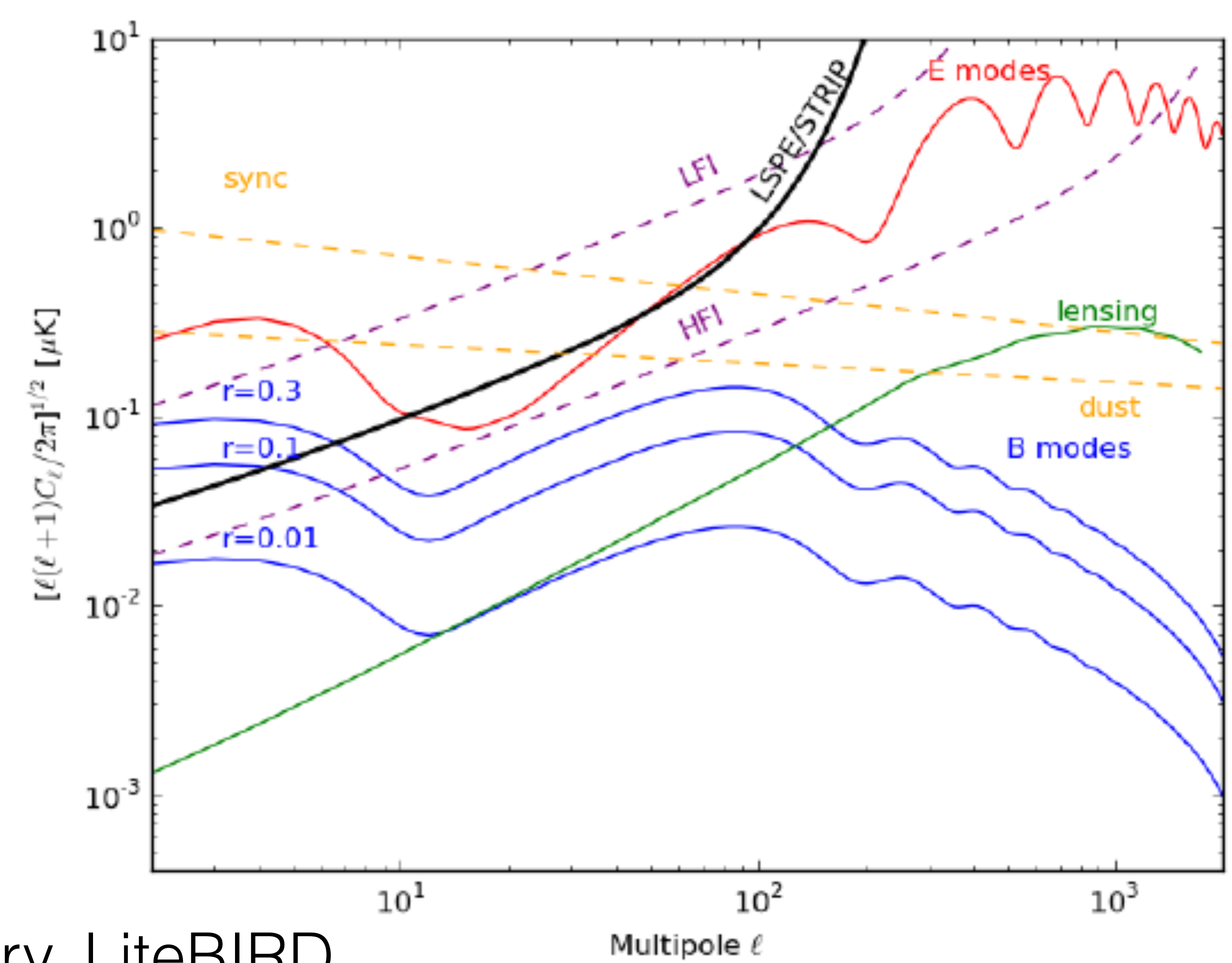

BICEP3/KECK array, Simons Observatory, LiteBIRD, …

¡Many Thanks!